

เคอร์คิวมินกราฟต์พอลิไวนิลแอลกอฮอล์สำหรับห่อหุ้มแอสคอร์บิลปาลมิเตต

นางสาวศิริินภา เจนศิริสกุล

วิทยานิพนธ์นี้เป็นส่วนหนึ่งของการศึกษาตามหลักสูตรปริญญาวิทยาศาสตรมหาบัณฑิต

สาขาวิชาปิโตรเคมีและวิทยาศาสตร์พอลิเมอร์

คณะวิทยาศาสตร์ จุฬาลงกรณ์มหาวิทยาลัย

ปีการศึกษา 2554

ลิขสิทธิ์ของจุฬาลงกรณ์มหาวิทยาลัย

บทคัดย่อและแฟ้มข้อมูลฉบับเต็มของวิทยานิพนธ์ตั้งแต่ปีการศึกษา 2554 ที่ให้บริการในคลังปัญญาจุฬาฯ (CUIR)

เป็นแฟ้มข้อมูลของนิสิตเจ้าของวิทยานิพนธ์ที่ส่งผ่านทางบัณฑิตวิทยาลัย

The abstract and full text of theses from the academic year 2011 in Chulalongkorn University Intellectual Repository (CUIR)

are the thesis authors' files submitted through the Graduate School.

CURCUMIN GRAFTED POLY(VINYL ALCOHOL) FOR
ASCORBYL PALMITATE ENCAPSULATION

Miss Sirinapa Janesirisakule

A Thesis Submitted in Partial Fulfillment of the Requirements
for the Degree of Master of Science Program in Petrochemistry and Polymer Science
Faculty of Science
Chulalongkorn University
Academic Year 2011
Copyright of Chulalongkorn University

Thesis title CURCUMIN GRAFTED POLY(VINYL ALCOHOL) FOR
ASCORBYL PALMITATE ENCAPSULATION
By Miss Sirinapa Janesirisakule
Field of study Petrochemistry and Polymer Science
Thesis Advisor Associate Professor Supason Wanichwaecharungruang, Ph.D.

Accepted by the Faculty of Science, Chulalongkorn University in
Partial Fulfillment of the Requirements for the Master's Degree

..... Dean of the Faculty of Science
(Professor Supot Hannongbua, Dr.rer.nat.)

THESIS COMMITTEE

..... Chairman
(Assistant Professor Warinthorn Chavasiri, Ph.D.)

..... Thesis Advisor
(Associate Professor Supason Wanichwaecharungruang, Ph.D.)

..... Examiner
(Associate Professor Mongkol Sukwattanasinitt, Ph.D.)

..... External Examiner
(Nantanit Wanichacheva, Ph.D.)

ศิริณา เจนศิริสกุล : เคอร์คิวมินกราฟต์พอลิไวเนิลแอลกอฮอล์สำหรับการห่อหุ้มแอสคอร์บิล
 ปาลมิเตต CURCUMIN GRAFTED POLY(VINYL ALCOHOL) FOR ASCORBYL
 PALMITATE ENCAPSULATION) อ. ที่ปรึกษาวิทยานิพนธ์หลัก: รศ.ดร. ศุภศร วณิชเวชารุ่งเรือง
 , 77 หน้า.

งานวิจัยนี้ทำการสังเคราะห์อนุภาคนาโนจากพอลิเมอร์ 2 ชนิดคือ curcumin-grafted PV(OH) (Cur-PV(OH) และ cinnamate-grafted PV(OH) (Cin-PV(OH) เพื่อใช้ห่อหุ้มแอสคอร์บิลปาลมิเตต (AP) โดยการทดลองครอบคลุมตั้งแต่การสังเคราะห์พอลิเมอร์ การสร้างอนุภาค และการกักเก็บ เมื่อเปรียบเทียบความเสถียรของ AP อิสระที่ไม่ถูกห่อหุ้มกับ AP ที่ถูกห่อหุ้มในอนุภาคที่สังเคราะห์ขึ้นทั้ง 2 ชนิดในรูปของแข็งและอนุภาคแขวนลอยในน้ำ พบว่า AP ที่ถูกห่อหุ้มมีความเสถียรมากกว่า AP อิสระที่ไม่ถูกห่อหุ้ม โดย AP ในรูปของแข็งมีความเสถียรมากกว่าในรูปอนุภาคแขวนลอยในน้ำ AP ในสภาวะที่ไม่มีแสงจะมีความเสถียรมากกว่าที่มีแสงการเปรียบเทียบความเสถียรของ AP พบว่า AP ที่ถูกห่อหุ้มในอนุภาคนาโนของ Cur-PV(OH) มีความเสถียรมากกว่า AP ที่ถูกห่อหุ้มในอนุภาค Cin-PV(OH) ที่มีการเติมเคอร์คิวมินอิสระลงไปรวมกักเก็บด้วย อนุภาค Cur-PV(OH) สามารถบรรจุ AP ได้สูงถึง $29.00 \pm 0.3\%$ โดยน้ำหนัก โดยกระบวนการกักเก็บมีประสิทธิภาพ $80.85 \pm 0.2\%$ และอนุภาค AP-Cur-PV(OH) มีขนาดประมาณ 269.8 ± 19.4 นาโนเมตร การศึกษาการซึมผ่านของอนุภาค AP-Cur-PV(OH) โดยใช้ผิวหนังส่วนของหนูอายุ 6 เดือนด้วยกล้องจุลทรรศน์ที่ใช้ลำแสงเลเซอร์สำหรับมองภาพตัวอย่างในลักษณะ 3 มิติ (Confocal Laser Fluorescence Scanning Microscope, CLFM) พบว่าอนุภาคเป็นเส้นทางหลักที่อนุภาค AP-Cur-PV(OH) เข้าสู่ชั้นผิวหนังได้ดี และอนุภาคสามารถปลดปล่อย AP ออกจากอนุภาคและเข้าสู่เนื้อเยื่อบริเวณรอบรูขุมขนได้

สาขาวิชา...ปิโตรเคมีและวิทยาศาสตร์พอลิเมอร์. ลายมือชื่อ.....
 ปีการศึกษา.....2554..... ลายมือชื่อ อ.ที่ปรึกษาวิทยานิพนธ์หลัก.....

5272663523: MAJOR PETROCHEMISTRY AND POLYMER SCIENCE

KEYWORDS : ASCORBYL PALMITATE/ENCAPSULATION /NANOPARTICLE
AND PENETRATON

SIRINAPA JANESIRISAKULE CURCUMIN GRAFTED POLY(VINYL
ALCOHOL) FOR ASCORBYL PALMITATE ENCAPSULATION.
ADVISOR: ASSOC. PROF. SUPASON WANICHWAECHARUNGUANG,
Ph.D., 77 pp.

In this work, encapsulation of ascorbyl palmitate (AP) into two polymeric nanoparticles of curcumin-grafted PV(OH) (Cur-PV(OH)) and cinnamate-grafted PV(OH) (Cin-PV(OH)) was carried out. The experiment covers polymer synthesis, particle fabrication, and encapsulation. Then, the stability of AP in the two polymeric nanoparticles and free AP in freeze-dried form and suspension form. The result showed that the encapsulated AP was more stable than the unencapsulated AP. AP in a freeze-dried form was more stable than AP in the suspension form. Moreover, AP kept under light-proof condition was more stable than that kept expected to light. AP inside the Cur-PV(OH) particles was more stable than AP co-encapsulated with curcumin inside the Cin-PV(OH) particles. Cur-PV(OH) nanospheres could be loaded with AP at the encapsulation efficiency of $80.85 \pm 0.2\%$ at loading of $29.00 \pm 0.3\%$ (wt of AP/total wt). An average particle size of AP-loaded Cur-PV(OH) particles was 269.80 ± 19.4 nm. The skin penetration study of AP-loaded Cur-PV(OH) particles on the ear skin of 6 month old pig using confocal laser fluorescence scanning microscope (CLFM) showed that hair follicle was the skin penetrating route of the AP-Cur-PV(OH) particles. Moreover, the accumulated Cur-PV(OH) at the hair follicles could release AP out into the surrounding tissue.

Field of Study : Petrochemistry and Polymer Science Student's Signature.....

Academic Year:.....2011..... Advisor's Signature.....

ACKNOWLEDGEMENTS

I have many people to thank for their introduce and encouragement for this project. First of all, I would like to express my sincere appreciation and gratitude to my beloved advisor, Associate Professor Dr. Supason Wanichweacharungruang, for all her valuable suggestions, guidance, and encouragement throughout my study.

I am also grateful to the other members of my committee, Associate Professor Dr. Mongkol Sukwattanasinitt, Assistance Professor Dr. Warinthorn Chavasiri, and Dr. Nantanit Wanichacheva for their technical guidelines, comments, and advice given to me especially during the proposal presentation.

Gratefully thanks are wxtended to Graduate School, Chulalongkorn University, Scientific and Technological Research Equipment Centre Foundation, Chulalongkorn University and National Nanotechnology Center (NANOTEC), National Science and Technology Development Agency

Moreover, I also acknowledge all members of research group for the good working environment, opinion, and helpful. Without all of them as mentions, this thesis would not be possible.

CONTENTS

	Page
ABSTRACT (THAI).....	iv
ABSTRACT (ENGLISH).....	v
ACKNOWLEDGEMENTS.....	vi
CONTENTS.....	vii
LIST OF TABLES.....	x
LIST OF FIGURES.....	xi
LIST OF SCHEMES.....	xiii
LIST OF ABBREVIATIONS.....	xiv
CHAPTER I INTRODUCTION.....	1
1.1 Phenolic compounds.....	1
1.2 Vitamin C Ester (Ascorbyl palmitate).....	3
1.3 Curcumin.....	5
1.4 Poly(vinyl alcohol)	6
1.5 Encapsulation.....	7
1.5.1 Encapsulation technique.....	7
1.5.1.1 Micro or nano emulsions.....	8
1.5.1.2 Liposome and vesicles.....	8
1.5.1.3 Solid lipid nanoparticles.....	10
1.5.1.4 Polymeric nanoparticles.....	11
1.6 DPPH radical scavenging assay.....	14
1.7 Literature reviews.....	15
1.7.1 Literature reviews about curcumin antioxidant.....	15
1.7.2 Literature reviews about ascorbyl palmitate (AP).....	18
1.7.3 Literature reviews about ascorbyl palmitate (AP) encapsulation.....	19
1.7.4 Literature reviews about poly(vinyl alcohol)	25
1.8 Research objectives.....	26
CHAPTER II EXPERIMENTAL.....	27
2.1 Materials and Chemicals.....	27

	Page
2.2 Instrument and Equipments.....	27
2.3 Synthesis of mono-substituted glutarylcurcumin.....	28
2.4 Synthesis of curcumin-grafted poly(vinyl alcohol).....	29
2.5 Synthesis of cinnamate-grafted poly(vinyl alcohol).....	30
2.6 Encapsulation of ascorbyl palmitate into polymeric nanoparticles.....	31
2.7 Morphology and particle size of AP-encapsulated nanopaticles	33
2.8 Stability of ascorbyl palmitate.....	34
2.9 <i>Ex vivo</i> skin penetration by using confocal laser scanning fluorescence microscopy (CLFM).....	35
2.10 DPPH• free radical scavenging activity.....	35
CHAPTER III RESULTS AND DISCUSSION.....	37
3.1 Synthesis and characterization.....	38
3.1.1 Synthesis of mono-substituted glutarylcurcumin.....	38
3.1.2 Synthesis of curcumin-grafted poly(vilnyl alcohol).....	39
3.1.3 Synthesis of cinnamate-grafted poly(vinyl alcohol).....	45
3.2 Encapsulation of ascorbyl palmitate into nanoparticles.....	47
3.3 Encapsulation efficiency and loading.....	50
3.4 Stability of the encapsulated ascorbyl palmitate (AP).....	51
3.5 <i>Ex vivo</i> skin penetration by using confocal laser scanning fluorescence microscopy (CLFM).....	53
3.6 DPPH• free radical scavenging activity.....	54
CHAPTER IV CONCLUSION.....	56
REFERENCES.....	57
APPENDIX.....	69
VITAE.....	77

LIST OF FIGURES

Figure	Page
1.1 Structure of ascorbic acid.....	3
1.2 Structure of ascorbyl palmitate (AP).....	4
1.3 Structure of (a) curcumin, (b) desmethoxycurcumin and (c) bis- demethoxycurcumin.....	5
1.4 Structure of poly(vinyl alcohol), (partially hydrolyzed).....	7
1.5 (A) Two immiscible liquids, not yet emulsified, (B) An emulsion of Phase II dispersed in Phase I, (C) The unstable emulsion progressively separates and (D) The surfactant (blue outline around particles) positions itself on the interfaces between Phase II and Phase I, stabilizing the emulsion.....	8
1.6 Structure of liposome.....	8
1.7 Structure of 2,2-Diphenyl-1-picrylhydrazyl (DPPH radical).....	14
1.8 Structure of natural curcuminoids.....	15
1.9 Chemical structures of curcumin (1) and the radical reaction products (2, 4 and 5).....	16
1.10 Structure of antioxidants.....	17
1.11 Chemical structures of (a) ascorbyl palmitate and (b) sodium ascorbyl Phosphate.....	18
1.12 EPR spectra of ascorbyl radicals recieved from blood samples equilibrated with ascorbic acid (A) and ascorbyl palmitate (C) in equimolar concentration 200 $\mu\text{mol/l}$ compared with control signal from the blood alone is shown in (B) DPPH use as the standard to determine the coefficient.....	19
1.13 13 % AP remaining in NLC prepared from different types of solid lipid matrices at 25 °C and 4 °C after 1 month of storage.....	21
1.14 % AP remaining in degassing condition at different storage temperature (25 °C and 4 °C) at day 30.....	21

Figure	Page	
1.15	Photograph of (a) SEM image of PCPLC particles prepared by self-assembling at the polymer concentration of 600 ppm, (b) SEM image of AP-loaded PCPLC particles prepared at PCPLC concentration of 6000 ppm with the loading 56% (w/w) AP in the particles and (c) TEM image of the same AP loaded PCPLC particle.....	22
1.16	SEM micrographs at 15 kV of (a) chitosan particles (10,000x) and (b)-(d) AP-loaded chitosan particles with different CTS to AP weight ratios of 1:1.00 (100,000x) to AP weight ratios: (b) 1:1.00 (1000x), (c) 1:1.00 (10,000x) and (d) 1:1.50 (10,000x).....	23
1.17	TEM micrographs at 80 kV of (a) chitosan particles 100,000X and (b) AP-loaded chitosan particles with CTS to AP weight ratios of 1:1.00 (100,000x).....	24
1.18	SEM photograph of poly(vinylalcohol-co-vinylcinnamate) by (a) micellar particles (dialyzed against water) and (b,c) reverse micellar particles (dialyzed against hexane).....	24
1.19	TEM of HTCC/CMCS nanoparticles (n^+/n^- , a = 1.67; b = 1.25; c = 1.....	25
1.20	Schematic illustration of the interaction between PV(OH) and ND particles.....	26
3.1	$^1\text{H-NMR}$ spectrum of curcumin in CDCl_3	41
3.2	$^1\text{H-NMR}$ spectrum of mono-substituted glutarylcurcumin in CDCl_3	42
3.3	$^1\text{H-NMR}$ spectrum of curcumin-grafted PV(OH) in DMSO-d_6	42
3.4	UV-visible spectra of curcumin (blue), mono-substituted glutarylcurcumin (red), curcumin-grafted poly(vinyl alcohol) (green) in DMSO	43
3.5	FT-IR spectrum of mono-substituted glutarylcurcumin.....	44
3.6	FT-IR spectrum of curcumin-grafted PV(OH).....	44
3.7	$^1\text{H-NMR}$ spectrum of cinnamate-grafted PV(OH) in DMSO-d_6	46
3.8	UV-visible spectra of cinnamate-grafted poly(vinyl alcohol) in DMSO	46
3.9	FT-IR spectrum of cinnamate-grafted PV(OH).....	47
3.10	Suspension of (a) AP-encapsulated curcumin-grafted PV(OH), (b) AP-encapsulated cinnamate-grafted PV(OH) and (c) AP	

Figure	Page
	48
3.11	48
3.12	49
3.13	49
3.14	52
3.15	53
3.16	

Figure	Page
of AP into the tissue: (a) unresolved fluorescent image of the skin tissue at ~40 μm depth for the stratum corneum surface for 30 min after the AP-loaded curcumin-grafted PV(OH) nanoparticles suspension was applied; (b) fluorescent spectrum of curcumin-grafted PV(OH) (red), AP (green), and skin tissue (grey); (c) superimposed image of the three resolved fluorescent images (d) superimposed image of the AP (green) and curcumin-grafted PV(OH) nanoparticles (red) resolved fluorescent images.....	54
A.1 Calibration curve of ascorbyl palmitate (AP) in methanol solution.....	70
A.2 Retention time and area of ascorbyl palmitate (AP) at 1,000 ppm.....	70
A.3 Retention time and area of ascorbyl palmitate (AP) at 800 ppm.....	71
A.4 Retention time and area of ascorbyl palmitate (AP) at 400 ppm.....	71
A.5 Retention time and area of ascorbyl palmitate (AP) at 200 ppm.....	72
A.6 Retention time and area of ascorbyl palmitate (AP) at 100 ppm.....	72

LIST OF TABLES

Table	Page
1.1 The structure of phenol group compounds.....	1
1.2 Degradation of AP after 4 weeks in different colloidal carrier systems at an initial concentration of 1% w/w (mean \pm S.D).....	20
1.3 The influence of two carrier systems on the effectiveness of AP against free radical formation in UV irradiated skin at different concentration of AP (mean \pm SE, $n = 5$, skin of different pigs).....	20
1.4 Loading capacity and encapsulation efficiency of AP-loaded chitosan nanoparticles.....	23
2.1 Concentration (ppm) of polymer (curcumin-grafted poly(vinyl alcohol) and cinnamate-grafted poly(vinyl alcohol)) and active (ascorbyl palmitate and ascorbyl palmitate together with curcumin).....	32
3.1 The mole ratios of curcumin : glutaric anhydride.....	39
3.2 Particle size of AP (or together with curcumin)-encapsulated polymeric nanoparticles.....	50
3.3 % loading and % encapsulation efficiency (%EE) of AP-encapsulated particles.....	51
3.4 % inhibition of DPPH [*] of 4 substances in various concentratio(mg/mL)...	55

LIST OF SCHEMES

Scheme	Page
1.1 The nonenzymatic antioxidant process of the phenolic material	6
1.2 Mechanism of DPPH [•] and antioxidant (RO-H)	15
1.3 H-atom transfer reactions of curcumin	16
2.1 Synthesis of mono-substituted glutarylcurcumin	28
2.2 Synthesis of curcumin-grafted poly(vinyl alcohol)	29
2.3 Synthesis of cinnamate-grafted poly(vinyl alcohol)	30
3.1 (a) Synthesis of mono-substituted glutarylcurcumin, (b) Synthesis of curcumin-grafted poly(vinyl alcohol)	37
3.2 Mechanism of synthesis of mono-substituted glutarylcurcumin	38
3.3 Mechanism of synthesis of curcumin-grafted poly(vinyl alcohol)	40
3.4 Mechanism of synthesis of cinnamate-grafted poly(vinyl alcohol)	45

LIST OF ABBREVIATIONS

AP	Ascorbyl palmitate
AP-Cin-PV(OH)	AP-encapsulated cinnamate-grafted poly(vinyl alcohol)
APCur-Cin-PV(OH)	AP (together with curcumin)-encapsulated cinnamate-grafted poly(vinyl alcohol)
AP-Cur-PV(OH)	AP-encapsulated curcumin-grafted poly(vinyl alcohol)
°C	Degree Celsius
CDCl ₃	duterated chloroform
CLFM	Confocal laser fluorecence scanning microscopy
Cin-PV(OH)	Cinnamate-grafted poly(vinyl alcohol)
Cur-PV(OH)	Curcumin-grafted poly(vinyl alcohol)
DSC	differential scanning calorimeter
DMF	dimethyl formamide
DMSO	dimethyl sulfoxide
DMSO-d ₆	duterated dimethyl sulfoxide\
EDCI	1-Ethyl-3-(3-dimethylaminopropyl)carbodiimide
h	hour(s)
HOBt	hydroxy benzotriazole
HPLC	High performance liquid chromatography
FT-IR	Fourier transform infared spectroscopy
mg	milligram
mL	milliliter
MW	molecular weight
nm	nanometer
NMR	nuclear magnetic resonance
ppm	parts per million
PV(OH)	poly(vinyl alcohol)
SEM	scanning electron microscope
TEM	transmission electron microscope
UV	ultraviolet

μg	microgram(s)
μL	microliter(s)
μm	micrometer(s)
λ	wavelength

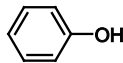
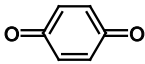
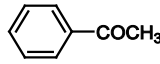
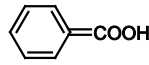
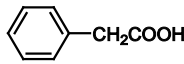
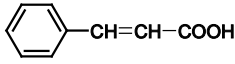
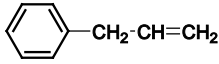
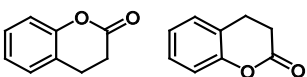
CHAPTER I

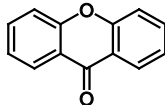
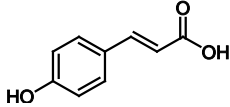
INTRODUCTION

1.1 Phenolic compounds

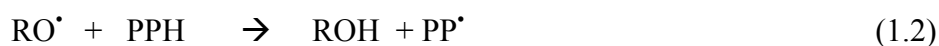
Phenolic compounds are substances that have been created to capitalize on the growth and propagation of each plant. Thus, the patterns of phenolic compounds in plants are different. At the present, the phenolic compounds have more than 8,000 species such as phenolic acid, lignins, etc. showed in Table 1.1.

Table 1.1 The structure of phenol group compounds [1]

Class	Basic skeleton	Basic structure
Simple phenols	C_6	
Benzoquinones	C_6	
Acetophenones	C_6-C_2	
Phenolic acids	C_6-C_1	
Phenylacetic acids	C_6-C_2	
Hydroxycinnamic acids	C_6-C_3	
Phenylpropenes	C_6-C_3	
Coumarins, isocoumarins	C_6-C_3	

Class	Basic skeleton	Basic structure
Xanthones	$C_6-C_1-C_6$	
Lignins	$[C_6-C_3]_n$	

Important biological activities of phenolic compounds include antioxidant and antimutagens, thus phenolic compounds can prevent the onset of many diseases associated with oxidation and mutagenesis, e.g., ischemic heart disease and cancer. Phenolic compounds can eliminate free radicals and metal ions that cause lipid peroxidation and other molecules by the following mechanism:



When ROO^{\bullet} , RO^{\bullet} are free radicals and PPH is phenolic compound.

When the phenolic compounds transfer hydrogen atom to the free radical, free radical of the phenolic compounds are quite stable. Therefore, it cannot react to others. Moreover, free radical of the phenolic compounds can react with other free radicals, from equation (1.3) and equation (1.4).



Phenolic compounds can be found in various parts of plants such as grains (including soybeans, peanuts, cotton, rice and sesame seeds), fruit (including grapes, orange, and black pepper), and leaves (including potatoes, and onions) [2].

1.2 Vitamin C Ester (Ascorbyl palmitate)

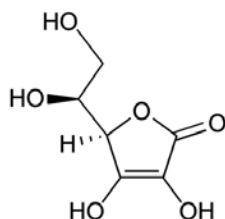


Figure 1.1 Structure of ascorbic acid

Vitamin C, L-ascorbic acid, or L-ascorbate, Figure 1.1 is an essential nutrient for humans and other animal species. Vitamin C is a water soluble compound. Vitamin C is an antioxidant and can prevent the body for oxidative stress [3], boost the immune system, prevent and heal infections caused by viruses and bacteria [4]. Moreover, the compound is a cofactor in leastways eight enzymatic reactions including several collagen synthesis reactions that cause the most severe symptoms of scurvy when they are dysfunctional [5]. . Vitamin C is found in citrus fruits such as guava, tamarind, orange, lemon, and some green vegetables [6].

Degradation of vitamin C occurs through both aerobic and anaerobic pathways [7] and depends on many factors such as heat, oxygen, moisture, storage temperature, metals, and storage time [8]. While the absorption of water soluble vitamin C by the body is quite quick, its availability to cells, especially skin cells is limited. Therefore, vitamin C is not stored in the body [9]. For this reason, synthesis of vitamin C derivatives, both water-soluble form such as sodium ascorbyl phosphate [10], magnesium ascorbyl phosphate [11] and fat-soluble form such as ascorbyl palmitate [12] have been proposed to ease its degradation problem.

Ascorbyl palmitate (AP) is a synthetic ester comprised of the 16-carbon chain saturated fatty acid, palmitic acid and L-ascorbic acid [13]. The ester linkage is at the 6 carbon of ascorbic acid. AP is a fat-soluble, and highly bioavailable derivative of vitamin C [14], (Figure 1.2). AP possess overall the benefits of vitamin C, unlike the water-soluble form, AP can be stored in the lipid cell membranes until the body is ready to put it to use [15]. AP is used as an antioxidant in foods, pharmaceuticals, skin care and cosmetics, and is

also used as a preservative for the natural oils, oleates, fragrances, colors, vitamins, waxes, and other edible oils [16].

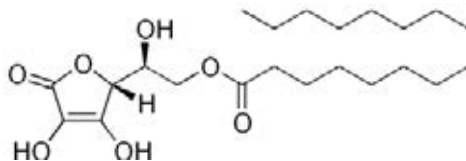


Figure 1.2 Structure of ascorbyl palmitate (AP)

Ascorbyl palmitate is a capable free radical-scavenging antioxidant, its antioxidative activity is stronger than vitamin E [17]. It also acts synergistically with vitamin E, helping to regenerate the vitamin E radical on a steady basis [18].

Ascorbyl palmitate protects fats from peroxidation [19], and can be stored in the body in small amounts [20]. Taking ascorbic acid together with ascorbyl palmitate seems to be the most ideal combination. This combination allow the body to be filled with vitamin C at all times [21].

Ascorbyl palmitate acts synergistically with other antioxidants such as vitamin?? to inhance immunity in our bodies [22]. It has been reported to promote nitric oxide activity as well as to help maintain healthy platelet function [23]. It is also essential for the formation and maintenance of intercellular ground substance and collagen, important for joint health. It aids in the absorption of iron and the formation of red blood cells and the conversion of folic acid precursor to its active forms [24-25].

Ascorbyl palmitate can be found in food as a preservative [26]. Restaurants may choose to fry their food in oils that have been fortified with ascorbyl palmitate because it keeps the oil from burning and food from overcooking. Potato chips are usually fried in oils that contain ascorbyl palmitate, the additive keeps the product fresher for longer periods of time [27-28]. Ascorbyl palmitate is also used to prolong the freshness of dried and powdered milk products [29].

Numerous skin care products containing ascorbyl palmitate are commercially available [30]. It helps dramatically plump up thinning skin by increasing its production of new collagen. When ascorbyl palmitate is properly delivered into skin cells, there is a very good chance to reduce the appearance of wrinkles and improve skin texture [31-33].

1.3 Curcumin

Curcumin (diferuloylmethane) is a polyphenol derived from the plant *Curcuma longa*, commonly called turmeric [34]. It is used in other spicy dishes from India and South East Asia.

Curcumin consists of curcumin, demethoxycurcumin and bisdemethoxycurcumin [35] (Figure 1.3). The curcuminoid is a natural phenols that have at least two tautomeric forms, enol and keto. The enol form is more stable in solution and in the solid phase [36]. The structure formula of curcumin is $C_{20}H_{21}O_6$, molecular weight is 368.38 g/mol, boiling point is $183^{\circ}C$ and maximum absorption wavelength is 420 nm [37].

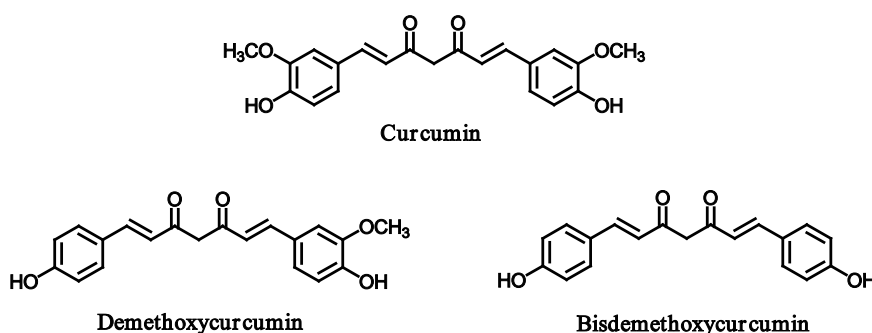


Figure 1.3 Structure of (a) curcumin, (b) demethoxycurcumin and (c) bisdemethoxycurcumin [38]

Curcumin commonly used as a food ingredients in Asia for a long time. The Food and Drug Administration (FDA) of the United States are considered that turmeric is an herb that is safe [39]. It possesses diverse pharmacologic effects including anti-Alzheimer's disease [40], anti-angiogenic [41] anti-oxidant [42], anti-tumor [35], anti-inflammatory [44], anti-ischemic [45], anti-cancer [46] activities.

One of the most significant factors of curcumin is its antioxidant properties to scavenge reactive oxygen species (ROX) [47] and inhibit the process of lipid peroxidation [48]. The structure of curcumin consists of all conjugated of β -diketone moiety and two O-methoxylated phenol. The antioxidation process is through to be distributed into two parts, Schemes 1.1

(1) Radical trapping part



(2) Radical termination part



Where S is the substance for antioxidant

AH is the antioxidant

A^\bullet is the antioxidant radical

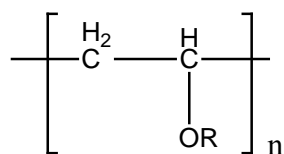
X^\bullet is another radical species

Scheme 1.1 The nonenzymatic antioxidant process of the phenolic material [49].

Anywise, curcumin was limited toward its water-insolubility, instability, and low bioavailability such as low serum level, limited tissue distribution [50]. Furthermore, curcumin also changed to many compounds that have low activity [51]. Metabolism study of curcumin showed that 99% of curcumin changed into glucoronide, easy to release from animal body [52].

1.4 Poly(vinyl alcohol)

Poly(vinyl alcohol), (PVA, PV(OH) or PVAL) is a well known synthetic polymer that soluble in water, white powder, tasteless and odorless. It is a highly crystalline which prepared by radical polymerization of vinyl acetate followed by saponification of poly(vinyl acetate) [53]. The chemical structure of the vinyl alcohol repeating units is:



where R = H or COCH₃

Figure 1.4 Structure of poly(vinyl alcohol), (partially hydrolyzed)

Poly(vinyl alcohol) is non-toxic [54], biodegradable [55], biocompatible [56], non-carcinogen [57], good oxygen permeable [58] and no immunogenic effects [59]. It has high tensile strength and flexibility, as well as high oxygen and aroma barrier properties [60].

Poly(vinyl alcohol) used in four majors sections of PV(OH) consumption consist of : paper coating [61], film used in the water transfer printing process [62], textile sizing agent [63] and paper adhesive with boric acid in spiral tube winding [64]. Moreover, the hydrophilic characteristic of PVOH is satisfactory to generate hydrogel for pharmaceutical utilization generally as drug delivery medium [65], anti-shearing agent in cell fermentation processes [66] and tissue replacement [67].

1.5 Encapsulation

Encapsulation is the storage of any substance in the capsule to protect, control release of the substance or make the substance dispersed in a solvent solution [68]. In medical, an encapsulation techniques were used in the manufacture of drug delivery to the target to optimize the treatment better [69].

1.5.1 Encapsulation technique.

Vesicle preparations can be classified into four types according to the structure:

- 1.5.1.1 Micro- or nano emulsions.
- 1.5.1.2 Liposome and vesicles.
- 1.5.1.3 Solid lipid nanoparticles.
- 1.5.1.4 Polymeric nanoparticles.

1.5.1.1 Micro or nano emulsions.

Emulsion are mixture of two or more immiscible liquids that consist of oil, water and surfactant [70]. Emulsion particles may be found in the form of oil-in-water (O/W) or water-in-oil (W/O), Figure 1.5. A factor for create of emulsion with a high energy level with high-pressure homogenizers, HPH) and ultrasound generator [71] is temperature, pressure and frequency of homogenized. The number of homogenization necessary to reduce the dispersion of the particles. Moreover, high temperature is necessary to produce a small particle size [72-73].

The particle sizes of microemulsions had between 10-140 nm. Microemulsions made from a mixture of compounds in a suitable ratio from ternary phase diagram. Nanoemulsions is a dispersion of oil and water that stabilized with emulsifying agent, particle sizes between 20-200 nm [74]

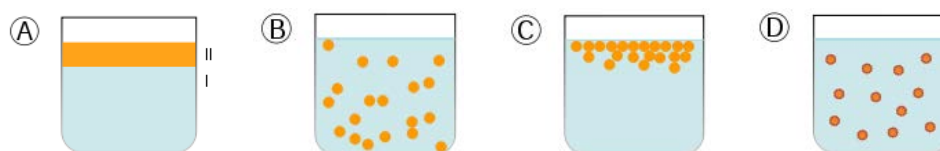


Figure 1.5 (A) Two immiscible liquids, not yet emulsified, (B) An emulsion of Phase II dispersed in Phase I, (C) The unstable emulsion progressively separates, and (D) The surfactant (blue outline around particles) positions itself on the interfaces between Phase II and Phase I, stabilizing the emulsion.

1.5.1.2 Liposome and vesicles.

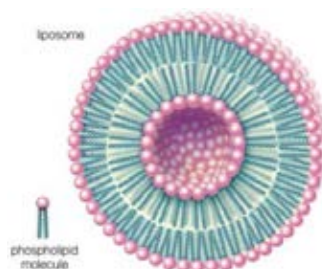


Figure 1.6 Structure of liposome [75]

Liposome are artificially prepared vesicle from lipid bilayer that have hydrophilic part and hydrophobic part (amphiphilic), Figure 1.6 Liposome are used for delivery drug for cancer and other diseases. A liposome encapsulates a region of aqueous solution inside a hydrophobic membrane, dissolved hydrophilic solutes cannot readily pass through the lipids. Hydrophobic chemicals can be dissolved into the membrane. The liposome is dependent on nature of lipid, components of isotonic pressure and method to prepare liposome [76].

The preparation of liposome consisted of specific additives and phospholipid such as lecithin as a neutral. The charge of the liposome wall come from phospholipid such as phosphatidylglycerol dimeriatoyl phosphatidylcholine. In the wall of liposome included 1) sterol, phytosterol, chloesterol and dihydrocholesterol help for controlled chemical and physical properties and 2) buffer, electrolyte, phosphatidic acid, dicetylphosphate, steylamine help for encapsulated substances and increased the stability of liposome [77].

The preparation of liposome had several method depending on appropriateness of the drug and ability for contained and encapsulated drug. There are five ways to prepare liposome;

Film hydration method is the most popular method. First, dissolved phospholipid in organic solvents. Next, prepared phospholipid film by evaporation to remove organic solvents. Then, rehydrated film with water or buffer solution at temperature over than T_c of phospholipid. Finally, created MLV liposomes for encapsulated drug into liposome carriers. [78].

Dehydration-rehydration method is a method to mix film from drying lipid solution by using lyophilization or evaporation method in the presence of the drug in an aqueous solution. Drug is encapsulated into mixed film between lipid layer and then become to MLV liposome [79].

Reverse phase evaporation method is a method to soluble fat in diethyl ether, diisopropyl ether, or mixture of both in chloroform. Then, added water into lipid solution and reduced particles by using sound wave. After that, evaporated organic solvents. In this method, system is a reverse phase to MLV liposome [80].

Solvent injection method is a method to inject lipid solution at high pressure for example ether, fluorocarbon, or ethanol into aqueous phase under reducing pressure. Temperature of aqueous phase is upper T_c and releasing pressure lead to evaporated solvent during injection. The method to make LUV liposome [81].

Supercritical liposome method is a method to prepare liposome do not use organic solvents. First, prepared phospholipid and cholesterol solution in compressed carbon dioxide gas. Next, increased the temperature, pressure and compressed carbon dioxide gas again. Then, adjusted the temperature and pressure to separate liposome [82].

1.5.1.3 Solid lipid nanoparticles.

Solid particles consist of solid lipid nanoparticles (SLN) and nanostructured lipid carriers (NLC), that are several advantages such as the ability to control release, increase the chemical stability of drug storage, easy to increase of the large-scale production, and can encapsulate of hydrophilic drug and lipophilic drug [84]. There are two types of solid lipid nanoparticles [83];

Solid lipid nanovesicles contained of lipid, surfactant or emulsion, and water. Lipid that have triglyceride, fatty acid, steroid, and wax. The principle properties such as high physical stability, protection of drug degraded, deliver to the target. The disadvantage of the SLN for example drug released from particles after the change of polymorphic transition between drug encapsulated and content of water [84].

Nanostructured lipid carriers are three types; 1) Imperfect crystal type 2) Amorphous type 3) Multiple type [84]. The preparation of SLN and NLC are three method; High speed stirring or ultrasound (HPH), microemulsion technique, solvent emulsification and evaporation, and W/O/W double emulsion method [85].

High speed stirring or ultrasound (HPH) is the most popular method since ensure consistency in production. The principle of HPH, reducing the particle size to pass through the cavitation and turbulences [86]. In general, use the amount of the lipid about 5-10%. Moreover, temperature influences for the preparation of particles [87]. For the preparation of

particles at high temperature made by mixed drug and lipid solutions at high temperature that more than melting point of lipid about 5°C. Next, mixed with an aqueous solution of surfactant at the same temperature and stirred at high speed until was the pre-emulsion. Then, homogenized with a pressure at 500 bars for three times until were SLN or NLC [88-89]. For the preparation of particles at low temperature made by mixed drug and lipid solutions under liquid nitrogen to be solid lipid microparticles. Next, stirred at high speed in aqueous solution of cold surfactant until was the per-emulsion. Then, homogenized with a pressure lower or equal room temperature with a pressure at 500 bars for five times until were SLN or NLC [90].

Microemulsion technique prepare by stirred lipid solution about 10%, surfactant about 15%, and co-surfactant about 10%. Next, distributed microemulsion in cold water and stirred all the time. Then, removed water by using lyophilization [91].

Solvent emulsification and evaporation is the method to precipitate in suitable solution by soluble fat in organic solvents such as toluene, chloroform [91]. Then, evaporating the solvent under reduced pressure, fat is precipitated as a SLN. The advantages of this method is without heat during the preparation. Therefore, it is appropriate to encapsulate drug that easy to degrade [92].

W/O/W double emulsion method developed from solvent emulsification and evaporation method to prepare SLN for encapsulated hydrophilic drug together with sterbilizer. The particle size in the range of micrometers that called lipospheres [93].

1.5.1.4 Polymeric nanoparticles.

Polymeric nanoparticles is a crucial in the process of drug delivery or ingredients to success. When using a conductive polymer (carrier) is a drug or substance to the organ causing disease [94]. The process for forming a polymer in the form of nanoparticles, it is interesting. The advantages of nanoparticles have many such particles are very small, can penetrate easily through the cell without being eliminated by the immune system [95]. In addition, small particles have a high ratio of surface area to volume, which can be packed into the particulate matter in large quantities. However, the small particles tend to be very stable

when left for long periods could cause aggregation of the particles [96]. The factors that have to consider in the preparation of polymeric nanoparticles and the particle size and form of which depends on the method of preparation and the type of polymers used in polymeric nanoparticles. There are various forms, such as nanospheres are also different [97]. In addition, nanocapsules can be classified according to their retention, which may be water or oil. The type and density of the charge on the surface of the particles, type of substance to be delivered, stability of the particles, and toxicity of the particles [98].

The preparation of polymeric nanoparticles have many ways, such as ionic gelation, emulsification, emulsion polymerization, self-assembly, supercritical fluid precipitation and spray-drying [99]. In this case, it discusses how to prepare polymeric nanoparticles. With the emulsifier film applications. (emulsification) and his relation to ionic (ionic gelation).

Preparation of polymeric nanoparticles with ionic gelation.

The ionic gelation is a simple method for prepared nanoparticles. This method relies on the principle of attraction between opposite charges of the polymer solution was diluted in water [100]. However, there are various other factors to control such that the concentration of the polymer, the molecular weight of polymer, the ratio of polymer used, the type of polymer, and rate of stirring [101]. Because these factors affect the size and size distribution. Therefore, it is important to find the optimal conditions for preparation of polymeric nanoparticles [102].

Preparation of polymeric nanoparticles by emulsification.

Emulsion is a type of colloid, formed by two or more liquids that do not dissolve into a homogenous distribution coexist [103]. There are divided into two types: water in oil emulsion (w/o emulsion), and oil in the water emulsion (o/w emulsion) [104].

Emulsification-solvent evaporation: this method consists of two steps. The first step is emulsifier film applications (emulsification) by dissolved polymer in volatile organic solvents

such as chloroform, ethyl acetate, or dichloromethane. A process that requires high energy to achieve compatibility of the two-phase phase (organic solvents and water solution) [105]. In the second step is the removal of the organic solvent of the polymer by precipitated polymer in form of the o/w nanocapsules [106]. The size of the particles depends on the agitation rate during the emulsification, the type and amount of dispersing agent, viscosity of the organic solvents and aqueous solutions, and temperatures [107]. The average of droplet size can be prepared more than 250 nm. However, this method cannot be used in the industry because the solvents used are highly toxic [108].

Emulsification-solvent diffusion or Emulsification-solvent displacement: this method will soluble polymer in an organic solvent that can be water-soluble portion, such as propylene carbonate, benzyl alcohol ethyl acetate, isopropyl acetate, methyl acetate, methyl ethyl ketone, benzyl alcohol, butyl lactate, and isovaleric acid. Then, emulsification with polymer that can soluble in water, which can add the surfactants in a phase of water such as pluronic, F68, poly(vinyl alcohol), and sodium taurodeoxycholate [109]. The droplet size depends on the properties of water mixed compatibility with organic solvents, rate of stirring, and the concentration of stabilizing agent is added in the emulsion [110].

Emulsification–reverse salting out: the principle of this method is to separate the water-soluble organic solvents from aqueous solutions containing high concentrations of salt [111]. This method is similar to the *emulsification-solvent diffusion* method but that the composition of the emulsion polymer that is soluble in organic solvents such as acetone. The aqueous solutions should have a high concentration of salt. The salt used may be of electrolytes such as magnesium chloride, calcium chloride, and magnesium acetate or of non-electrolytes such as sucrose is also used as colloidal stabilizer such as polyvinylpyrrolidone or hydroxyethylcellulose [112]. When emulsification is the o/w droplet of the diluted emulsion with water enough to make the organic solvent soluble in water diffusion in aqueous solutions and the salt concentration high enough polymer formed. Polymer was precipitated by the salting out of aqueous solutions [113]. The selected a type of salt important for the encapsulation efficiency. This method can be used in a pilot scale [114]. The preparation of the size of polymeric nanoparticles in a pilot scale by the emulsification-reverse salting between 557 to 174 nm, if the rate of stirring in the range of 790 to 2,000 rpm. Whereas the size of polymeric nanoparticles in emulsification-solvent diffusion between 562

to 203 nm [115]. For the preparation of emulsion, the rate of agitation is an important affected to the size of the particles [116]. It was found that appropriate for the rate of stirring in emulsification-reverse salting out is 790 rpm, while the emulsification-solvent diffusion method to be used up to 1,000 rpm to ensure uniform particle size distribution are prepared every time [117].

For the preparation of polymeric nanoparticles by using emulsification method to purify the emulsion have many type depending on the type of emulsion preparation techniques such as evaporation under low pressure, centrifugation, ultracentrifugation techniques filtration through mesh or filters, dialysis, gel filtration, ultrafiltration, diafiltration, and cross-flow [118]. In addition, have polymeric nanoparticles prepared by using the machinery developed to prepare polymeric nanoparticles used in the industry. The small particle size is not equal and very large for the distribution of particles. Therefore, in industrial use a colloidal mil for controlling the particle size similar to each production [119].

1.6 DPPH radical scavenging assay

DPPH, or 2,2-Diphenyl-1-picrylhydrazyl, (Figure 1.9) is a stable free radical with purple color, absorbed at 517 nm [120]. Its free radical has been scavenged, DPPH will generate from purple to yellow. The DPPH radical scavenging assay uses this character to show herbs free radical scavenging activity [121].

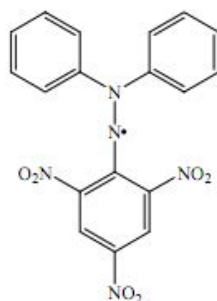
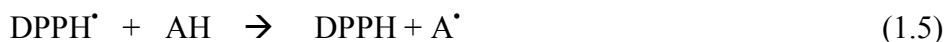


Figure 1.7 Structure of 2,2-Diphenyl-1-picrylhydrazyl, (DPPH radical)

DPPH[•] reacted with antioxidant (AH[•]) or radical species (R[•]), from equation (1.5), and (1.6) [122].



Scheme 1.2 Mechanism of DPPH^{\bullet} and antioxidant (RO-H)

The advantages of this assay are convenient, high reproducibility, and easy to analyze. But this assay cannot analyze the antioxidant activity of blood [123].

1.7 Literature reviews

1.7.1 Literature reviews about curcumin antioxidant

In 1995, Ruby and coworker compared antioxidant activities, cytotoxic, and tumor reducing of curcumin I, II, and III isolated from turmeric (*Curcuma longa*). Curcumin III was found to be more active of antioxidant activity and cytotoxic agent than curcumin I and II. The concentration of curcuminoids (I, II, and III) required for 50% prevention of superoxide, lipid peroxidase, and hydroxyl radical were the most in curcuminoid I, II and III, respectively. The capability of these compounds to repress the superoxide production by macrophages activated with phorbol-1,2-myristate-1,3-acetate (PMA) indicated that all of curcuminoids (I, II, and III) stopped superoxide production and curcumin III generated maximum effect. The result showed that curcumin III is the most active of the curcuminoids offer in turmeric, Figure 1.8 [124].

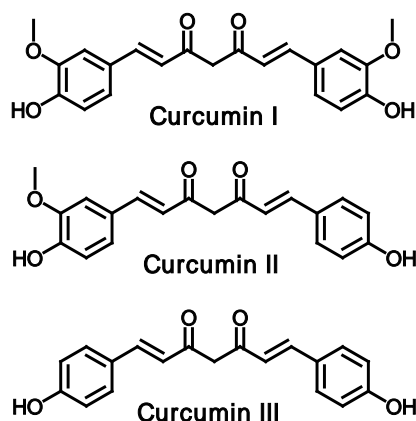
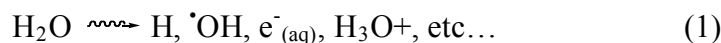


Figure 1.8 Structure of natural curcuminoids.

In 1999, Slobodan and coworker studied the antioxidant mechanisms of curcumin, bis(4-hydroxy-3-methoxyphenyl)-1,6-heptadiene-3,5-dione by pulse radiolysis and laser flash photolysis. Curcumin is insoluble in water at neutral pH but in lightly acidic, curcumin is likely in the keto form that presents to prefer H-atom transfer reactions. The rate constants of H-atom transfer reactions, curcumin is an excellent H-atom donor. Therefore, it summarized that H-atom transfer plays a crucial part in the antioxidant action of curcumin, Scheme 1.3 [125].



Scheme 1.3 H-atom transfer reactions of curcumin.

In 1999, Toshiya and coworker studied the antioxidant mechanism of curcumin by reacted with radical species from the pyrolysis of 2,2'-azobis(isobutyronitrile) under an oxygen atmosphere, and were observed the reaction products from curcumin by HPLC. The reaction at 70 °C for several products, three of structure classified to be ferulic acid, vanillin, and a dimer of curcumin after their separated. The dimer was a lately classified compound bearing a dihydrofuran moiety, and its chemical structure was explicated by using 2D NMR techniques. A mechanism for the dimer production is presented and its relativity to curcumin's antioxidant activity considered. The results show that the dimer is a radical-terminated product in the initial stage, Figure 1.9. [126].

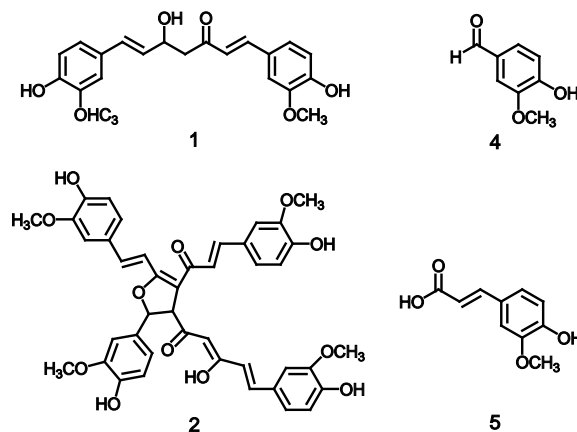
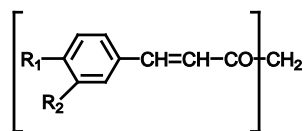


Figure 1.9 Chemical structures of curcumin (1) and the radical reaction products (2,4 and 5).

In 2000, Roberto and coworker showed curcumin to have capable antioxidant, anti-inflammatory, and antitumor promoting properties *in vitro* and *in vivo*. The data showed that curcumin is a certain leader of heme oxygenase (HO-1) in vascular endothelial cells both in hypoxic and normoxic conditions, and enlarged heme oxygenase activity. The biological performances of curcumin including antioxidant capacities, adjustment of inflammatory processes, and inhibition of cell proliferation have also been mentioned to overexpression of HO-1 [127].

In 2000, Ross and coworker studied the antioxidant activity of curcumin (1,7-bis(4-hydroxy-3-methoxyphenyl)-1,6-heptadiene-3,5-dione) by inhibition of managed beginning of styrene oxidation. Synthetic nonphenolic curcuminoids indicated no antioxidant activity; so, curcumin is a phenolic chain-breaking antioxidant, donating H-atoms from the phenolic groups. Moreover, the antioxidant activities of o-methoxyphenols are whittled in hydrogen bond accepting media, Figure 1.10 [128].



$R_1 = \text{OH}, R_2 = \text{OCH}_3$: Antioxidant

$R_1 = R_2 = \text{OCH}_3$: No activity

Figure 1.10 Structure of antioxidants.

In 2004, Venugopla and coworker studied the antioxidant and anti-inflammatory

properties of curcumin. They founded a literal natural product in curing an extensive diseases. Its antioxidant property to the possess of various functional groups, inclusive carbon-carbon double bonds, phenoxy, and methoxy in its structure. The anti-inflammatory property stored it in the limelight over the decades in remedying inflammatory-mediated diseases including diabetes, so forth, cancer, rheumatoid arthritis, and atherosclerosis. Its anti-inflammatory property presents to be mediated through the inhibition of lipoxygenase (LOX), cyclooxygenase (COX) and nitric oxide synthase (iNOS) [129].

1.7.2 Literature reviews about ascorbyl palmitate (AP)

In 2001, Spiclin and coworker compared the stability of vitamin c derivatives such as ascorbyl palmitate and sodium ascorbyl phosphate by examined in microemulsions were both w/o and o/w types and performed of the same ingredients for topical use as carrier systems. The stability of ascorbyl palmitate is highly conditional on its initial concentration, its base in the microemulsion, the quantity of oxygen dissolved in the system and storing conditions. Furthermore, ascorbyl palmitate is more suitable for topical application than sodium ascorbyl phosphate, toward its lead to penetrate in the skin. On the other hand, sodium ascorbyl phosphate was stable in both kind of microemulsions [130].

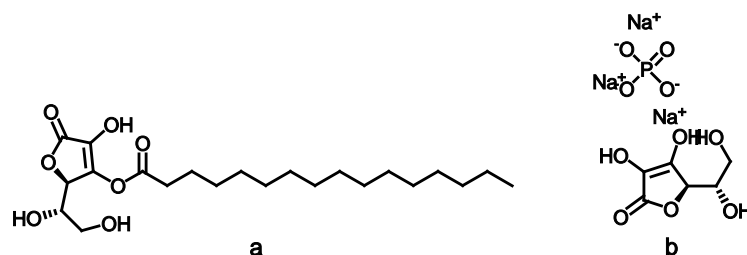


Figure 1.11 Chemical structures of (a) ascorbyl palmitate and (b) sodium ascorbyl phosphate. [130]

In 2003, Gopinath and coworker founded that vesicles of ascorbyl palmitate (Aspasomes) in owning of cholesterol and charge leader dicetylphosphate, solution of AZT encapsulated. The antioxidant capacity of aspasome was much better than ascorbic acid. Therefore, the found applications as drug delivery in disorders involved with reactive oxygen

species. Aspasomes increased the transdermal permeation of aqueous azidothymidine (AZT). The skin penetration and antioxidant property indicate a promising future for aspasome as a transdermal drug delivery system. [131]

In 2003, Pokorski and coworker compared the electron spin resonance (EPR) emitted by human blood loaded with ascorbyl palmitate (AP), hydrophobic derivative of ascorbic acid (AA), or with AA. The result showed that the blood with AP released an EPR signal whose singlet shape, location, and width absolutely relate with the known qualifications of AP and was homologous of AP. In addition, the ascorbate moiety of AP is biologically active because it generates ascorbyl radicals with spectrum of EPR are indistinguishable from those AA. This may help to solve the high scavenging capacity represented by AP. Moreover, AP capability could be more effectively applied, because AP is able to spread in biomembranes on account of its lipophilicity. [132]

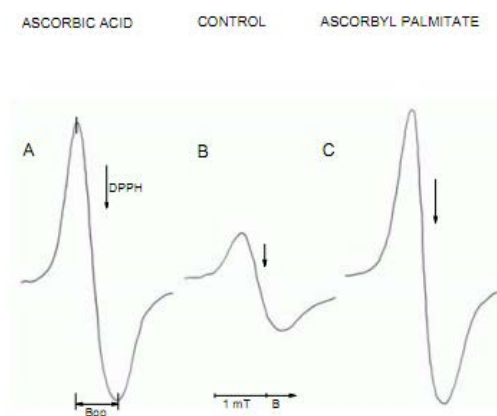


Figure 1.12 EPR spectra of ascorbyl radicals received from blood samples equilibrated with ascorbic acid (A) and ascorbyl palmitate (C) in equimolar concentration 200 $\mu\text{mol/l}$ compared with control signal from the blood alone is shown in (B). DPPH use as the standard to determine the coefficient [132].

1.7.3 Literature reviews about ascorbyl palmitate (AP) encapsulation

In 2003, Julijana and coworker compared the stability effect of carrier systems for ascorbyl palmitate encapsulated in microemulsions (ME), liposomes, and solid-lipid nanoparticles (SLN). AP was reactive to oxidation and most stable in systems which least

exposed to the hydrophilic environment. The result showed that AP was stable in SLN and non-hydrogenated soybean lecithin (NSL) liposomes than in hydrogenated soybean lecithin (HSL) liposomes and in ME. Furthermore, in SLN, the distinguished incorporation of a ratio of the drug into the solid lipid active is also predicted to longer AP stability. They summarized that the location of the sensitive molecule of drug in a carrier system is important for its stability. [133]

Table 1.2 Degradation of AP after 4 weeks in different colloidal carrier systems at an initial concentration of 1% w/w (mean±S.D.) [133]

Carrier system	Amount of non-degraded AP (%)
w/o ME	19±1
o/w ME	13±1
NSL liposomes	26±2
HSL liposomes	7±4
SLN	25±12

In 2003, Polona and coworker studied the effective of UV radiation to free radical formation in the skin. In this work, applied ascorbyl palmitate (AP) in microemulsions to scavenge free radical that consist of carbon-centred acyl ($C=O^{\bullet}$) and sulphur centred radical (SO_3^{\bullet}) radical in UV irradiated porcine skin. The effect of AP was subordinate its kind of microemulsion and concentration. O/w microemulsions carried AP to the skin better than w/o microemulsions. Moreover, the effect of concentration on the effectiveness of AP is very important because AP can act pro-oxidatively for antioxidatively if its concentration is too low. [134]

Table 1.3 The influence of two carrier systems on the effectiveness of AP against free radical formation in UV irradiated skin at different concentration of AP (mean ± SE, $n = 5$, skin of different pigs) [134]

Samples	0.5% w/w	1.0% w/w	2.5% w/w	5.0% w/w
o/w thickened microemulsion	0.54 ± 0.05	0.46 ± 0.09	0.65 ± 0.06	0.68 ± 0.09
w/o thickened microemulsion	-0.12 ± 0.17	0.20 ± 0.09	0.40 ± 0.05	0.50 ± 0.08

In 2006, Tangsumranjit and coworkers encapsulated ascorbyl palmitate (AP) in poly(D,L-lactide) (PLA) and poly(D,L-lactide-co-glycolide) (PLGA) nanoparticles by solvent displacement method. The particles size average 115-150 nm. and zeta potential was around -30 mV for all formulations. Decreasing temperature and pHs around neutrality increased the AP stability in both PLGA and PLA nanoparticles. Moreover, AP-loaded PLA was more stable in distilled water than in diverse phosphate buffer systems and degassing of the distilled water led to the best AP protection in PLA nanoparticles when stored under atmospheric condition [135].

In 2006, Sangkil and coworker prepared ascorbyl palmitate (AsP) encapsulated in liposomes by before and after freeze-dried. Then, studied the skin penetration, stability test, and localization test. The result showed that freeze-dried liposome can pleasant AsP formulation for anti-aging, skin whitening treatment, and skin delivery [136].

In 2007, Veerawat and coworker increased the chemical stability of ascorbyl palmitate (AP) after encapsulated into nanostructure lipid carriers (NLC). The result showed that AP can improve the stability by selecting proper type of lipid, surfactant, and storage in cold temperature and flushing with nitrogen gas or inert gas. Furthermore, the degradation of AP was outdo by incorporation of antioxidants into NLC between the percentage of AP-loaded NLC remaining and the production step after keep for 3 months until more than 90% after flushing with inert gas or nitrogen gas, adding gathered antioxidants and storage at 4°C [137].

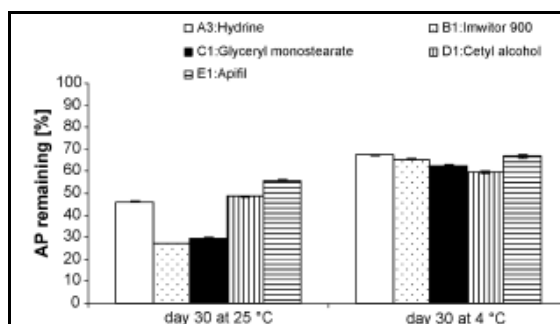


Figure 1.13 % AP remaining in NLC prepared from different types of solid lipid matrices at 25 °C and 4 °C after 1 month of storage.

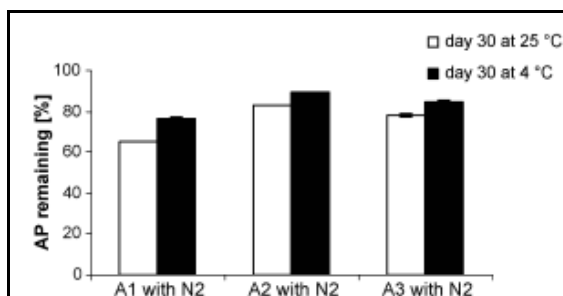


Figure 1.14 % AP remaining in degassing condition at different storage temperature (25 °C and 4 °C) at day 30.

In 2007, Veerawat and coworker studied the physicochemical properties and *in vitro* release of ascorbyl palmitate from semi-solid lipid nanoparticles based on nanostructured lipid carriers (NLC gels) systems with the purposed viscosity for dermal delivery. NLC with purposed viscosity were generated by high pressure homogenization (HPH) technique. After the production, the particle size of free-AP and AP-loaded NLC of all explicated formulations were in the colloid size range from 174 to 233 nm and polydispersity index (PI) less than 0.3. From X-ray diffraction and DSC showed that AP involved the inside structure of lipids. The release study indicated that a modified release profile could be obtained by using different kinds of lipid. Furthermore, the data from TGA supported that hot HPH technique prospered for produce physically stable AP-loaded NLC. [138]

In 2010, Wittayasuporn and coworker prepared, characterized and self-assembled poly(ethylene oxide)-4-methoxycinnamoylchitosan (PCPLC) nanoparticles for encapsulated ascorbyl palmitate (AP). The size of AP encapsulated into PCPLC gave 689 ± 0.98 nm., encapsulation efficiency is 84% and loading capacity is 56%. The particles represented no short-term cytotoxicity against the human skin melanoma A-375 cell line using the MTT assay and no short-term skin irritation on human volunteers. Moreover, aqueous suspension of PCPLC nanoparticles resisted the growth of *Escherichia coli* ATCC 25922 and *Staphylococcus aureus* ATCC 25923 [139].

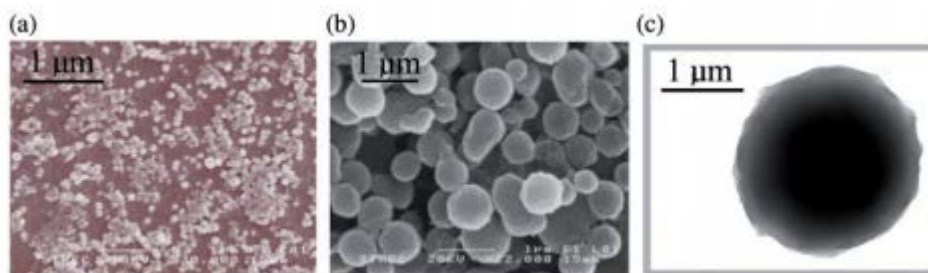


Figure 1.15 Photograph of (a) SEM image of PCPLC particles prepared by self-assembly at the polymer concentration of 600 ppm, (b) SEM image of AP-loaded PCPLC particles prepared at PCPLC concentration of 6000 ppm with the loading 56% (w/w) AP in the particles and (c) TEM image of the same AP-loaded PCPLC particle [139].

In 2010, Rangrong and coworker encapsulated ascorbyl palmitate (AP) in chitosan particles by oil-in-water emulsion, followed by ionic gelation using sodium triphosphate pentabasic (TPP) as a cross-linking agent. The morphology of AP-loaded chitosan particles that observed by SEM and TEM showed a spherical shape with an average diameter of 30-100 nm. Loading capacity (LC) and encapsulation efficiency (EE) of AP in the nanoparticles were about 8-20% and 39-73%, respectively. The amount of AP released from the nanoparticles in TPP buffer (pH~8.0) and ethanol increased with increasing LC and decreasing TPP concentration [140].

Table 1.4 Loading capacity and encapsulation efficiency of AP-loaded chitosan nanoparticles

Sample		LC ^a (%)	EE ^b (%)
CTS:AP	TPP (%)		
1:0.25	0.5	8.46	76.67
1:0.50	0.5	8.45	68.78
1:1.00	0.5	13.87	43.27
1:1.50	0.5	19.78	38.91

$$^a \text{LC} = (\text{weight of loaded AP} / \text{weight of sample}) \times 100$$

$$^b \text{EE} = (\text{weight of loaded AP} / \text{weight of AP in feed}) \times 100$$

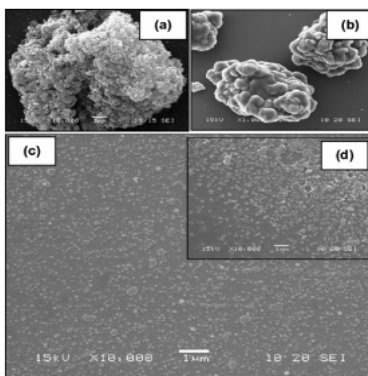


Figure 1.16 SEM micrographs at 15 kV of (a) chitosan particles (10,000x) and (b)-(d) AP-loaded chitosan particles with different CTS to AP weight ratio of 1:1.00 (100,000x) to AP weight ratios: (b) 1:1.00 (1000x), (c) 1:1.00 (10,000x) and (d) 1:1.50 (10,000x)

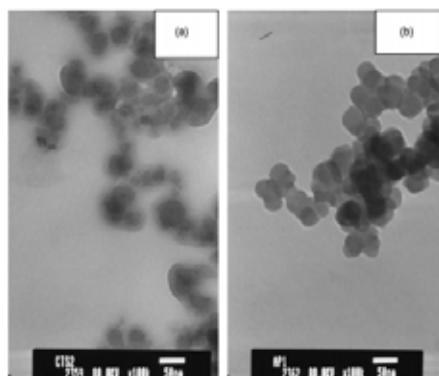


Figure 1.17 TEM micrographs at 80 kV of (a) chitosan particles 100,000X and (b) AP-loaded chitosan particles with CTS to AP weight ratios of 1:1.00 (100,000x)

1.7.4 Literature reviews about poly(vinyl alcohol)

In 2008, Luadthong and coworker prepared polymeric nanoparticle of poly(vinylalcohol-co-vinylcinnamate) from PV(OH) grafted *trans*-substituted cinnamic acid at various substitution degree. The micro/nanoparticle could be performed by dialysis with water and non-polar solvent such as hexane. Molecular weight of PV(OH) did not influence to morphology and particle size of nanoparticle. Self-assembly of the derivatives of

poly(vinylalcohol-co-vinylcinnamate) gave spherical both micellar particles and reverse micellar particles. [141]

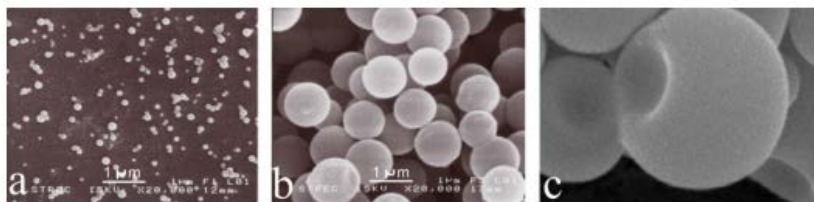


Figure 1.18 SEM photograph of poly(vinylalcohol-co-vinylcinnamate) by (a) micellar particles (dialyzed against water) and (b,c) reverse micellar particles (dialyzed against hexane) [141]

In 2009, Sheikh and coworker prepared nanoparticles (NPs) of poly(epsilon-caprolactone) (PCL) grafted poly(vinyl alcohol) (PVA) copolymer (PCL-g-PVA) to carry the hydrophilic and hydrophobic drug. Stannous octoate (Sn(II)Oct(2)) is a catalyst to increase side chain polymerization reaction for the applied epsilon-caprolactone monomer to form poly(epsilon-caprolactone) (PCL). The synthesis of grafted copolymer can self-aggregate into NPs by direct dialysis method. Moreover, in vitro drug release experiments were conducted; the loaded NPs reveal continuous and sustained release form for both drugs, up to 20 and 15 days for paclitaxel and doxorubicin, respectively. [142]

In 2009, Yufend and coworker synthesized and characterized a thermosensitive chitosan (CS)/poly(vinyl alcohol) (PV(OH)) hydrogel nanoparticles with different charge between $-N^+(CH_3)_3$ and $-COO^-$, the nanoparticles of *N*-(2-hydroxyl) propyl-3-trimethyl ammonium chitosan chloride (HTCC) and carboxymethyl chitosan (CM) for drug delivery. The electrostatic interaction of $-N^+(CH_3)_3$ and $-COO^-$ was a main factor on the formation of nanoparticles. They had monodisperse and spherical shape (average sizes, 200-300 nm) at the charge ratio of n^+/n^- . Furthermore, the rheological analysis showed that the gel strength was reduce by the formation of negative nanoparticles. [143]

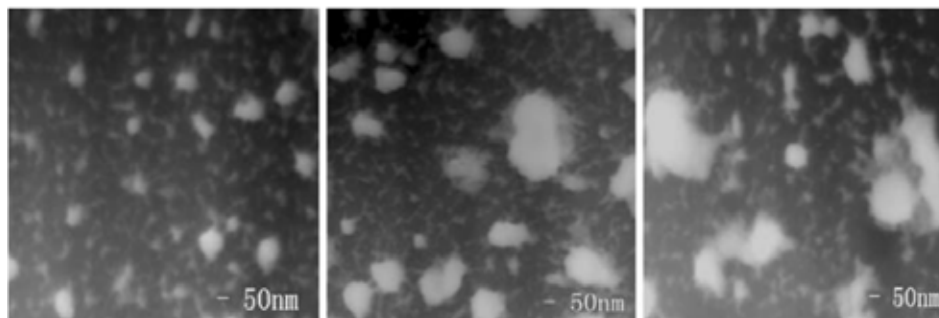


Figure 1.19 TEM of HTCC/CMCS nanoparticles (n^+/n^- , $a=1.67$; $b=1.25$; $c=1$) [143]

In 2011, Seira and coworker synthesized nanocomposites of poly(vinyl alcohol) (PV(OH))/nanodiamond (ND) by simple casting method from medium of aqueous and attained the high dispersibility of ND in the PVA(OH) matrices. The result showed that nanocomposites has superb properties acquired both ND and PVA. The thermal conductivity, the thermal properties, and the Young's modulus of nanocomposites increased 2.5 times compared with PV(OH) film with only 1% w/w of ND loading. Moreover, it was displayed that PV(OH)/ND nanocomposites remained high transparency of PV(OH) even if ND particles were provided. [144]

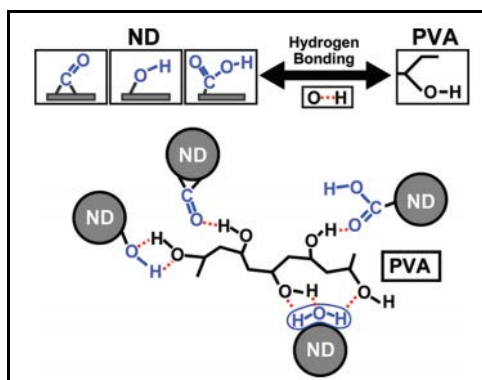


Figure 1.20 Schematic illustration of the interaction between PV(OH) and ND particles. [144]

In 2011, Semenzim and coworker synthesized a highly crystalline poly(vinyl alcohol) and poly(vinyl alcohol)/poly(vinyl acetate) microspheres for delivered drug through targeted processes and controlled rate. Crystallinity very important for the degradation of polymeric matrixes; it can involve the drug-release rate, particularly in chemoembolization. The

particles characterized by cross-polarization/magic angle spinning nuclear magnetic resonance, scanning electron microscopy (SEM), differential scanning calorimetry (DSC), and X-ray diffraction (XRD) [145].

1.8 Research objectives.

1. To synthesize and characterize curcumin-grafted poly(vinyl alcohol) and cinnamate-grafted poly(vinyl alcohol) nanoparticles.
2. To encapsulate ascorbyl palmitate (AP) into curcumin-grafted poly(vinyl alcohol) and cinnamate-grafted poly(vinyl alcohol) nanoparticles.
3. To compare the stability of AP-encapsulated curcumin-grafted poly(vinyl alcohol), AP-encapsulated cinnamate-grafted poly(vinyl alcohol), AP (together with curcumin)-encapsulated curcumin-grafted poly(vinyl alcohol), and free-AP.
4. To study skin penetration and release of the AP-encapsulated nanoparticles.
5. To compare the antioxidant activity between free-curcumin and curcumin-grafted PV(OH) nanoparticles by using DPPH radical scavenging assay.

CHAPTER II

EXPERIMENTAL

2.1 Materials and Chemicals

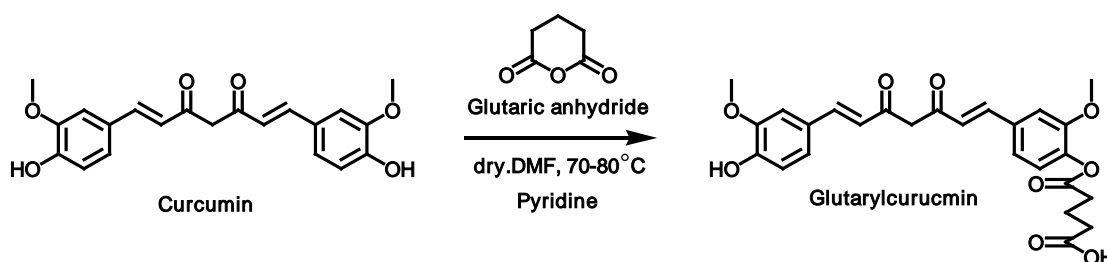
Ascorbyl palmitate (AP) was obtained from Roche (Basle, Switzerland). Poly(vinyl alcohol), MW 124,000-186,000, 87-89% deacetylated (PV(OH)), was from Aldrich Chemical Company (Steinheim, Germany). Cinnamoyl chloride, 1-ethyl-3-(3-dimethylaminopropyl) carbodiimide (EDCI) and curcumin (>98% purity) were purchased from Acros Organics (Geel, Belgium). Glutaric anhydride and hydroxybenzotriazole (HOBt) were from Aldrich Chemical Company (Steinheim, Germany). Dimethyl formamide (DMF) (RCI labscan, Bangkok, Thailand), pyridine (Carlo Ebra reagent, MI, Italy) were dry and triply distilled before use. Ethyl acetate, hexane, methanol distilled from commercial grade solvent. 1,1-Diphenyl-2-picryl-hydrazyl (DPPH) was purchased from Sigma-Aldrich (USA). Butylated hydroxytoluene (BHT) and Silica gel 60 (0.063-0.200 nm) for column chromatography were purchased from Merck KGaA (Darmstadt, Germany). Centrifugal-filtering devices (MWCO 100,000, Amicon Ultra-15) was purchased from Millipore (County cock, Ireland). Cellulose tubular membrane (CeluSep T4, MWCO 12,000-14,000, 75 mm. flatwidth, 17.9 mL/cm volume capacity, Membrane Filtration Products, Seguin, TX, USA).

2.2 Instrument and Equipments

The ATR-FT-IR spectra were obtained using a Nicolet Fourier transform Infrared spectrophotometer: Impact 410 (Nicolet Instruments Technologies, Inc., Madison, WI, USA). ¹H NMR analyses were performed using 400.00 MHz of a Varian Mercury spectrometer (Varian Company, Palo Alto, CA, USA) in deuterated chloroform (CDCl₃) or deuterated dimethylsulfoxide (DMSO-d₆). UV Absorption spectra at 200-500 nm were acquired with a UV2500 UV/vis spectrophotometer (Shimadzu Corporation, Kyoto, Japan) using a quartz cell with 1 cm path-length. Centrifugation was carried out on an Allegra™ 64R : 5000 rpm for 10 min. (Beckman Coulter, Inc, Tokyo, Japan). The particle suspension

was freeze-dried using Freeze-Dry/Shell Freeze System Model 7753501 (Labconco Corp., Kansas, MI, USA.) Transmission electron micrographs (TEM) was performed from JEM-2010 (JEOL, Tokyo, Japan) and scanning electron microscopes (SEM) was performed from JSM-6400 (JEOL, Tokyo, Japan). Confocal laser scanning fluorescence microscopy (CLFM) was measured using Nikon Digital Eclipse C1si Confocal Microscope system (Tokyo, Japan). High performance liquid chromatography (HPLC) was obtained with a ThermoFinnigan P4000 pump, connected to UV6000LP (UV/VIS detector) and 100 mm x 4.6 mm column packed with 5 μ m Hypersil C-18 reverse phase (Thermo Fisher Inc, Waltham, Massachusetts, USA).

2.3 Synthesis of mono-substituted glutarylcurcumin



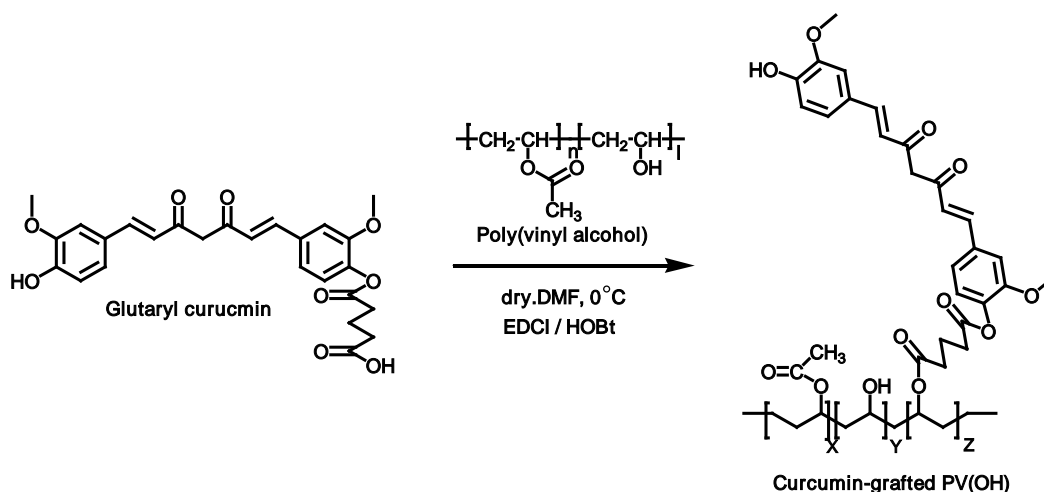
Scheme 2.1 Synthesis of mono-substituted glutarylcurcumin

The attachment of glutaryl group to the hydroxyl moiety of curcumin was carried out by reacting between curcumin and glutaric anhydride. The mono-substituted glutaryl curcumin was first prepared by reacting 1 mol equivalent of curcumin and 1.5 mol. equivalent of glutaric anhydride in a presence of 5% pyridine under dry DMF. The mixture was stirred at 70–80 °C for 4 h under $\text{N}_{2(g)}$ atmosphere. Then the solvent was evaporated and crude mixture of mono-substituted glutarylcurcumin was purified by column chromatography on silica gel column, using a 20-50% EtOAc gradient in hexane. The product obtained 76.47% yields of yellow powder. Then, product was characterized by $^1\text{H-NMR}$, FT-IR, UV-visible spectroscopic analyses.

Glutarylcurcumin: $^1\text{H-NMR}$ (CDCl_3 , 400 MHz, δ , ppm) 7.60 (Ar-CH=CH-C=O- CH_2 -C=O-CH=CH-Ar-, dd, $J = 16, 4.4$ Hz, 2H), 6.92-7.16 (Ar-H, m, 6H), 6.47-6.57 (Ar-CH=CH-C=O- CH_2 -C=O-CH=CH-Ar-, d, $J = 16$ Hz, 2H), 5.83 (-C=O-CH $_2$ -C=O-, s, 1H), 5.81 (-C=O-CH $_2$ -C=O-, s, 1H), 5.80 (-C=O-CH $_2$ -C=O-, s, 1H), 3.94 (CH $_3$ -O-Ar-O-C=O-

CH₂-CH₂-, s, 3H), 3.87 (CH₃-O-Ar-O-H, s, 3H), 2.70 (-Ar-O-C=O-CH₂-CH₂-, t, J = 7.2 Hz, 2H), 2.57 (HO-C=O-CH₂-CH₂-, t, J = 7.2 Hz, 2H) and 2.11 (-C=O-CH₂-CH₂-CH₂-C=O-OH, p, J = 7.2 Hz, 2H); UV-visible spectroscopy (DMSO) λ_{max} at 412 nm; FT-IR (cm⁻¹) C-H stretching at 2918.12 cm⁻¹, C=O stretching of the ester functionality at ~1705.54 cm⁻¹, C=C stretching at 1624.84 cm⁻¹, C=O of keto-enol at 1567.48 and C-H bending at 1201.19.

2.4 Synthesis of curcumin-grafted poly(vinyl alcohol), Cur-PV(OH)

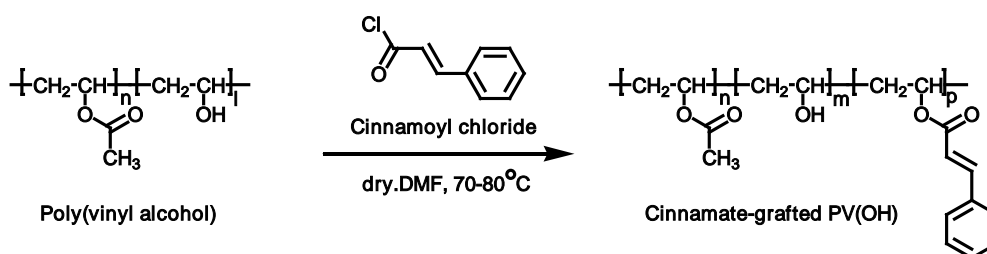


Scheme 2.2 Synthesis of Cur-PV(OH)

The Cur-PV(OH) was synthesized by esterification reaction between mono-substituted glutarylcurcumin and poly(vinyl alcohol) or PV(OH). The mono-substitute glutarylcurcumin was activated by EDCI (0.05 g, 3 mol. equivalent of glutarylcurcumin), then, the compound was coupled with PV(OH) (0.09 g, 20 mol. equivalent of glutaryl curcumin) using HOBt (0.06 g, 4 mol. equivalent of glutaryl curcumin) as a catalyst. The reaction was carried out in dry DMF at 0 °C for 24 h under N_{2(g)} atmosphere. EDCI and HOBt were eliminated by dialyzing the reaction mixture against 40% aqueous methanol for five times using a regenerated cellulose tubular membrane (CeluSep T4 dialysis tube (MWCO 12,000-14,000, 75 mm. flatwidth, 17.9 ml/cm volume capacity, Membrane Filtration Products, Seguin, TX, USA.) Dry particles were obtained by freeze drying the aqueous suspension. Product was then subjected to ¹H-NMR, FT-IR and UV-visible spectroscopic analyses. The degree of curcumin substitution on PV(OH) backbone was estimated from ¹H NMR information.

Cur-PV(OH): $^1\text{H-NMR}$ (DMSO, 400 MHz, δ , ppm) 7.54 (Ar- $\underline{\text{C}}\text{H}=\text{CH}-\text{C}=\text{O}-\text{CH}_2-\text{C}=\text{O}-\text{CH}=\underline{\text{C}}\text{H}-\text{Ar}$ -, d, $J = 13$ Hz, 2H), 6.82-7.32 (Ar- $\underline{\text{H}}$, m, 6H), 6.75 (Ar- $\text{CH}=\underline{\text{C}}\text{H}-\text{C}=\text{O}-\text{CH}_2-\text{C}=\text{O}-\underline{\text{C}}\text{H}=\text{CH}-\text{Ar}$ -, d, $J = 15$ Hz, 2H), 6.14 ($-\text{C}=\text{O}-\underline{\text{C}}\text{H}_2-\text{C}=\text{O}-$, s, 1H), 6.06 ($-\text{C}=\text{O}-\underline{\text{C}}\text{H}_2-\text{C}=\text{O}-$, s, 1H), 6.02 ($-\text{C}=\text{O}-\underline{\text{C}}\text{H}_2-\text{C}=\text{O}-$, s, 1H), 4.54 ($-\underline{\text{C}}\text{H}_2-\text{CH}-\text{OH}$ -, s, 1H), 4.17 ($-\underline{\text{C}}\text{H}_3-\text{Ar}-\text{H}$, s, 6H), 3.82 ($-\text{CH}_2-\underline{\text{C}}\text{H}-\text{OH}$) $_m$ - $(\text{CH}_2-\underline{\text{C}}\text{H}-\text{O}-\text{C}=\text{O}-\text{CH}_3)$ $_n$, br, 1H), 2.70 ($-\text{Ar}-\text{O}-\text{C}=\text{O}-\underline{\text{C}}\text{H}_2-\text{CH}_2-$, t, $J = 7.2$ Hz, 2H), 2.61 ($\text{HO}-\text{C}=\text{O}-\underline{\text{C}}\text{H}_2-\text{CH}_2-$, t, $J = 7.2$ Hz, 2H), 2.23 ($-\text{C}=\text{O}-\text{CH}_2-\underline{\text{C}}\text{H}_2-\text{CH}_2-\text{C}=\text{O}-\text{OH}$, p, $J = 7.2$ Hz, 2H), 1.93 ($-\text{CH}_2-\text{CH}-\text{OH}$) $_m$ - $(\text{CH}_2-\text{CH}-\text{O}-\text{C}=\text{O}-\underline{\text{C}}\text{H}_3)$ $_n$, s, 3H) and 1.22-1.74 ($-\underline{\text{C}}\text{H}_2-\text{CH}-\text{OH}$) $_m$ - $(\underline{\text{C}}\text{H}_2-\text{CH}-\text{O}-\text{C}=\text{O}-\text{CH}_3)$ $_n$ - $(\underline{\text{C}}\text{H}_2-\text{CH})$ $_o$, br, 2H); UV-visible spectroscopy (DMSO) λ_{max} at 402.5 nm; FT-IR (cm^{-1}) O-H stretching at 3422.34, C-H stretching at 2923.23, C=O stretching of the ester functionality at ~ 1735.56 and C=C stretching at 1629.27.

2.5 Synthesis of cinnamate-grafted poly(vinyl alcohol), Cin-PV(OH)



Scheme 2.3 Synthesis of Cin-PV(OH)

The Cin-PV(OH) was synthesized according to method of Luadthong *et al*, 2008. Briefly, PV(OH) (0.40 g, 9 mmol monomeric units) was dissolved in heated anhydrous DMF (20 mL). Then, pyridine (0.73 ml, 9 mmol) was added. The obtained clear solution was poured into a round bottom flask containing the freshly prepared cinnamoyl chloride (4.00 g, 9 mmol). The mixture was stirred at 80–90 °C for 2-3 h. The substituted polymer was separated by precipitation with 1.0% w/v aq. Na_2CO_3 . The precipitate was washed with distilled water and the obtained solid was dried under vacuum to constant weight. Product was then subjected to $^1\text{H-NMR}$, UV-Visible spectrophotometric and FT-IR spectroscopic analyses. The degree of curcumin substitution on PV(OH) backbone was estimated from ^1H NMR information.

Cin-PV(OH): $^1\text{H-NMR}$ (DMSO, 400 MHz, δ , ppm) 7.68 (Ar- $\underline{\text{C}}\underline{\text{H}}=$, br), 7.57 (Ar- $\underline{\text{H}}$, br), 7.39 (Ar- $\underline{\text{H}}$, br), 6.53 ($=\underline{\text{C}}\underline{\text{H}}-\text{COOR}$, br), 4.67, 4.46 and 4.22 ($-\text{O}\underline{\text{H}}$, s), 3.86 ($-\underline{\text{C}}\underline{\text{H}}-\text{OCOCH}_3$, br), 3.81 ($-\underline{\text{C}}\underline{\text{H}}-\text{OH}$, br) and 1.14-2.31 ($-\underline{\text{C}}\underline{\text{H}}_3-\text{CO}$ and $-\text{CH}-\underline{\text{C}}\underline{\text{H}}_2-\text{CH}-$, br of PV(OH) backbone); UV-visible spectroscopy (DMSO) λ_{max} at 279 nm; FT-IR (cm^{-1}) O-H stretching at 3431.58, C-H stretching at 3024.90, C=O stretching of the ester functionality at \sim 1710 and C=C stretching at 1629.27.

2.6 Encapsulation of AP into polymeric nanoparticles

Two types of polymeric nanoparticles, Cur-PV(OH) and Cin-PV(OH), were induced at room temperature by solvent displacement method by using dialysis technique.

For Cur-PV(OH), polymer (30 mg) was dissolved in DMF (10 mL) to get polymeric solution at concentration of 3,000 ppm. In a separate container, 15 mg of AP were dissolved in 10 mL of DMF to get AP solution at concentration of 1,500 ppm (Table 2.1). The two solutions were then mixed together and the obtained mixture solution of polymer and loaded chemicals (AP) was then transferred into the dialysis bag (regenerated cellulose tubular membrane (CeluSep T4 dialysis tube (MWCO 12,000-14,000, 75 mm. flatwidth, 17.9 mL/cm volume capacity, Membrane Filtration Products, Seguin, TX, USA) and dialyzed against 1,000 mL deionized water. Five mL of each obtained particle suspension was centrifugally filtered using centrifugal-filtering devices with MWCO 10,000 (Amicon Ultra-15, Millipore, Ireland) at 5,000 rpm for 10 min. The filtered product was very quickly rinsed with methanol to remove all the unencapsulated AP molecules.

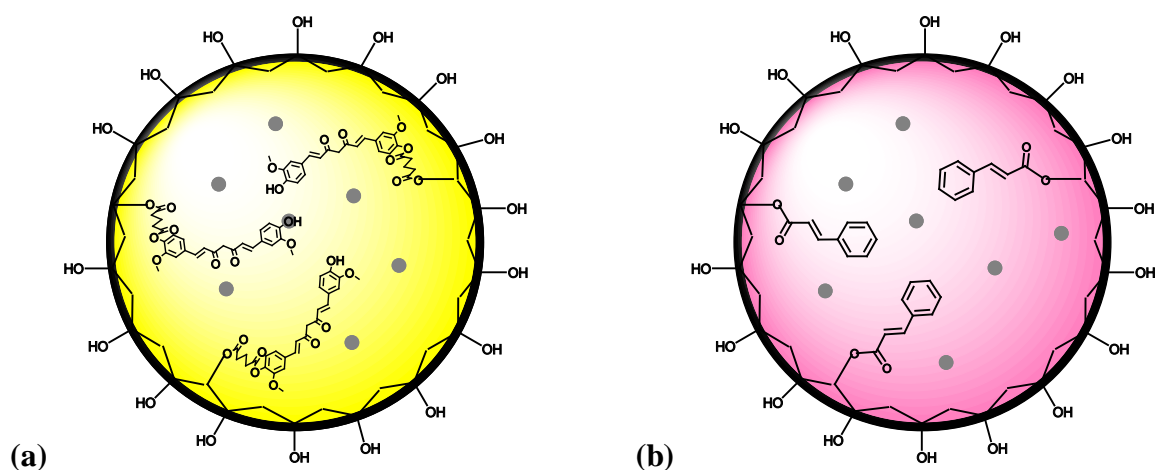
For Cin-PV(OH), polymer (30 mg) was dissolved in DMF (10 mL) to get polymeric solution at concentration of 3,000 ppm. In a separate container, 15 mg of AP (alone or together with 15 mg of curcumin) were dissolved in 10 mL of DMF to get AP solution at concentration of 1,500 ppm (Table 2.1). The two solutions were then mixed together and the obtained mixture solution of polymer and loaded chemicals (AP alone or AP and curcumin) was then transferred into the dialysis bag (regenerated cellulose tubular membrane (CeluSep T4 dialysis tube (MWCO 12,000-14,000, 75 mm. flatwidth, 17.9 mL/cm volume capacity, Membrane Filtration Products, Seguin, TX, USA) and dialyzed against 1,000 ml deionized water. Five mL of each obtained particle suspension was centrifugally filtered using

centrifugal-filtering devices with MWCO 10,000 (Amicon Ultra-15, Millipore, Ireland) at 5,000 rpm for 10 min. The filtered product was very quickly rinsed with methanol to remove all the unencapsulated AP (alone or together with curcumin) molecules.

The expected outcome of model of AP-Cur-PV(OH), AP-Cin-PV(OH) and APCur-Cin-PV(OH) nanoparticles showed in Figure 2.1(a), Figure 2.1(b) and Figure 2.1 (c), respectively.

Table 2.1 Concentration (ppm) of polymer (Cur-PV(OH) and Cin-PV(OH)) and active (AP and AP together with curcumin)

Types	Concentration of polymer (ppm)	Concentration of AP (ppm)	Concentration of curcumin (ppm)
Cur-PV(OH)	3,000	1,500	-
Cin-PV(OH)	3,000	1,500	-
Cin-PV(OH)	3,000	1,500	1,500



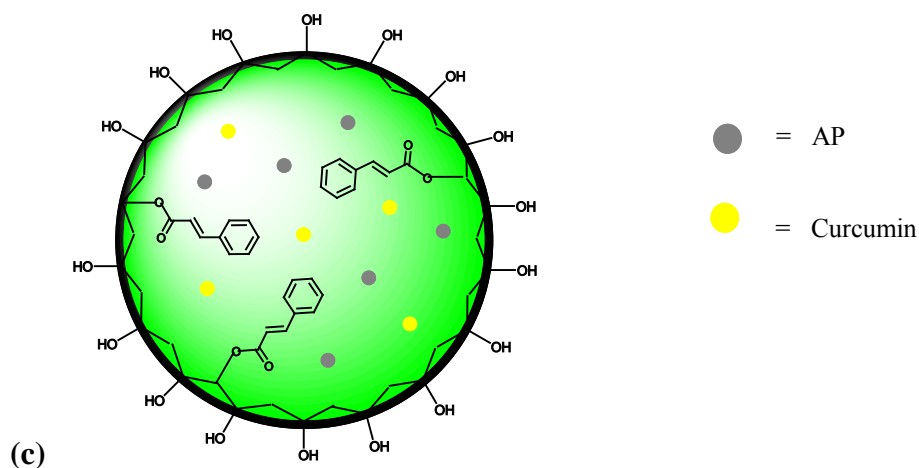


Figure 2.1 Model of (a) AP-Cur-PV(OH), (b) AP-Cin-PV(OH) and (c) APCur-Cin-PV(OH)

The obtained supernatant was analyzed by HPLC to get the concentration of unencapsulated active chemicals (AP/curcumin). The encapsulation efficiency and loading was calculated according to the following equations:

$$\% \text{ Encapsulation efficiency (\%EE)} = \frac{\text{Weight of encapsulated AP} \times 100}{\text{Weight of AP used}}$$

$$\% \text{ Loading} = \frac{\text{Weight of encapsulated AP} \times 100}{\text{Weight of polymer used}}$$

HPLC was performed with a ThermoFinnigan P4000 (pump), connected to a UV6000LP (UV/VIS detector). The stationary phase was 100 mm×4.6 mm column packed with Hypersil C-18 and the mobile phase was methanol : acetonitrile : 0.02 M phosphate buffer pH 2.5 (75 : 10 : 15). The flow rate was set at 1.5 ml/min and the detection by UV detection at 254 nm.

2.7 Morphology and particle size of AP-encapsulated nanoparticles

The morphology and particle size of AP-encapsulated polymeric nanoparticles were elucidated by scanning electron microscope (SEM) and transmission electron microscope (TEM).

SEM photographs were acquired by scanning electron microscope (JEM-6400, JEOL, Tokyo, Japan). A drop of nanoparticles suspension was placed on a glass slide and dried in desiccators overnight. The sample was coated with a gold layer under vacuum at 15 kV about 90 s. Analysis was carried out at $25\pm 2^\circ\text{C}$.

TEM photographs were obtained by transmission electron microscope (JEM-2100, JEOL, Tokyo, Japan). Observation was presented at 100-120 kV.

Each instrument was repeated three times and average value was reported.

2.8 Stability of AP

The stability study of the encapsulated-AP (and curcumin) and the free-AP were carried out under solid condition using freeze-dried samples and also under aqueous suspension condition.

Stability test on the solid product was carried out as follows. Three freeze-dried, AP-encapsulated curcumin-grafted PV(OH), (AP-Cur-PV(OH)), AP-encapsulated cinnamate-grafted PV(OH), (AP-Cin-PV(OH)), AP (together with curcumin)-encapsulated cinnamate-grafted PV(OH), (APCur-Cin-PV(OH)) and free-AP were kept at room temperature for 60 days under normal light and under light-proof conditions. At various time intervals, 5 mg of each sample were subjected to AP extraction and quantitation. Briefly, 5 mL of methanol were added and stirred to extract out the AP (and curcumin), then the mixture was centrifugally filtered (MWCO 100,000, Amicon Ultra-15, Millipore, Ireland). The obtained solid was soaked in methanol, sonicated, filtered and the methanol extract was quantitatively analysed for AP content by HPLC.

Stability test on the aqueous product was carried out as follows. Three freeze-dried, AP-Cur-PV(OH), AP-Cin-PV(OH), APCur-Cin-PV(OH), and free-AP were kept at room temperature for 24 hours under normal light and under light-proof conditions. At various time intervals, 5 mL of each freshly prepared suspension of AP (and curcumin)-encapsulated nanoparticles (AP concentration is 1,000 ppm), as well as 1,000 ppm of free-AP solution for comparison. At various time intervals, 5 mL of aliquot was withdrawn and centrifugally

filtered (MWCO 100,000, Amicon Ultra-15, Millipore, Ireland). Then, analysed for AP content by HPLC.

2.9 *Ex vivo* skin penetration by using confocal laser scanning fluorescence microscopy (CLFM)

The skin specimens (pig ear skin) of the fresh six month-old pig were purchased from Manoch Farm (Phetchabun, Thailand) that consisted of epidermis and dermis layers and cut about $1 \times 2 \text{ cm}^2$ pieces.

The experiment was started by dropping 10 μL of the AP-encapsulated curcumin-grafted PV(OH) suspension (1,430 ppm of curcumin-grafted PV(OH) and 705 ppm of AP) onto the surface of fresh pig ear skin piece ($1 \times 2 \text{ cm}^2$ area), thus to give the coverage of $\sim 3.52 \mu\text{g}/\text{cm}^2$ AP and $\sim 7.15 \mu\text{g}/\text{cm}^2$ polymer. Then, rolled the AP-encapsulated curcumin-grafted PV(OH) suspension with roller for 10 minutes and kept at room temperature for 30 minutes before being subjected to Confocal laser scanning fluorescence microscopy (CLFM) analysis. The CLFM system used was a Nikon Digital Eclipse C1-Si (Tokyo, Japan) equipped with Plan Apochromat VC 100x, Diode Laser and Ar Laser (405 nm and 488 nm, respectively, Melles Groit, Carlsbad, CA, USA), a Nikon TE2000-U microscope, a 32-channel-PMT-spectral-detector and Nikon EZ-C1 Gold Version 3.80 software. CLFM was used to capture the fluorescent signals of the curcumin-grafted PV(OH) nanoparticles moieties together with the released AP in the skin piece. Excitation was carried out at 405 and 488 nm while detection was done spectrally at 405-750 nm were collected from the sample piece, at various depth starting from 40 μm (from the stratum corneum surface) down to 400 μm depth. Then, unmixed the fluorescent spectrum of curcumin-grafted PV(OH) nanoparticles, AP and fresh pig ear skin with red, green and grey colors, respectively.

2.10 DPPH[•] free radical scavenging activity

The total radical scavenging capacity of the tested compounds was defined and compared to that of BHT, curcumin and Cur-PV(OH) by using the DPPH[•] radical scavenging methods. The hydrogen atom or electron donation abilities of some pure compounds were measured by the bleaching of a purple colored methanol solution of the stable DPPH radical.

This spectrophotometric assay uses the stable radical, 1,1-diphenyl-2-picryl-hydrazyl (DPPH[•]), as a reagent.

DPPH[•] scavenging activity was measured according to method of Khajeelak, 2010. Briefly, prepared 11.8 mg/100 mL of DPPH and 1 mg/1 mL sample solutions of BHT, free curcumin and curcumin-grafted PV(OH) in methanol. Next, added 50 μ L of each sample solutions in a 96-well plate. Then, added 250 μ L of DPPH solution mixed together with each sample solutions. These solutions were vortexed thoroughly and incubated at room temperature in the dark for 30 minutes. Absorbance spectra by UV-visible spectrophotometry of the test mixture was read at 515 nm against blank samples (methanol) lacking scavenger. Residual DPPH free radicals were determined from the absorbance.

The capability to scavenge the DPPH[•] radical was calculated by comparing the results of the test with those of the control using the formula:

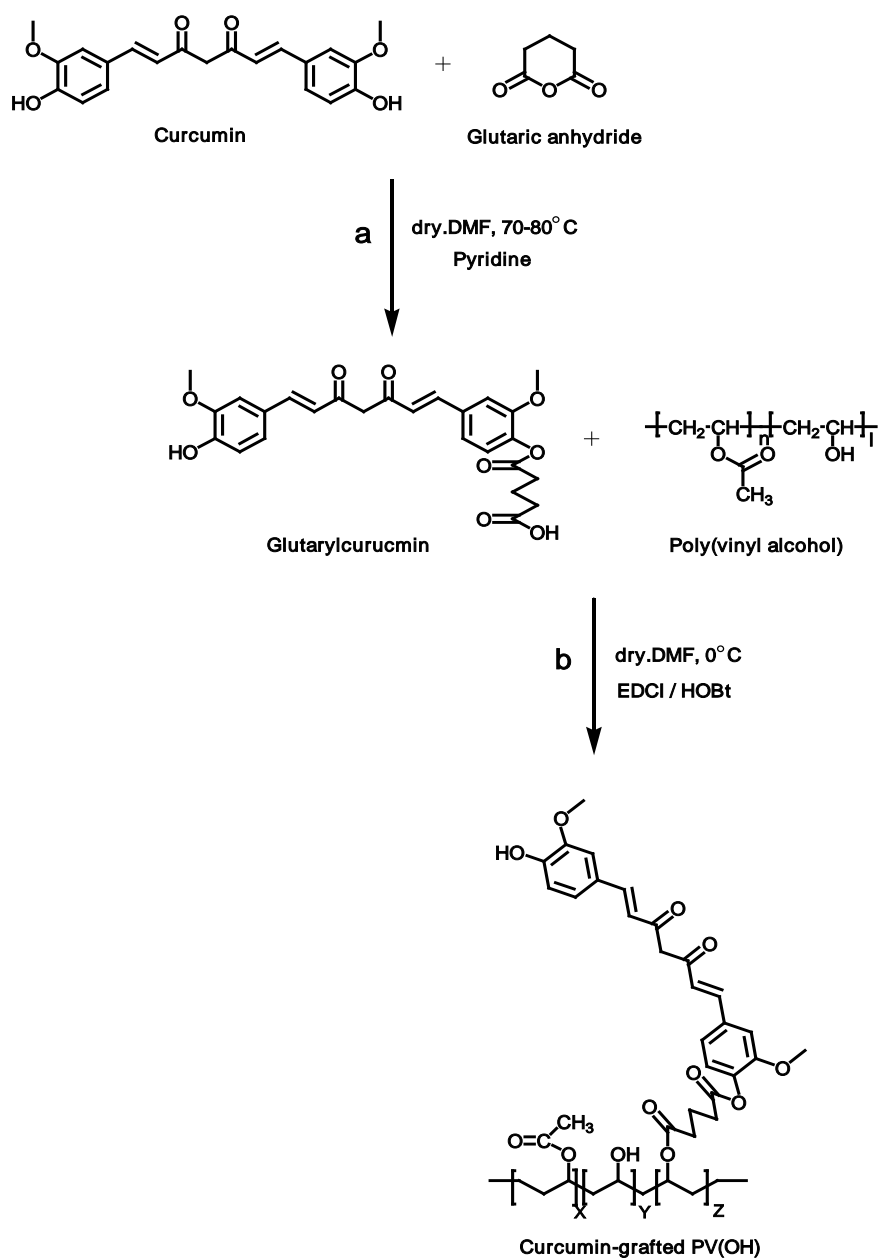
$$\% \text{ Inhibition} = \frac{\text{Absorbance of control} - \text{Absorbance of test}}{\text{Absorbance of control}} \times 100$$

DPPH[•] decreases significantly upon exposure to radical scavengers.

CHAPTER III

RESULTS AND DISCUSSION

3.1 Synthesis and characterization

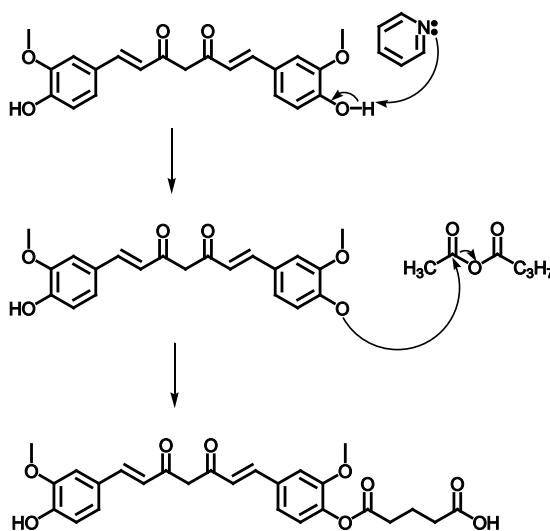


Scheme 3.1 Synthesis of (a) mono-substituted glutarylcurcumin and (b) Cur-PV(OH)

The Cur-PV(OH) was synthesized by first esterification curcumin with glutaric anhydride, then grafting the obtained glutarylcurcumin onto the hydroxyl groups of the PV(OH) via ester linkage.

3.1.1 Synthesis of mono-substituted glutarylcurcumin

The preparation of mono-substituted glutarylcurcumin was carried out according to Scheme 3.1 (a). Mono-substituted glutarylcurcumin was successfully synthesized using esterification between hydroxyl group of curcumin and carbonyl group of glutaric anhydride. Hydroxyl groups of curcumin were deprotonated by pyridine and carbonyl groups of glutaric anhydride reacted as nucleophiles to form ester bonds. The mechanism is shown in Scheme 3.2



Scheme 3.2 Mechanism of ester bond formation in mono-substituted glutarylcurcumin.

In this step, mole ratios between curcumin and glutaric anhydride affected the yield of mono-substituted product, therefore, various mole ratios of curcumin : glutaric anhydride were experimented (Table 3.1)

Table 3.1 The mole ratios of curcumin : glutaric anhydride

Molar ratios curcumin : glutaric anhydride	% yield of mono-substitution product
1 : 1.2	43.25
1 : 1.5	76.47
1 : 2.0	50.06

Mole ratios of curcumin : glutaric anhydride of 1 : 1.5 gave the highest yields (76.47%) of the mono-substituted glutarylcurcumin (Table 3.1). The crude from reaction was purified by silica gel column chromatography using 20-50% EtOAc gradient in hexane to gain the pure mono-substituted glutarylcurcumin as yellow powder. Identification of the product was attained through FT-IR, ¹H-NMR and UV-visible spectroscopy.

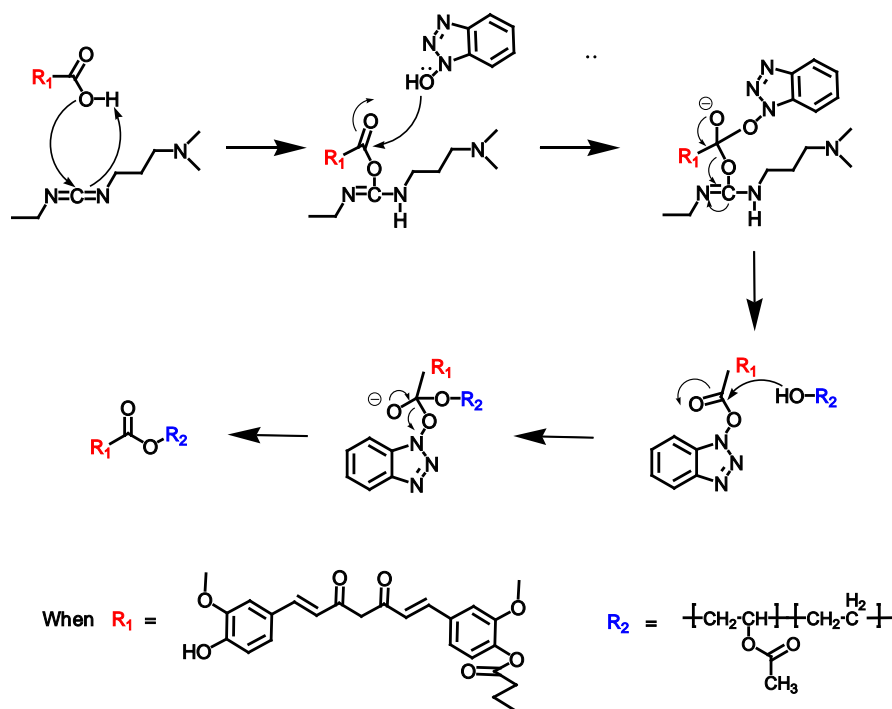
Curcumin: ¹H-NMR (CDCl₃, 400 MHz, δ, ppm) 6.92-7.13 (Ar-H), 7.61 (Ar-CH=), 6.46-6.49 (=CHC(O)-), and 5.80-5.89 (-C(O)CHC(O)-)

When comparing the ¹H-NMR spectrum of mono-substituted glutarylcurcumin (Figure 3.2) to that of the curcumin (Figure 3.1), it is apparent that the signals of methoxy proton (H_{h,h'}) of mono-substituted glutarylcurcumin are splitted into two-singlet peaks at a ratio of H_h : H_{h'} = 1 : 1 (comparing to one singlet peak of methoxy of unmodified curcumin). In addition, instead of 3 sets of aromatic protons observed in curcumin, 6 sets of aromatic protons were observed in the product. Also, instead of two sets of protons from the double bond next to aromatic ring observed in the curcumin, the product showed four sets of such protons and thus confirming the derivatization of just only one side of the molecules.

3.1.2 Synthesis of Cur-PV(OH)

The synthesis pathway of Cur-PV(OH) is shown in Scheme 3.1 (b). The carboxylic group of mono-substituted glutarylcurcumin was reacted with 1-ethyl-3-(3-dimethylaminopropyl) carbodiimide (EDCI) to form O-acyl isourea, which have higher reactivity than the free acid. This intermediate will react with hydroxybenzotriazole (HOBT) to generate the reactive amide intermediate, which can rapidly react with hydroxyl group of

PV(OH) without side product from intramolecular reaction. From this reaction, product is a yellow powder.



Scheme 3.3 Mechanism of synthesis of Cur-PV(OH)

Glutarylcurcumin: $^1\text{H-NMR}$ (CDCl_3 , 400 MHz, δ , ppm) 7.60 (Ar- $\underline{\text{C}}\text{H}=\text{CH}-\text{C}=\text{O}-\text{CH}_2-\text{C}=\text{O}-\text{CH}=\underline{\text{C}}\text{H}-\text{Ar}$ -, dd, $J = 16, 4.4$ Hz, 2H), 6.92-7.16 (Ar- $\underline{\text{H}}$, m, 6H), 6.47-6.57 (Ar- $\text{CH}=\underline{\text{C}}\text{H}-\text{C}=\text{O}-\text{CH}_2-\text{C}=\text{O}-\underline{\text{C}}\text{H}=\text{CH}-\text{Ar}$ -, d, $J = 16$ Hz, 2H), 5.83 ($-\text{C}=\text{O}-\underline{\text{C}}\text{H}_2-\text{C}=\text{O}-$, s, 1H), 5.81 ($-\text{C}=\text{O}-\underline{\text{C}}\text{H}_2-\text{C}=\text{O}-$, s, 1H), 5.80 ($-\text{C}=\text{O}-\underline{\text{C}}\text{H}_2-\text{C}=\text{O}-$, s, 1H), 3.94 ($\underline{\text{C}}\text{H}_3-\text{O}-\text{Ar}-\text{O}-\text{C}=\text{O}-\text{CH}_2-\text{CH}_2-$, s, 3H), 3.87 ($\underline{\text{C}}\text{H}_3-\text{O}-\text{Ar}-\text{O}-\text{H}$, s, 3H), 2.70 ($-\text{Ar}-\text{O}-\text{C}=\text{O}-\underline{\text{C}}\text{H}_2-\text{CH}_2-$, t, $J = 7.2$ Hz, 2H), 2.57 ($\text{HO}-\text{C}=\text{O}-\underline{\text{C}}\text{H}_2-\text{CH}_2-$, t, $J = 7.2$ Hz, 2H) and 2.11 ($-\text{C}=\text{O}-\text{CH}_2-\underline{\text{C}}\text{H}_2-\text{CH}_2-\text{C}=\text{O}-\text{OH}$, p, $J = 7.2$ Hz, 2H)

The $^1\text{H-NMR}$ spectrum of the Cur-PV(OH) (Figure 3.3) showed the signals of PV(OH) backbone between 1.22-1.74 ppm ($-\underline{\text{C}}\text{H}_2-\text{CH}-\text{OH}-$) $_m$ -($\underline{\text{C}}\text{H}_2-\text{CH}-\text{O}-\text{C}=\text{O}-\text{CH}_3$) $_n$ -($\underline{\text{C}}\text{H}_2-\text{CH}-$) $_o$, br, 2H) and signals of 6.92-7.13 ppm (Ar- $\underline{\text{H}}$) of curcumin.

The degree of curcumin substitution on PV(OH) is 5.9 % (Figure 3.3), as deduced from the integration of peaks from 1.22-1.74 ppm (PV(OH) backbone $-\underline{\text{C}}\text{H}_2-\text{CH}-\text{OH}-$) $_m$ -

$(\underline{\text{C}}\text{H}_2\text{-CH-O-C=O-CH}_3)_n\text{-(}\underline{\text{C}}\text{H}_2\text{-CH-C=O-R-)}_o$, br, 2H) against the two singlet peaks at 6.08 ppm (curcumin $\text{-C=O-}\underline{\text{C}}\text{H}_2\text{-C=O-}$, 2H)

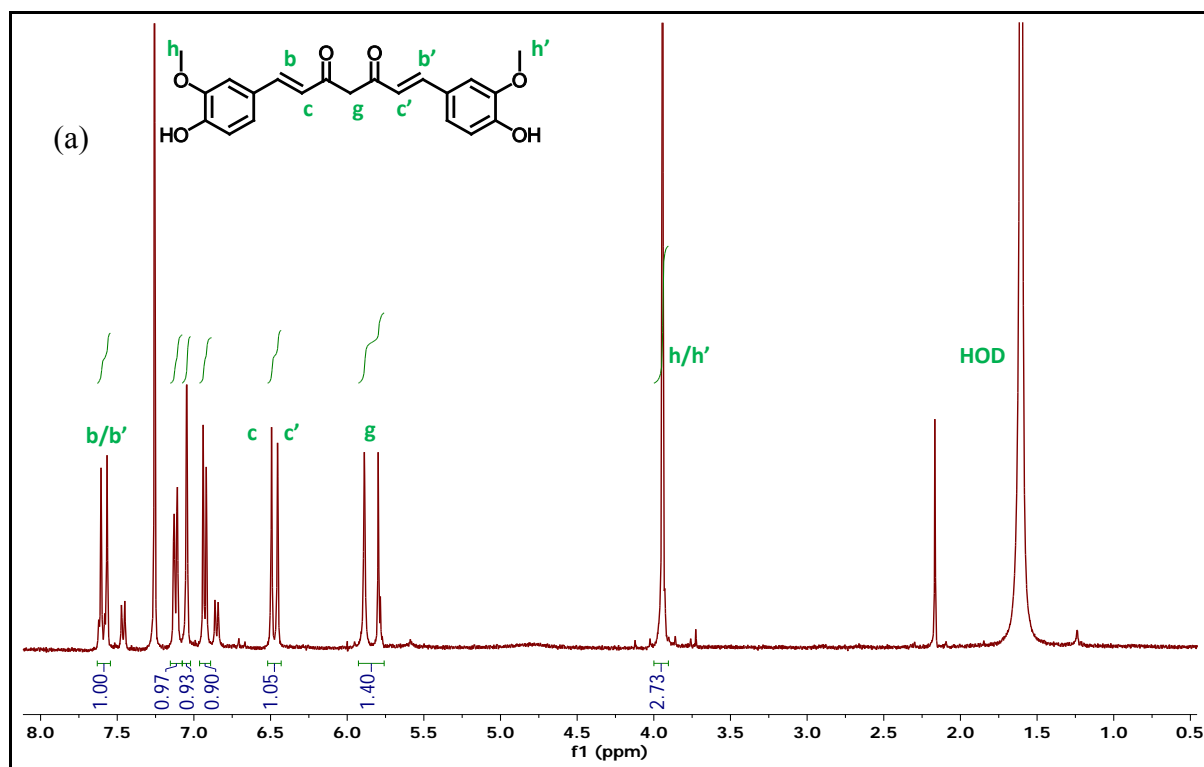


Figure 3.1 $^1\text{H-NMR}$ spectrum of curcumin in CDCl_3

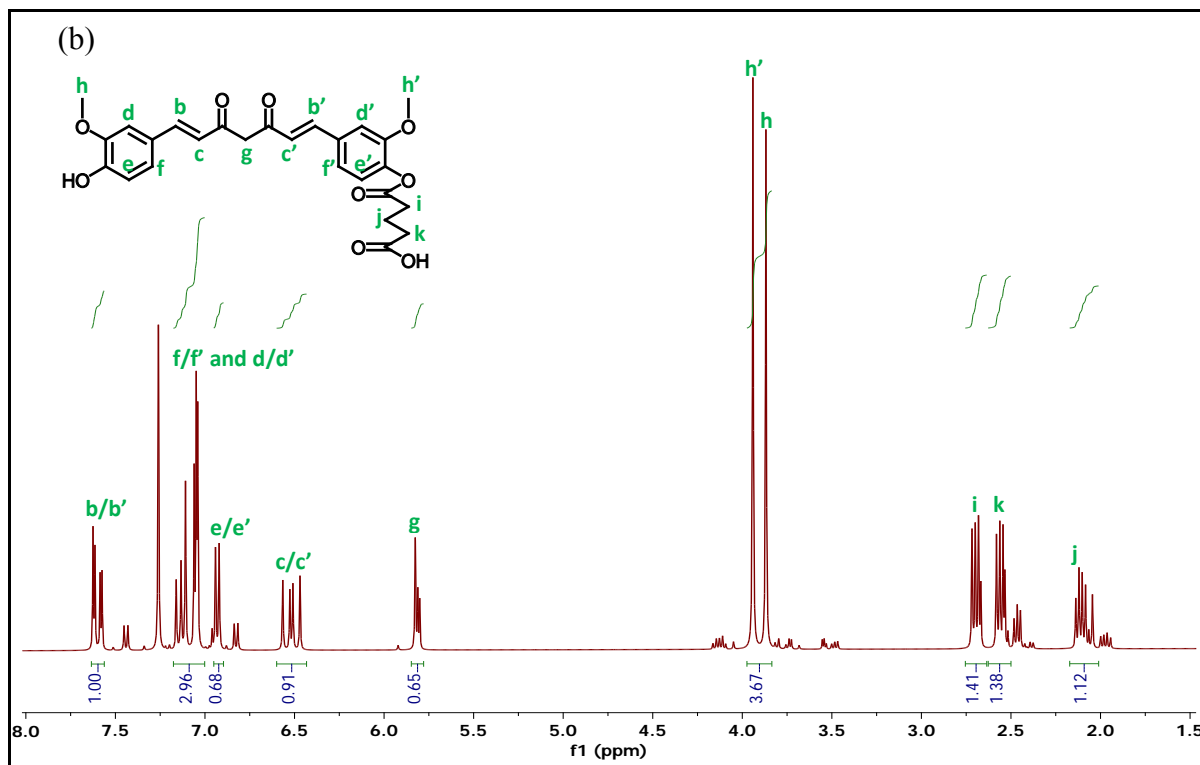


Figure 3.2 $^1\text{H-NMR}$ spectrum of mono-substituted glutarylcurcumin in CDCl_3

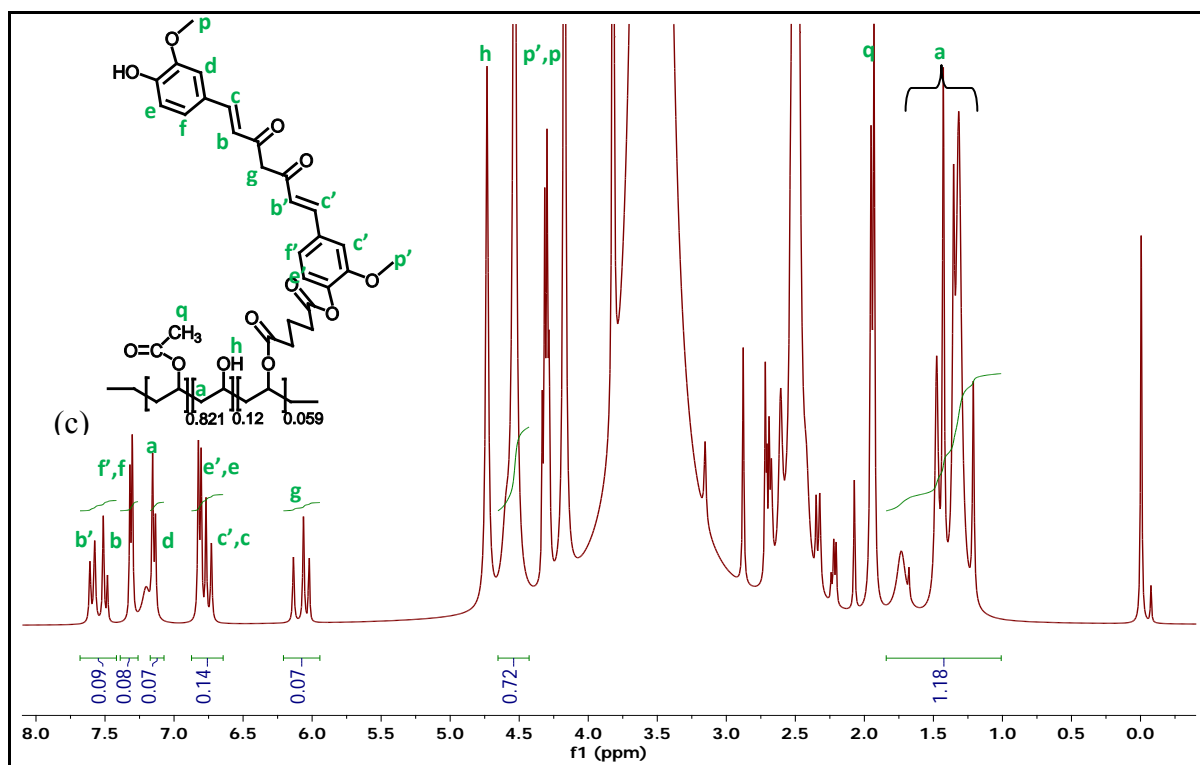


Figure 3.3 $^1\text{H-NMR}$ spectrum of Cur-PV(OH) in DMSO-d_6

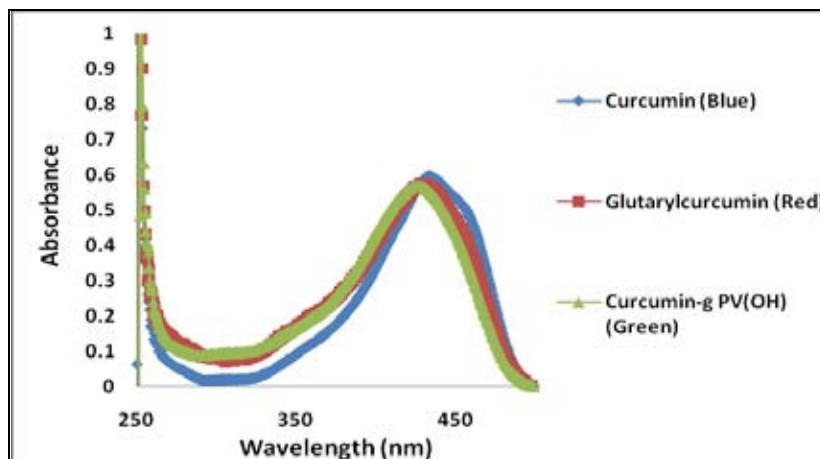


Figure 3.4 UV-visible spectra of curcumin (blue), mono-substituted glutarylcurcumin (red) and Cur-PV(OH) (green) nanoparticles in DMSO

The solutions of curcumin (blue), mono-substituted glutarylcurcumin (red) and Cur-PV(OH) (green) in DMSO showed a broad characteristic UV-visible absorption spectra around 250-500 nm. UV-visible absorption spectra showed λ_{\max} of curcumin, mono-substituted glutarylcurcumin, Cur-PV(OH) and Cin-PV(OH) at 428, 412 and 402.5, respectively (Figure 3.4). Maximum absorption of mono-substituted glutarylcurcumin and Cur-PV(OH) is blue-shifted from that of curcumin. The blue-shift indicated less conjugation in the curcumin core structure resulting from the replacement of hydroxyl group with acyl groups.

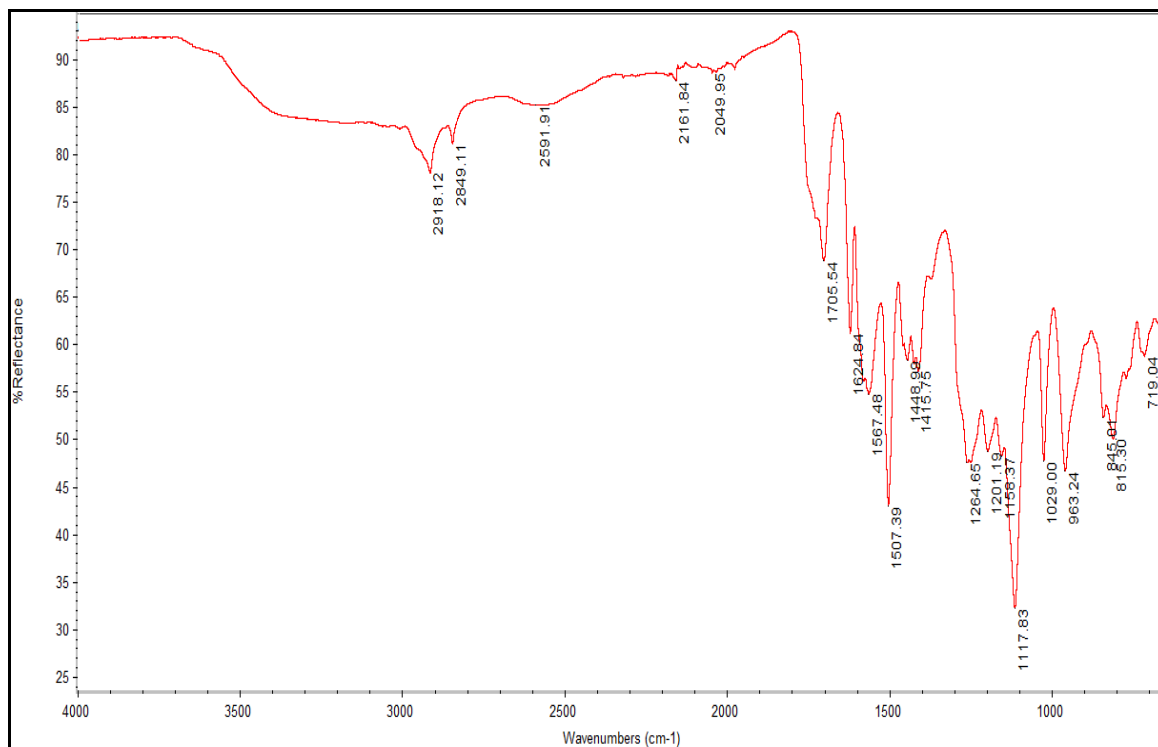


Figure 3.5 FT-IR spectrum of mono-substituted glutarylcurcumin

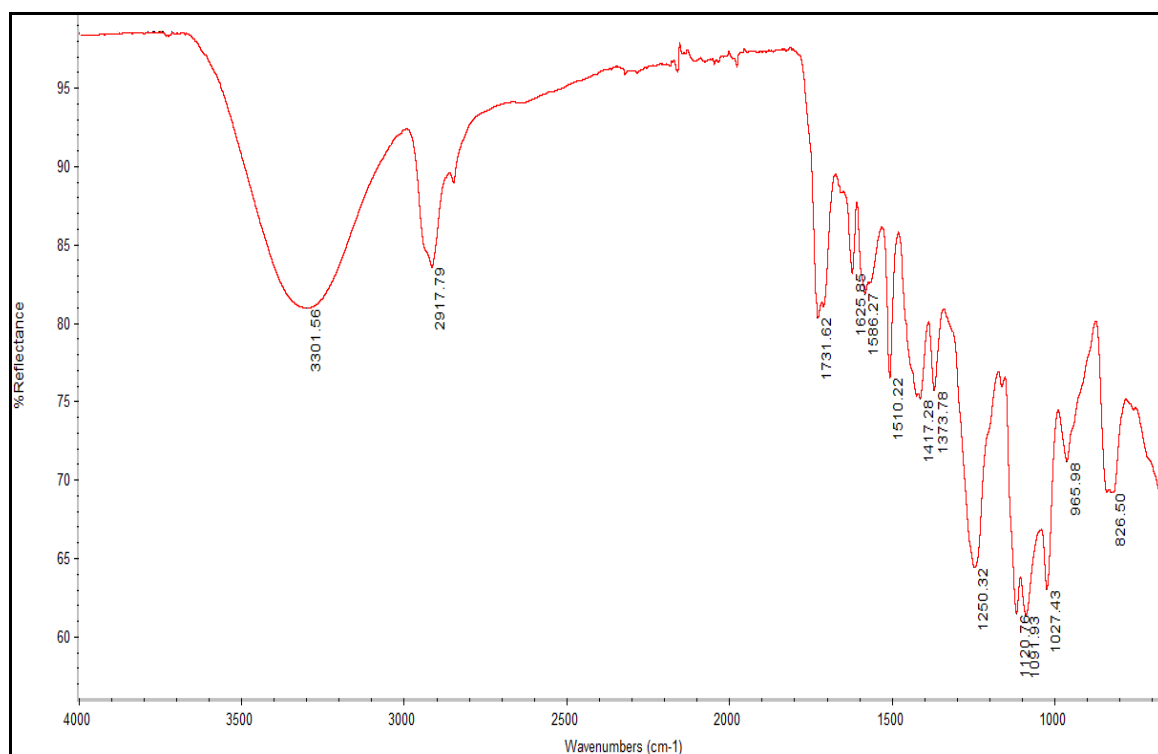
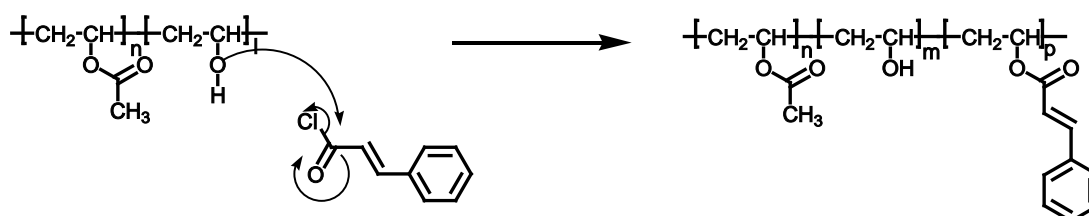


Figure 3.6 FT-IR spectrum of Cur-PV(OH)

FT-IR spectrum of mono-substituted glutarylcurcumin (Figure 3.5) showed the absorption peak of C-H stretching vibration at 2918.12 cm^{-1} , C=O stretching vibration at $\sim 1705.54\text{ cm}^{-1}$, informing the new ester functionality, and C=C stretching vibration at 1624.84 cm^{-1} . FT-IR spectra of Cur-PV(OH) (Figure 3.6) showed the absorption peak of O-H stretching vibration at 3301.56 cm^{-1} , C-H stretching vibration at 2917.79 cm^{-1} , C=O stretching vibration at $\sim 1731.62\text{ cm}^{-1}$, informing the ester functionality and C=C stretching vibration at 1625.85 cm^{-1} .

3.1.3 Synthesis of Cin-PV(OH)

The preparation of Cin-PV(OH) was carried out according to method of Luadthong *et al.* 2008. Grafting of cinnamoyl moieties onto PV(OH) could be done successfully using a classical esterification reaction that utilized the hydroxyl functionality of PV(OH) and cinnamoyl chloride. The sample is a white solid. The mechanism of the reaction is shown in Scheme 3.4.



Scheme 3.4 Mechanism of synthesis of Cin-PV(OH)

The degree of cinnamoyl substitution is 17.69 % (Figure 3.7) as deduced from the integration of peaks at 6.53-7.68 ppm (all six cinnamoyl protons) against peaks at 1.14-2.31 ppm ($-\text{CH}-\underline{\text{C}}\text{H}_2-\text{CH}-$ and $\underline{\text{C}}\text{H}_3-\text{CO}-$ of PV(OH) backbone).

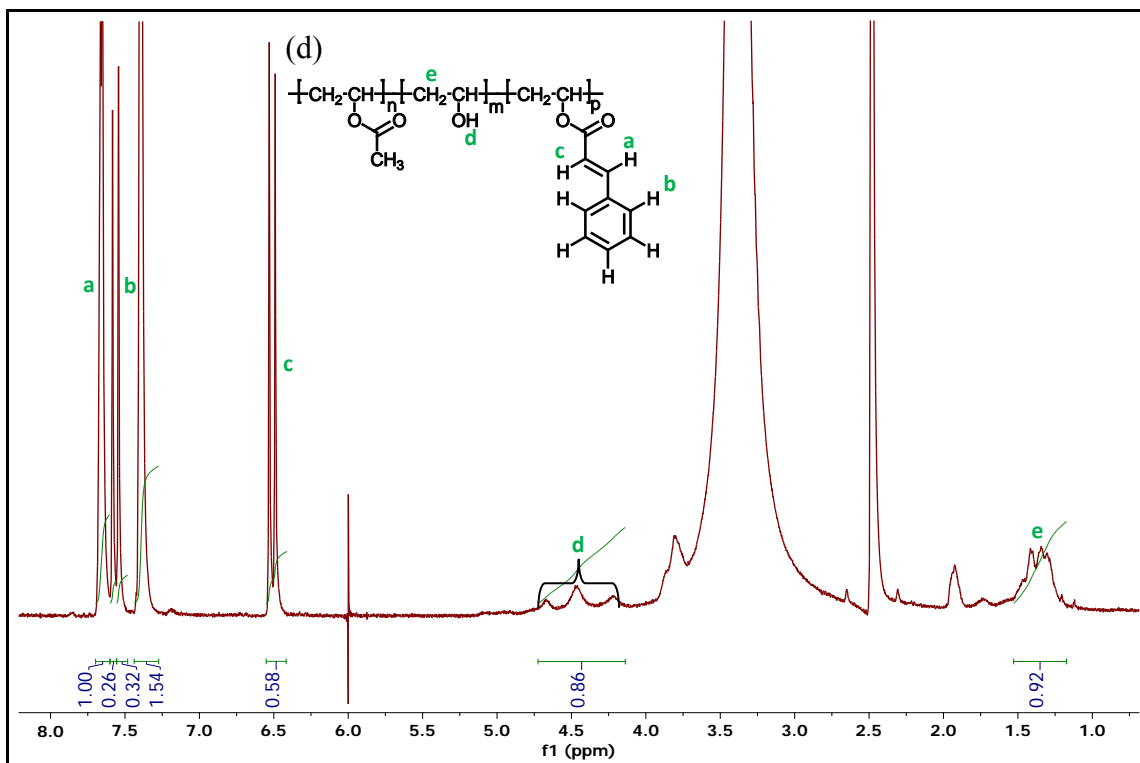


Figure 3.7 $^1\text{H-NMR}$ spectrum of Cin-PV(OH) in DMSO-d_6

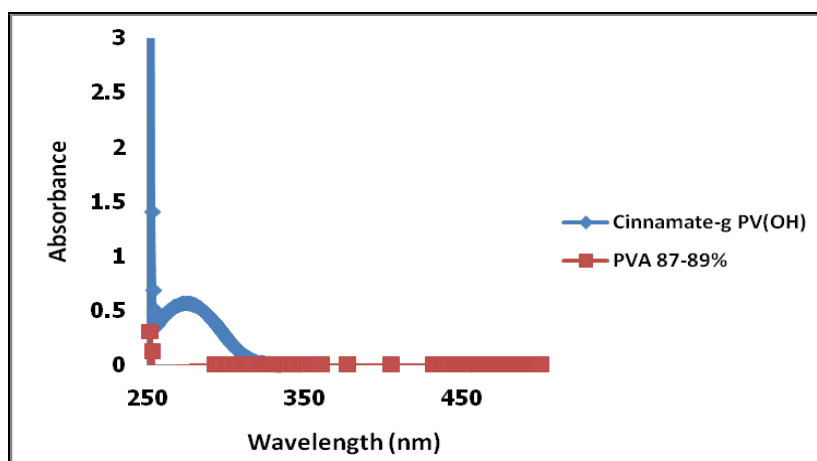


Figure 3.8 UV-visible spectra of Cin-PV(OH) in DMSO

UV-Vis absorption spectrum of Cin-PV(OH) possesses maximum absorption at 279 nm (blue) which is the characteristic absorption of cinnamoyl chromophore. This, therefore, confirm successful grafting of the cinnamoyl moiety on to the PV(OH) chains. As expected,

the UV-Vis absorption spectrum of PV(OH) (red) shows no absorption in that region (Figure 3.8).

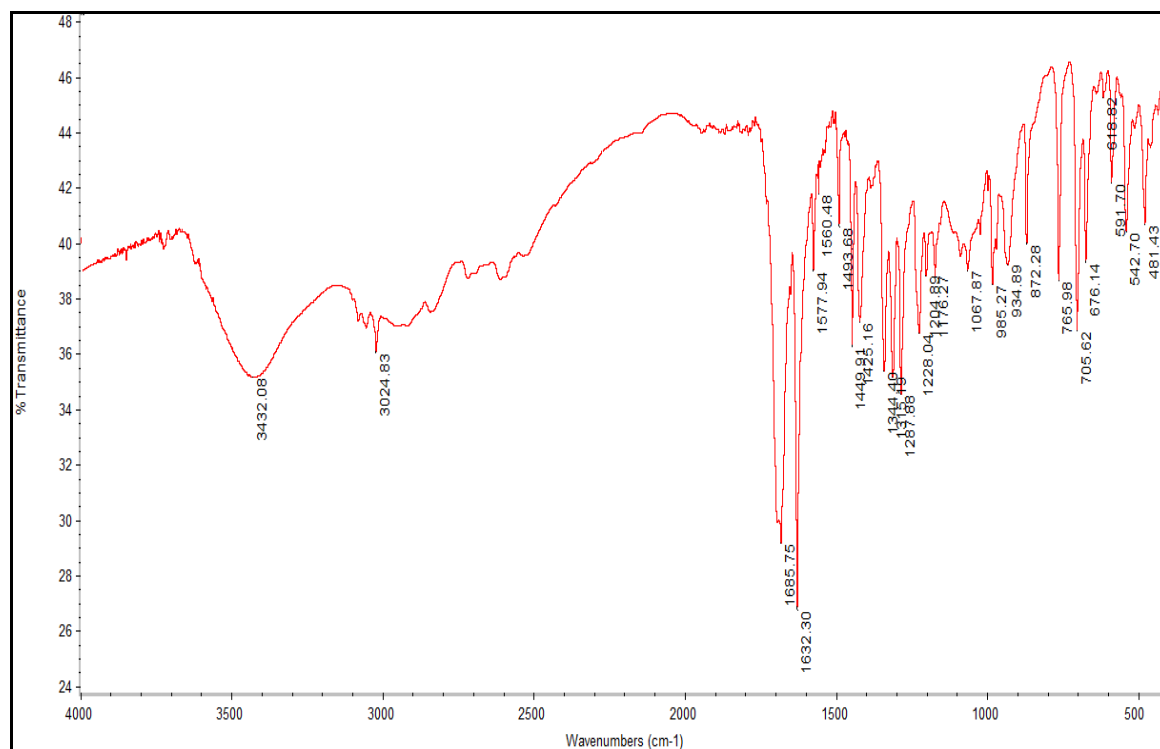


Figure 3.9 FT-IR spectrum of Cin-PV(OH)

FT-IR spectrum of Cin-PV(OH) (Figure 3.9) showed the absorption peak of O-H stretching vibration at 3432.08 cm^{-1} , C-H stretching vibration at 3024.83 cm^{-1} , C=O stretching vibration at $\sim 1710.00\text{ cm}^{-1}$ of the ester functionality and C=C stretching vibration at 1632.30 cm^{-1} .

3.2 Encapsulation of AP into nanoparticles

Encapsulation of AP was carried out by dialyzing 20 ml solution consisting of 30 mg of PV(OH) and 15 mg of AP (together with curcumin) in DMF. First, for the AP-Cur-PV(OH), milky yellow suspension (Figure 3.10 (a)) was obtained upon the dialysis. Analysis of the suspension by SEM (Figure 3.11 (a)) and TEM (Figure 3.11 (b)) indicated spherical particles with agreeable diameter of $269.84 \pm 19.44\text{ nm}$ and $259.44 \pm 16.90\text{ nm}$, respectively. Second, for the AP-Cin-PV(OH), milky white suspension (Figure 3.10 (b)) was obtained upon the

dialysis. Analysis of the suspension by SEM (Figure 3.12 (a)) and TEM (Figure 3.12 (b)) indicated spherical particles with agreeable diameter of 291.67 ± 32.27 nm and 275.00 ± 25.00 nm, respectively. Finally, for the APCur-Cin-PV(OH), milky orange suspension (Figure 3.10 (c)) was obtained upon the dialysis. Analysis of the suspension by SEM (Figure 3.13 (a)) and TEM (Figure 3.13 (b)) indicated spherical particles with agreeable diameter of 304.00 ± 13.47 nm and 300.00 ± 25.00 nm, respectively.

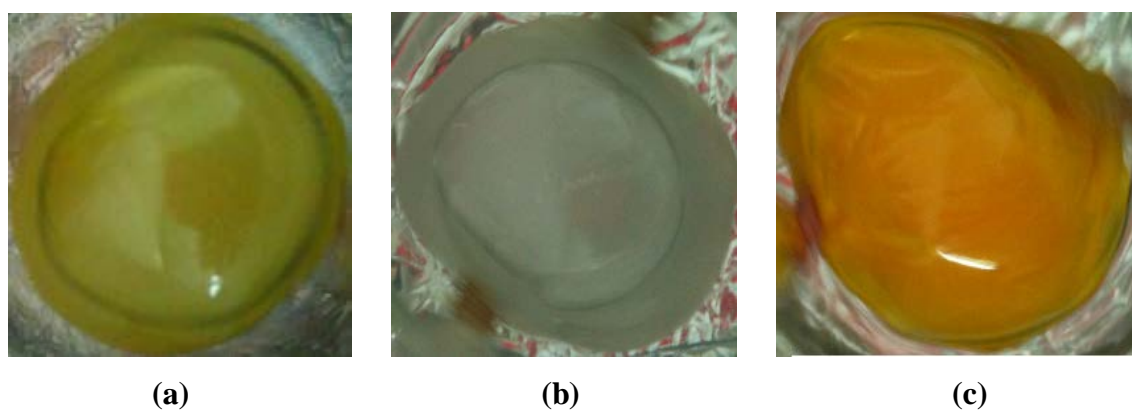


Figure 3.10 Suspension of (a) AP-Cur-PV(OH), (b) AP-Cin-PV(OH) and (c) APCur-Cin-PV(OH)

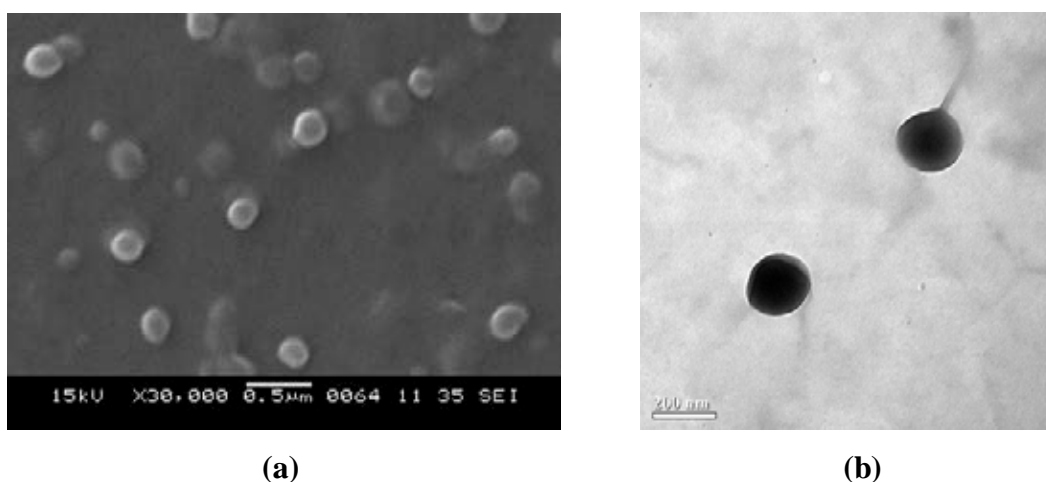


Figure 3.11 SEM (a) and TEM (b) photographs (at 10,000x magnification) of AP-Cur-PV(OH) prepared by dialysis at the initial PV(OH) and AP concentrations of 3,000 ppm and 1,500 ppm, respectively.

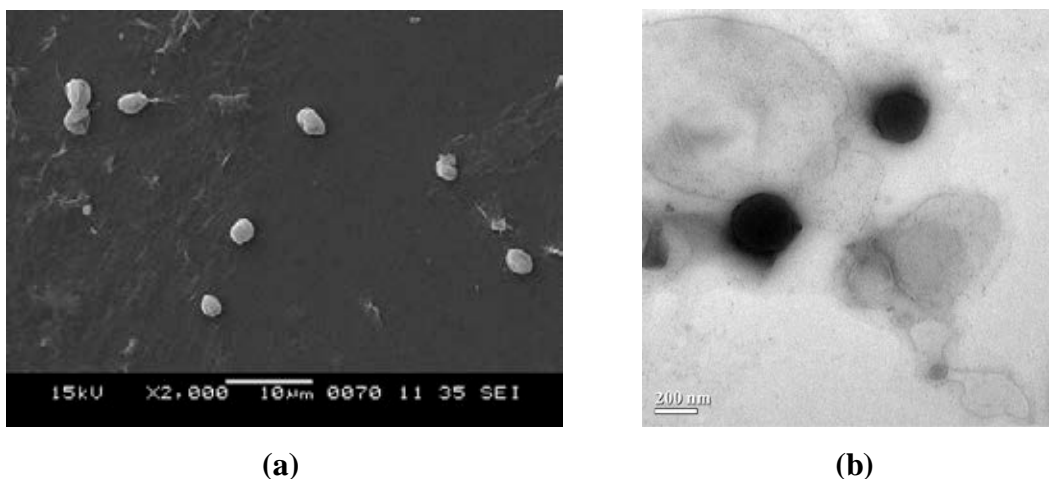


Figure 3.12 SEM (a) and TEM (b) photographs (at 10,000x magnification) of AP-Cin-PV(OH) prepared by dialysis at the initial PV(OH) and AP concentrations of 3,000 ppm and 1,500 ppm, respectively.

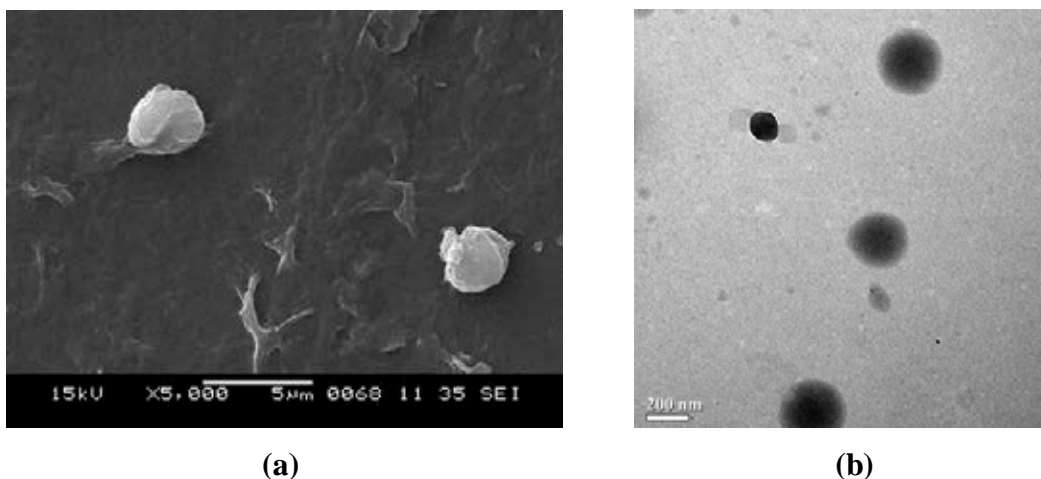


Figure 3.13 SEM (a) and TEM (b) photographs (at 10,000x magnification) of APCur-Cin-PV(OH) prepared by dialysis at the initial PV(OH) and AP concentrations of 3,000 ppm and 1,500 ppm, respectively.

It was speculated that when DMF was displaced by water, the hydrophobic groups (methylene, cinnamoyl and curcumin moieties) were directed to the inside of the sphere, while the hydrophilic domains of the PV(OH) backbone (hydroxyl groups) arranged themselves at the outer surface of the sphere to have maximal interaction with the hydrophilic water molecules,

leading to spontaneous particle formation. In a presence of AP, a hydrophobic form of vitamin C, AP was directed to the hydrophobic core of the sphere through van der Waal force. The result showed that morphology of three nanoparticles were spherical. The dry particle size (from SEM) is around 269-304 nm and the particle size obtained from TEM is around 259-300 nm. Moreover, the particle size of APCur-Cin-PV(OH) is bigger than AP-Cin-PV(OH) and AP-Cur-PV(OH), respectively (Table 3.2). The diameter of the particles increased with concentration of actives/polymer used during the encapsulation process and loading of the particles.

Table 3.2 Particle size of AP (or together with curucmin)-encapsulated polymeric nanoparticles

AP-encapsulated polymeric nanoparticles	Particle size distribution from SEM (nm)	Particle size distribution from TEM (nm)
Cur-PV(OH)	269.84 ± 19.44	259.44 ± 16.90
Cin-PV(OH)	291.67 ± 32.27	275.00 ± 25.00
Cin-PV(OH) + encapsulated curcumin	300.00 ± 25.00	304.75 ± 13.47

3.3 Encapsulation efficiency and loading

The encapsulation efficiency and loading were evaluated by measuring amount of AP which was loaded in the particles. The amounts of AP incorporated into the polymeric nanoparticles and in the dialysate water were determined using HPLC equipped with UV detector at 254 nm, with the aid of a calibration curve. Dialysate-water was subjected to HPLC analysis directly, while the freeze-dried nanoparticles were dissolved in methanol and filtered through the membrane with molecular weight cut-off 10,000, prior to the analysis. The encapsulation efficiency (EE) and loading capacity were calculated as follows:

$$\% \text{ Encapsulation efficiency (\%EE)} = \frac{\text{Weight of encapsulated AP} \times 100}{\text{Weight of AP used}} \quad (1)$$

$$\% \text{ Loading} = \frac{\text{Weight of encapsulated AP} \times 100}{\text{Weight of polymer used}} \quad (2)$$

HPLC condition: The stationary phase column was C-18 reverse phase and the mobile phase was methanol : acetonitrile : 0.02 M phosphate buffer pH 2.5 (75 : 10 : 15, v/v). UV detection was at 254 nm; injection volume 20 μ L and flow rate 1.5 mL/min. Calibration curve was created from a series of AP solutions freshly prepared in methanol at concentrations 100, 200, 400, 600, and 1,000 ppm. The obtained calibration curve was linear (Figure A1, Appendix A). The result indicated that retention time of AP solutions were between 6.2 to 6.5 min. (Figure A2-A6, Appendix A). Encapsulation efficiency and loading are shown in Table 3.3 (calculation of %EE and %loading showed in Appendix A)

Table 3.3 % loading and % encapsulation efficiency (%EE) of AP-encapsulated particles.

Type of carrier systems	% Loading of AP (\pm SD)	% EE of AP (\pm SD)	% Curcumin (\pm SD)
Cur-PV(OH)	29.00 \pm 0.32	80.85 \pm 0.16	28.43
Cin-PV(OH) + encapsulated curcumin	19.43 \pm 0.23	62.50 \pm 0.11	19.02 \pm 0.21 (%EE = 62.0 \pm 0.09)
Cin-PV(OH)	27.32 \pm 0.52	75.94 \pm 0.28	-

The results showed that Cur-PV(OH) gave maximum loading and AP maximum encapsulation efficiency of AP. We speculated that Cur-PV(OH) nanoparticles were more hydrophobic than Cin-PV(OH). So, Cur-PV(OH) might entrap AP and form spheres more quickly than Cin-PV(OH) did. The $^1\text{H-NMR}$ spectrum indicated 28.43 g of curcumin moieties per 100 g of the material. Whereas the loading of curcumin in the Cin-PV(OH) particles was 19.02 \pm 0.21 g per 100 g of the material.

3.4 Stability of the AP-encapsulated

In this research, the stability of AP-Cur-PV(OH), APCur-Cin-PV(OH), AP-Cin-PV(OH) and free-AP were studied in two forms, freeze-dried form and suspension form in water, under light and light-proof condition. In freeze-dried forms, AP under light-proof

condition is more stable than AP under light condition because the increasing of reactive oxygen species (ROS) was resulted from light activation that can cause the AP oxidized. Moreover, AP-Cur-PV(OH) is the most stable because it possess antioxidative properties from curcumin to scavenge the free radical before contact with AP. Follow by, APCur-Cin-PV(OH) because curcumin is separated with AP in nanospheres that ROS more easier to oxidize AP than in AP-Cur-PV(OH). Next, AP-Cin-PV(OH) and free-AP are less stable, respectively. In suspension forms, AP was degraded faster than in freeze-dried form. This is a result from AP more chance to react with hydroxyl radical in water.

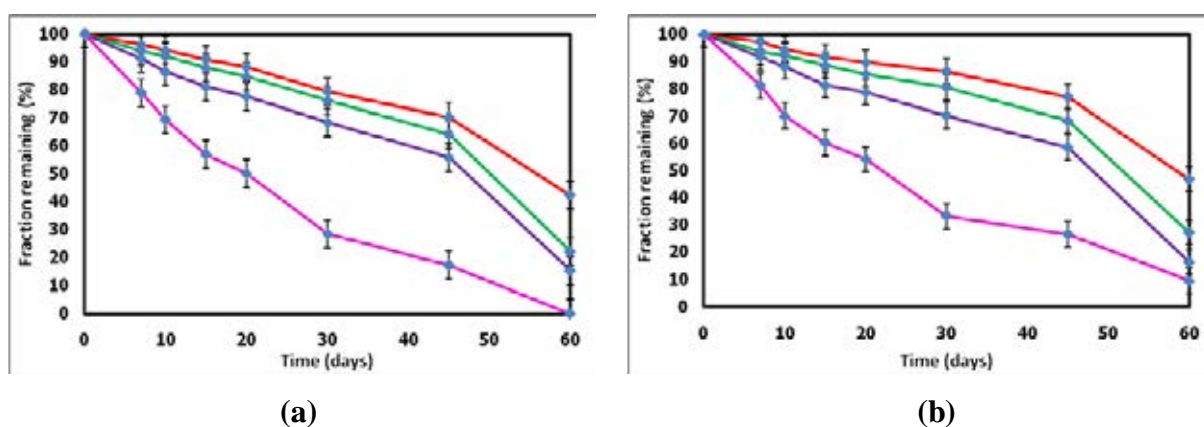


Figure 3.14 Content of AP-encapsulated particles after 2 months storage at room temperature (a) in normal light and (b) in light-proof condition of

- ◆— AP-Cur-PV(OH),
- ◆— APCur- Cin-PV(OH),
- ◆— AP-Cin-PV(OH), and
- ◆— unencapsulate AP.

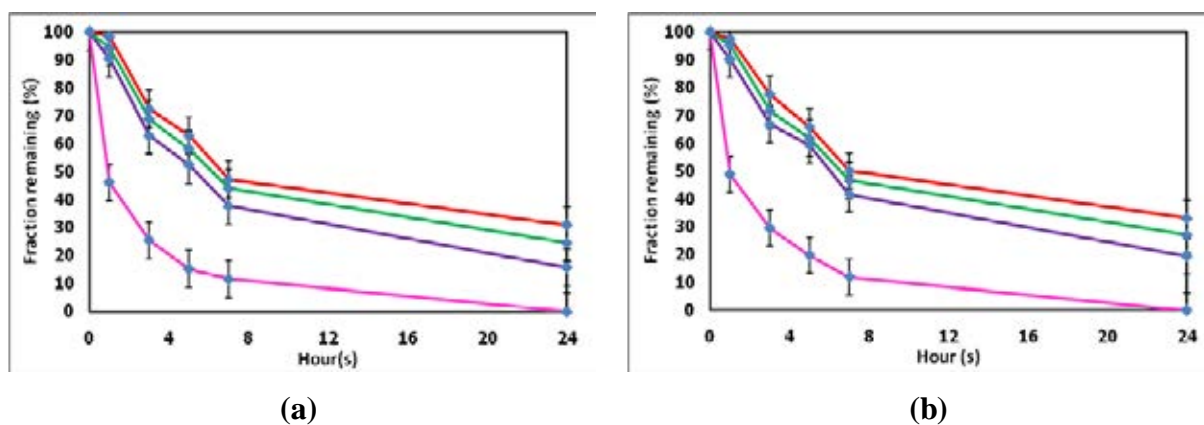
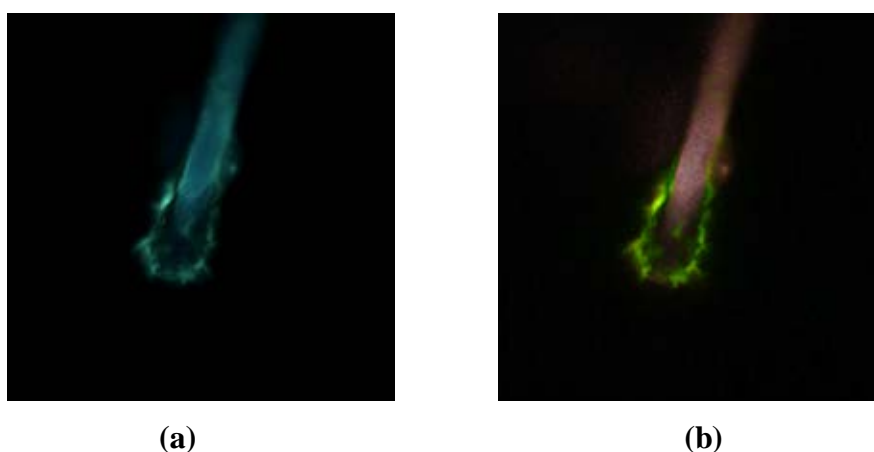


Figure 3.15 Content of AP-encapsulated particles for 24 h storage at room temperature **(a)** in normal light and **(b)** in light-proof condition of

- AP-Cur-PV(OH),
- APCur-Cin-PV(OH),
- AP-Cin-PV(OH), and
- unencapsulate AP.

3.5 *Ex vivo* skin penetration by using confocal laser scanning fluorescence microscopy (CLFM)

Ex vivo studies of the penetration of AP-Cur-PV(OH) and the AP release from the penetrated particles were carried out using fresh six month-old pig skin pieces. The experiment was based on the different fluorescent spectra of AP and of curcumin which enables the use of confocal laser scanning fluorescence microscope (CLFM) to locate the location of AP and Cur-PV(OH) in the skin tissue (figure 3.16(a)). The result showed that the AP-Cur-PV(OH) could penetrate into the skin tissue *via* hair follicle (figure 3.16(c) and (d)). Because the fluorescence signals from Cur-PV(OH) and from AP were not always at the same position (figure 3.16(d)). It was speculated that AP could be released from Cur-PV(OH).



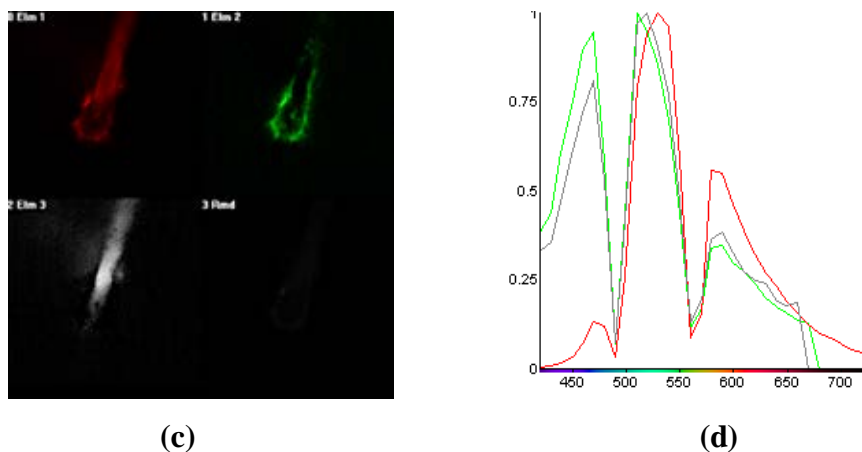


Figure 3.16 The confocal laser scanning fluorescence microscopy image showing (a) skin penetration of AP-loaded Cur-PV(OH) nanoparticles in hair follicle; (b) unresolved fluorescent image of the porcine ear skin at $\sim 40 \mu\text{m}$ depth for the stratum corneum surface, for 30 mins after the AP-loaded Cur-PV(OH) nanoparticles suspension was applied; (c) superimposed image of the AP (green), Cur-PV(OH) nanoparticles (red) and skin tissue (grey); (d) fluorescent spectrum of Cur-PV(OH) (red), AP (green), and skin tissue (grey).

3.6 DPPH[•] free radical scavenging assay activity

The antioxidant activity of free curcumin and Cur-PV(OH) nanoparticles were studied defined as free-radical scavenging activity with stable, non-biological implicate radical was expressed as BHT equivalents. As it was determined, the antioxidant activity is equal to the 1.0 mM concentration of a BHT solution having the antioxidant capacity equivalent to a 1.0 mM solution of the substance under investigation. The results of the antioxidant activity provided by scavenging activity of DPPH[•] solution were based on the reduction in the absorbance of the DPPH[•] solution at 515 nm.

Table 3.4 % Inhibition of DPPH[•] of 3 substances.

Substance	% Inhibition
BHT	13.11 ± 0.03
Free-curcumin	4.57 ± 0.20
Cur-PV(OH)	2.19 ± 0.10

From Table 3.4, the results for the antioxidant activity of curcumin against Cur-PV(OH) by BHT as a positive control showed that the ability as antioxidant of Cur-PV(OH) was reduced to half when compared with free-curcumin. Since one hydroxyl group on an aromatic ring of curcumin was grafted on polymer.

From finding the % weight of curcumin from Cur-PV(OH) and Cin-PV(OH), showed that weight of curcumin in Cur-PV(OH) was higher than APCur-Cin-PV(OH). However, from the result of grafting one phenyl group of glutarylcurcumin on polymer lead to reduce antioxidant properties of curcumin into a half. Then, we assumed that % weight of curcumin is the same equivalent.

CHAPTER IV

CONCLUSION

In this work, two polymeric nanoparticles were made, one with antioxidative property and the other with no such activity. The antioxidative nanocarriers were made from Cur-PV(OH) while the carriers with no antioxidative activity were made from Cin-PV(OH). Cur-PV(OH) which was synthesized by grafting the glutarylcurcumin onto the poly(vinyl alcohol) chains using esterification reaction. The substitution degree of curcumin on the PV(OH) chain was 5.9%. Cin-PV(OH) which was synthesized by grafting the cinnamoyl chloride onto the poly(vinyl alcohol) chains using esterification reaction. The substitution degree of Cur-PV(OH) chain was 17.69%. We conclude that antioxidative nanoparticles of Cur-PV(OH) have the best effective encapsulation and stabilization of ascorbyl palmitate (AP), %EE = 29.00 ± 0.32 and %loading = 80.85 ± 0.16 , followed by Cin-PV(OH) + curcumin-encapsulated, %EE = 19.43 ± 0.23 and %loading = 62.50 ± 0.11 , and Cin-PV(OH), %EE = 27.32 ± 0.52 and %loading = 75.94 ± 0.28 , respectively. The particle sizes from SEM and TEM of AP-Cur-PV(OH) are 269.84 ± 19.44 and 259.44 ± 16.90 , respectively. The stability of AP-Cur-PV(OH), AP-Cin-PV(OH) and APCur-Cin-PV(OH) were studied into two forms, suspension and freeze-dried, showed that AP-Cur-PV(OH) is the most stable. In freeze-dried form is more stable than in suspension form. Moreover, in light-proof condition, AP is more stable than in light condition. *Ex vivo* skin penetration studied of AP-Cur-PV(OH) by confocal laser scanning fluorescence microscopy (CLFM) showed that AP can penetrate into the skin. %Inhibition of Cur-PV(OH) by using DPPH[•] free radical scavenging activity assay is 2.19 ± 0.10 . The result showed that Cur-PV(OH) has antioxidant properties when compared with free-curcumin.

REFERENCES

- [1] Lo, K. M.; and Peter, C. K. Antioxidant Activity of Extracts from the Fruiting Bodies of *Agrocybeaeagerita* Var. Alba. Food Chemistry 89(4): 533-539.
- [2] Arts, M. J.; Guido, R. H.; Hans, V.; Peter, V.; and Aalt, B. Antioxidant Capacity of Reaction Products Limits the Applicability of the Trolox Equivalent Antioxidant Capacity (TEAC) Assay. Food and Chemical Toxicology 42(1): 45-59.
- [3] Padayatty, S. J.; Katz, A.; Wang, Y.; Ecj, P.; Kwon, O.; Lee, J. H.; Chen, S.; and Corpe, C. Vitamin C as an Antioxidant: Evaluation of its Role in Disease Prevention. Journal of the American College of Nutrition 22(2003): 18-35.
- [4] Carr, A. C.; and Frei, B. Toward a New Recommended Dietary Allowance for Vitamin C Based on Antioxidant and Health Effects in Humans. American Society for Clinical Nutrition 69(1999): 1086-1107.
- [5] Philips, C. L.; Combs, S.B.; and Pinell, S. Effects of Ascorbic Acid on Proliferation and Collagen Synthesis in Relation to the Donor Age of Human Dermal Fibroblasts. J. Invest. Dermatol 103(1994): 228–232.
- [6] Hande, S. B.; Nuray, K.; and Feryal, K. Degradation of Vitamin C in Citrus Juice Concentrates During Storage. Journal of Food Engineering 74(2) : 211-216.
- [7] Huelin, F. E.; Studies on the anaerobic decomposition of ascorbic acid. Journal of Food Science. 18(2006): 633-639.
- [8] Robertson, G. L.; and Samaniego, C. M. Effect of Initial Dissolved Oxygen Levels on the Degradation of the Ascorbic Acid and the Browning of Lemon Juice During Storage. Journal of Food Science 51(1): 187-187.
- [9] Schmalfluss, U.; Neubert, R.; and Wohlrab, W. Modification of Drug Penetration into Human Skin Using Microemulsions. J. Controlled Release. 46(1997): 279–285.
- [10] Shibayama, H.; Ueda, K.; Yoshio, K.; Matsuda, K.; Hisama, M.; and Miyazawa, M. Synthesis and Characterization of New Ascorbic Derivative: Sodium Isostearyl 2-O-L-Ascorbyl Phosphate. Journal of Oleo Science 54(2005): 601-608.
- [11] Sieb, A.; Deyoe, W.; and Hosney, C. Method of Preparation of 2-Phosphate Ethers of Ascorbic Acid. United States Patent 18: 1-16.
- [12] Cao, Z.; Yinghe, H.; Lixian, S.; and Xueqiang, C. Chemical Synthesis of Ascorbyl Palmate. Advanced Materials Research 236: 1962-1965.

- [13] Pierandrea, L.; Giulia, C.; Patrizia, P.; Nadia, M.; Annalisa, R.; and Franco, F.V. Self assembling and Antioxidant Activity of Some Vitamin C Derivatives. Colloids and Surfaces 167(1): 83-93.
- [14] Beddows, C. G.; Jagait, C.; and Kelly, M. J. Effect of Ascorbyl Palmitate on the Preservation of a Tocopherol in Sunflower Oil, Alone and with Herbs and Spices. Food Chemistry 73(2001): 255–261.
- [15] DeRitter, E.; Cohen, N.; and Rubin, S. H. Physiologic availability of dehydro-ascorbic acid and palmitoyl-L-ascorbic acid. Science 113: 628–631.
- [16] Segall, A. I.; and Moyano, M. A. Stability of Vitamin C Derivatives in Topical Formulations Containing Lipoic Acid, vitamin A and E. International Journal of Cosmetic Science 30: 453-458.
- [17] Spiclin, P.; Gasperlin, G.; and Kmetec, V. Stability of Ascorbyl Palmitate in Topical Microemulsions. International Journal of Pharmaceutics 222(2001): 271–279.
- [18] Yamazaki, H.; Yamakushi, T.; Ueno, A.; Yamaushi, A.; and Yamamoto, I. Food Additives on Acceptable Daily Intake (ADI) Level Affect the Agonist Induced Platelet Activation I. Antioxidants and Preservatives. Chemosphere 29(6): 1293-1299.
- [19] Nihro, Y.; Miyataka, H.; Sudo, T.; Matsumoto, H.; and Satoh, T. 3-O-alkylascorbic acids as Free-radical Quenchers: Synthesis and Inhibitory Effect on Lipid Peroxidation. J. Med. Chem 34(7): 2152-2157.
- [20] Jonston, C. S.; Monte, W. C.; Bolton, R. S.; and Chard, M.H. A Comparison of L-Ascorbic Acid and L-Ascorbyl 6-Palmitate Utilization in Guinea Pig and Humans. Nutrition Research 14(10): 1465-1471.
- [21] Albreksen, S.; Lie, L.; and Sandnes, K. Ascorbyl palmitate as a Dietary Vitamin C Source for Rainbow Trout (*Salmo gairdneri*). Agriculture 71(4): 359-368.
- [22] Ross, D.; Mendiratta, S.; Qu, Z.; Cobb, C. E.; and May, J. M. Ascorbate-6 palmitate Protects Human Erythrocytes from Oxidative Damage. Free Radical Biology and Medicine 26(1999): 81-89.
- [23] Perricone, N. The Hydroxyl Free Radical Reactions of Ascorbyl Palmitate as Measured in Various In Vitro Models. Biochem Biophys Res Commun 262(3): 661-665.
- [24] Pizarro, F.; Olivares, M.; Hertrampf, E.; Nuñez, S.; Tapia, M.; Cori, H.; and Romana, D. L. Ascorbyl palmitate enhances iron bioavailability in iron-fortified bread. American Journal of Clinical Nutrition 84(4): 830-834.
- [25] Teucher, B.; Olivares, M.; and Cori, H. Enhancers of iron absorption: ascorbic acid and

- other organic acids. International Journal Vitamin Nutrient Resource 2004;74:403–19.
- [26] Gordon, M. H. Food and Nutritional Analysis/Antioxidants and Preservative. Encyclopedia of Analytical Science (2005): 225-230.
- [27] Beddows, C. G.; Jagiat, C.; and Kelly, M. J. Effect of Ascorbyl Palmitate on the Preservative of α -tocopherol in Sunflower Oil Alone and with Herbs and Spices. Food Chemistry 73(3): 255-261.
- [28] Hudhes, R. E.; and Jones, E. Ascorbyl palmitate as a Source of ascorbic acid. Food Chemistry 22(1): 37-40.
- [29] Herr, B. Additive in Dietary Foods/Types and Functions of Additives in Dietary Products. Encyclopedia of Dietary Science (2011): 31-40.
- [30] Fox, C. Advances in the Cosmetic Science and Technology of Topical Bioactive Materials. Cosmet. Toil 112(1997): 67–84.
- [31] Jurkovi, P.; Sentjurc, M.; Gasperlin, M. Kristk, J.; and Pecer, S. Skin Protection Against Ultraviolet Induced Free Radicals with Ascorbyl Palmitate in Microemulsions. European Journal of Pharmaceutics and Biopharmaceutic 56(1): 59-66.
- [32] Darr, D.; Combs, S.; Dunston, S.; Manning, T.; and Pinell, S.; Tropical vitamin C protects porcine skin from ultraviolet radiation-induced damage. Br. J. Derm 127: 247–253.
- [33] Wang, S. Q.; Osterwalder, U.; and Jung, K. Ex Vivo Evaluation of Radical Sun Protection Factor in Popular Sunscreen with Antioxidants. Journal of the American Academy of Dermatology 65(3): 525-530.
- [34] Aggarwal, B. B.; Kuma, A.; and Bharti, A. C. Anticancer Potential of Curcumin Preclinical and Clinical Studies. Anticancer Research 23(2003): 363-39
- [35] Ray, S. N.; Chattopadhyay, N.; Mitra, A.; Siddiqi, M.; and Chatterjee, A. Curcumin Exhibits Anti-metastatic Properties by Modulating Integrin Receptors, Collagenase Activity, and Expression of Nm23 and E-cadherin. J Environ Pathol Toxicol Oncol 22(1): 49-58.
- [36] Kolev, T. M. DFT and Experimental Studies of the Structure and Vibrational Spectra of Curcumin". International Journal of Quantum Chemistry 102(6): 1069-1079.
- [37] Sherma, R.A.; Gescher, A.J.; and Steward, W.P. Curcumin: The Story so far. European Journal of Cancer 41(2005): 1955–1968.
- [38] Hatcher, H.; Planalp, R.; Cho, J; Torti, F. M.; and Torti S. V. Curcumin: from ancient medicine to current clinical trials. Cell. Mol. Life Sci 65(11): 1631–1652.

- [39] Aggarwal, B. B.; Bhatt, I. D.; Ichikawa, H.; Ahn, K. S.; Sethi, G; and Sandur, S. K. Turmeric: the Genus *Curcuma*. Journal of Pharmaceutical and Biomedical Analysis (2006): 297–368.
- [40] Ray, B.; and Lahiri, D. K. Current Opinion in Pharmacology"; Neuroinflammation in Alzheimer's Disease: Different Molecular Targets and Potential Therapeutic Agents Including Curcumin. Current Opinion in Pharmacology 9(4): 434-444.
- [41] Anand, P.; Kunnumakkara, A.; Newman, R.; and Aggarwal, B.B. Bioavailability of Curcumin: Problems and Promises. Mol. Pharmaceutics 4(6): 807–818.
- [42] Jayaprakasha, G. K.; Jaganmohan, R. L.; and Sakariah, K. K. Antioxidant Activities of Curcumin, Demethoxycurcumin and Bisdemethoxycurcumin. Food Chemistry 98 (2006): 720–724.
- [43] Choi, H.; Yang-Sook, C.; Curcumin Inhibits Hypoxia-Inducible Factor-1 by Degrading Aryl Hydrocarbon Receptor Nuclear Translocator: A Mechanism of Tumor Growth Inhibition. Molecular Pharmacology 70(5): 1664–1671.
- [44] Kavita, B.; Karl-Heinz, W.; and Andrew, C. B. Curcumin, Resveratrol and Flavonoids as Anti-inflammatory, Cyto- and DNA-Protective Dietary Compounds. Toxicology 278 (1) : 88-100.
- [45] Shukla, P. K.; Khanna, V. K.; Ali, M. M.; Khan, M. Y.; and Srimal, R. C. Anti-ischemic Effect of Curcumin in Rat Brain. Biomedical and Life Science 33(60): 1036-1043.
- [46] Mingxin, S.; Quifeng, C.; Luming, Y.; Yubin, M.; Yanlin, M.; and Gaoliang, O. Antiproliferation and Apoptosis Induced by Curcumin in Human Ovarian Cancer Cells. Cell Biology International 30(2006): 221-226.
- [47] Tuba, A.; and İlhami, G. Antioxidant and Radical Scavenging Properties of Curcumin. Chemico-Biological Interactions 174(1): 27-37.
- [48] Toshiya, M.; Tomomi, M.; Kayo, H.; Hiromi, B.; Yoshio, T.; and Hidemasa, Y. Chemical Studies on Antioxidant Mechanism of Curcumin: Analysis of Oxidative Coupling Products from Curcumin and Linoleate. J. Agric. Food Chem 49(5): 2539-2547.
- [49] Itokawa, H.; Shi, Q.; Morris-Natschke, S. L.; Kuo-Hsiung, L. Recent Advances in the Investigation of Curcuminoids. J. Med. Chem 40(1997): 3057-3063.
- [50] Ravindranath, V.; and Chandrasekhara, N. Absorption and Tissue Distribution of Curcumin in Rats. Toxicology 16(1980): 259-265.

- [51] Anand, P.; Ajaikumar, B. K.; Robert, A. N.; and Aggarwal, B. B. Bioavailability of Curcumin: Problems and Promises. Molecular Pharmaceutics 4(6): 807-818.
- [52] Pfeiffer, E.; Hoehle, S. I.; Walch, S. G.; Piess, A.; Solyom, A. M.; Metzler, A. Curcuminoids Form Reactive Glucuronides In Vitro. J. Agric. Food Chem 55(2007): 538-544.
- [53] Amiya, S.; Tsuchiya, S.; Qian, R.; and Nakajima, A. The Study of Microstructures of Poly(vinyl alcohol) by NMR. Pure and Applied Chemistry 62(11) : 2139-2146.
- [54] Oviedo, I. R.; Nogu, M. A.; Gmez, N.; and Rubio, M. Design of Physical and Nontoxic Crosslinked Poly(vinyl alcohol) Hydrogel. International Journal of Polymeric Materials 57(12): 1095-1103.
- [55] Shakesheff, K. M.; Evora, C.; Soriano, I.; and Langer, M. The Adsorption of Poly(vinyl alcohol) to Biodegradable Microparticles Studied by X-Ray Photoelectron Spectroscopy (XPS) Journal of Colloid and Interface Science 185(2): 538-547.
- [56] Noguchi, T.; Yamamuro, T.; Oka, M.; Kumar, P.; Kotoura, Y. and Ikadat, Y. Poly(vinyl alcohol) Hydrogels as an Artificial Articular Cartilage: Evaluation of Biocompatibility. Journal of Applied Biomaterials 2(2): 101-107.
- [57] Sheikh, F. A.; Barakat, N.; Kim, B. S.; Aryal, S.; Khil, M.; and Kim, H. Y. Self-Assembled Polyhedral Oligosilsesquioxane (POSS) grafted Poly(vinyl alcohol) (PVA) Nanoparticles. Materials Science and Engineering 29(3): 869-876.
- [58] Gennadios, A.; Weller, C. L.; and Testin, R. F. Temperature Effect on Oxygen Permeability of Edible Protein-based Films. Journal of Food Science 58(1): 210-214.
- [59] Gough, J.E.; and Scotchford, C.A. Cytotoxicity of Glutaraldehyde Crosslinked Collagen/poly(vinyl alcohol) Films is by the Mechanism of Apoptosis. Journal of Biomaterial Research 16(1): 121-130.
- [60] Park, S.Y.; Jun, S.T.; and Marsh, K.S. Physical Properties of Chitosan/PV(OH)-blended Films Cast from Different Solvents. Food Hydrocolloids 15(4): 499-502.
- [61] Finley, J. Spectrophotometric determination of polyvinyl alcohol in paper coatings. Anal. Chem 33(13): 1925-1927
- [62] Strawhecker, K.E.; and Manias, E. Structure and Properties of Poly(vinyl alcohol)/Na⁺ Monmorillonite Nanocomposites. Chem. Mater 20(12): 2943-2949.
- [63] Yu, Y. H.; Lin, C. Y.; Yeh, J. M.; and Lin, W. S. Preparation and Properties of Poly(vinyl alcohol)-Clay Nanocomposite Materials. Polymer 44(12): 3553-3560.
- [64] Mattheus, F.A.; and Sefton, M. Properties of a Heparin-poly(vinyl alcohol) Hydrogel

- Coating. Journal of Biomedical Materials Research 17(2): 359-373.
- [65] Narayan, B.; Jonathan, G.; Miqin, Z. Chitosan-based Hydrogels for Controlled, Localized Drug Delivery. Advanced Drug Delivery Reviews 62(1): 83-99.
- [66] Schertz, D. M.; Wang, J. H.; Gregory, J. P.; William, S. M. Method of Making Blend Compositions of an Unmodified Poly(vinyl alcohol) and a Thermoplastic Elastomer. United States Patent (2002): 1991-1998.
- [67] Cavalieri, F.; Miano, F.; D'Antona, P.; and Paradossi, G. Study of Gelling Behavior of Poly(vinyl alcohol)-Methacrylate for Potential Utilizations in Tissue Replacement and Drug Delivery. Biomacromolecules 5(6): 2439–2446.
- [68] Fairhurst, D.; and Loxley, A. Micro- and Nanoencapsulation of Water- and Oil-Soluble Actives for Cosmetic and Pharmaceutical Applications. Cosmetic Delivery Systems (2010): 1-24.
- [69] Patravale, V. B.; Abhijit, A.; and Kulkarni, R. M. Nanosuspensions: a Promising Drug Delivery Strategy. Journal of Pharmacy and Pharmacology 56(2004): 827-840.
- [70] Anjalic, H.; Madhusmita, D.; Chandrasekaran, N.; and Amitava, M. Anti Bacterial Activity of Sunflower Oil Microemulsion. International Journal of Pharmacy and Pharmaceutical Sciences 2(2010): 123-128.
- [71] Elaine, M.; Merisko, L.; and Gary, G., L. Drug Nanoparticles: Formulating Poorly Water Soluble Compounds. Toxicol Pathol 36(2008): 43-48.
- [72] Lawrence, M.J.; Rees, G.D.; Microemulsion-based media as novel drug delivery system. Adv. Drug Del. Rev 45(2000): 89–121.
- [73] Solans, C.; Izquierdo, P.; Nolla, J.; Azemar, N.; and Garcia-Celma, M.J. Nanoemulsions. Colloid and Interface Science 10(2005): 102–110.
- [74] Shah, P.; and Bhalodia, D.; and Shelat, P. Nanoemulsion: A Pharmaceutical Review. Sys. Rev. Pharm 1(1): 25-32.
- [75] Lewis, B.A.; and Engelman, D.M. Lipid Bilayer Thickness Varies Linearly with Acyl Chain Length in Fluid Phosphatidylcholine Vesicles. J. Mol. Bio 166(2): 211–217.
- [76] Uracha, R.; Usawadee, S.; Piyawan, B.; Praneet, O.; Nantavan, B.; Varaporn, J. and Satit, P. Effect of Lipid Types on Physicochemical Characteristics, Stability and Antioxidant Activity of Gamma-oryzanol-loaded Lipid Nanoparticles. Journal of Microcapsule 26(7): 614-626.
- [77] Thompson, A.K.; and Singh, H. Preparation of Liposomes from Milk Fat Globule Membrane Phospholipids Using a Microfluidizer. Journal of Dairy Science 89(2):

410-419.

- [78] Patrick, H.D.; Nigel, M.D.; Bianca, B.; and Thomas, R. Incorporation of ovalbumin into ISCOMs and related colloidal particles prepared by the lipid film hydration method. Journal of Pharmaceutics 278(2): 263-274.
- [79] Maria, J.C.; Angel, M.; Facundo, M.; Salima, Varona. Encapsulation and Co-precipitation Processes with Supercritical Fluids: Fundamentals and Applications. J. of supercritical Fluids 47 (2009) : 546-555.
- [80] Brynjelsen, S.; Doty, M.; Kipp, J. E.; and Narayanan, K. Preparation of Submicron Sized Nanoparticled Via Dispersion Lyophilization. United States Patent (2004):
- [81] Wolfgang, M.; and Karsten, M. Solid Lipid Nanoparticles: Production, Characterization and Applications. Lipid Assemblies for Drug Delivery 47(2003): 165-196.
- [82] Mehnert, W.; and Mäder, K.; Solid Lipid Nanoparticles: Production, Characterization and Applications. Adv. Drug. Deliv. Rev 47(2001): 165–196.
- [83] Wissing, S. A.; Kayser, O.; and Muller, R. H. Solid Lipid Nanoparticles for Parenteral Drug Delivery. Adv. Drug. Deliv. Rev 56(2004): 1257-1272.
- [84] Fu-Qiang, H.; Yu, Z.; Yong-Zhong, D.; and Hong, Y. Nimodipine Loaded Lipid Nanospheres Prepared by Solvent Diffusion Method in a Drugsaturated Aqueous System. International Journal of Pharmaceutic 348(2003): 146-152.
- [85] Manju, R. S.; Deependra, S.; and Swarnlata, S. Influence of Selected Formulation Variables on the Preparation of Peptide Loaded Lipospheres. Trends in Medical Research 6(2002): 101-115.
- [86] Anniemie, R.; Jeffery, A. H.; and Nicola, T. Oxidation-Sensitive Polymeric Nanoparticle. Langmuir 21(1): 411–417.
- [87] Taek, W. C.; Kwang, Y. C.; Jae, W. N.; Toshihiro, A.; and Chong, S. C. Chiral Recognition of Birirubin by Polymeric Nanoparticles. Langmuir 18(16): 6462-6464.
- [88] Eric, M. S.; Michael B. C.; and Shastri, V. P. Single-Step Process to Produce Surface Functionalized Polymeric Nanoparticles. Langmuir 23(24): 12275-12279.
- [89] Cabaleiro-Lago, C.; Lynch, I.; Dawson, K. A.; and Linse, S. Inhibition of IAPP and IAPP(20-29) Fibrillation by Polymeric Nanoparticles. Langmuir 26(5): 3453-3461.
- [90] Shilpa, S.; Matthias, T.; and Patrice, H. Microporous Structure and Drug Release Kinetics of Polymeric Nanoparticles. Langmuir 20(13): 5613-5620.
- [91] Chunbai, H.; Yiping, H.; Lichen, Y.; and Chunhua, Y. Effects of Particle Size and Surface Charge on Cellular Uptake and Biodistribution of Polymeric

- Nanoparticles. Biomaterials 31 (13) : 3657-3666.
- [92] Yan, S.; Changsheng, L.; Yuan, Y.; Xinyi, T.; Fan, Y.; Xiaoqian, S.; Huanjun, Z.; and Feng, X. Long-Circulating Polymeric Nanoparticles Bearing a Combinatorial Coating of PEG and Water-Soluble Chitosan. Int. J. of Pharm 377: 199-206.
- [93] Florindo, H. F.; Pandit, S.; Gonclaves, L. M.; and Almeida, A. J. Surface modification polymeric nanoparticles for Immunisation Against Equine Strangles. Int. J. of Pharm 390(1): 25-31.
- [94] Jagdish, J.; Suresh, K. G.; and Jorg, K. Preparation of Biodegradable Cyclosporine Nanoparticles by High-pressure Emulsification-solvent Evaporation Process. Journal of Control Release 96(1): 169-178.
- [97] Laura, M.E.; Richard, C.; and Justin, H. Oral drug delivery with polymeric nanoparticles: The gastrointestinal mucus barriers. Advanced Drug Delivery Reviews 1(7): 291-299.
- [98] Thomas, Y.; Jiamin, W.; and Tetsu, T. Kinetic stability of hematite nanoparticles: the effect of particle sizes. J. Nanopart. Res 4: 1-12.
- [99] Christine V.; and Kawthar, B. Methods for the Preparation and Manufacture of Polymeric Nanoparticles. Pharmaceutical Research 26(5): 1025-1058.
- [100] Wim, H.; De, J.; and Paul, B. Drug Delivery and Nanoparticles : Applications and Hazards. Int J Nanomedicine 3(2): 133-149.
- [101] Diana, G. V.; Hugh, S.; Dea, H. R.; and Ibrahim, M. A Novel Aerosol Method for the Production of Hydrogel Particles. Journal of Nanomaterials (2011) : 21-31.
- [102] Rajendran, N. N.; Natrajan, R.; Kumar, R.; and Selvaraj, S. Acyclovir-loaded chitosan nanoparticles for ocular delivery. Asian J Pharm 4(4): 220-226.
- [103] Soppimath, K. S.; Aminabhavi, T. M.; Kulkarni, A. R.; and Rudzinski, W.E. Biodegradable Polymeric Nanoparticles as Drug Delivery Devices. Journal of Controlled Release 70(2001): 1-20.
- [104] Mohapatra, M.; and Anand, S. Synthesis and applications of nanostructured ironoxides/hydroxides - a review. International Journal of Engineering, Science and Technology 2(8): 127-146.
- [105] Bagwe, R. P.; Kanicky, J. R.; Palla, B. J.; Patanjali, P. K.; and Shah, D. O. Improved Drug Delivery Using Microemulsions: Rationale, Recent, Progress and New Horizons. Therapeutic Drug Carrier System 18(1): 77-140.
- [106] Jager-Lezer, N.; Terrisse, I.; Bruneau, F.; Tokgoz, S.; Ferreira, L.; Calusse, D.; Seiller, M.; and Grossiord, J. L. Influence of Lipophilic Surfactant on the Release Kinetics of

- Water-Soluble Molecules Entrapped in a W/O/W Multiple Emulsion. Journal of Controlled Release 45(1): 1-13.
- [107] Solaro, R.; Chiellini, F.; and Battisti, A. Targeted Delivery of Protein Drugs by Nanocarriers. Materials 3(3): 1928-1980.
- [108] Delief, F.; Branco-Frieto, M. Polymeric Particulates to Improve Oral Bioavailability of Peptide Drugs. Molecules 10(2005): 65-80.
- [109] Catarina, P. R.; Ronald, J. N.; Antonio, J. R.; and Francisco, V. Nanoencapsulation I. Methods for Preparation of Drug-loaded Polymeric Nanoparticles. Nanomedicine: Nanotechnology, Biology and Medicine 2(1): 8-21.
- [110] Pegi, A. G.; and Julijana, K. The Manufacturing techniques of drug-loaded polymeric nanoparticles from preformed polymers. Journal of Microencapsulation (2011): 323-335.
- [111] Vanthier, C.; and Bouchemal, K. Methods for the Preparation and Manufacture of Polymeric Nanoparticles. Pharmaceutical Research 26(5): 1025-1032.
- [112] Sinha, V. R.; Bansal, K.; Kaushik, R.; Kumria, R.; and Trehan, A. Poly- ϵ -caprolactone Microspheres and Nanospheres: an Overview. International Journal of Pharmaceutics 278(1): 1-23.
- [113] Christine, V.; and Kawthar, B. Methods for the Preparation and Manufacture of Polymeric Nanoparticles. Pharmaceutical Research 25(5): 125-158.
- [114] Soppimath, K. S.; Aminabhavi, T. M.; Kulkarni, A. R.; and Rudzinski, W. E. Biodegradable Polymeric Nanoparticles as Drug Delivery Devices. Journal of Controlled Release 70(2001): 1-20.
- [115] Rao, J. P.; and Geckeler, K. E. Polymer nanoparticles: Preparation Techniques and Size-Control Parameters. Progress in Polymer Science 36(7): 887-913.
- [116] Kawashima, Y., Yamamoto, H., Takeuchi, H., and Kuno, Y. Mucoadhesive D-L lactide/glycolide Copolymer Nanospheres Coated with Chitosan to Improve Oral Delivery of Elcatonin. Pharm Dev Technol 5: 77-85.
- [117] Faraji, H. A.; and Wipf, P. Nanoparticles in cellular drug delivery. Bioorganic and medicinal chemistry 17(2009): 2950-2962.
- [118] Jing-ling, T.; Jin, S.; and Zhong-Gui, H. Self-Emulsifying Drug Delivery Systems: Strategy for Improving Oral Delivery of Poorly Soluble Drugs. Current Drug Therapy, 2007, 2, 85-93
- [119] Gupta, P. N.; Mahor, S.; Rawat, A.; Khatri, K.; Goyal, A. and Vyas, S. P. Lectin

- Anchored Stabilized Biodegradable Nanoparticles for Oral Immunization 1. Development and in vitro evaluation. Int. J. Pharm 318(2006): 163–173.
- [120] Buzea, C.; Blandino, I.; and Robbie, K. Nanomaterials and Nanoparticles: Sources and Toxicity. Biointerphases (2007): 17-27.
- [121] Wang, L. S.; and Hong, R.Y. Synthesis, Surface Modification and Characterisation of Nanoparticles. Advances in Nanocomposites (2008): 289-320.
- [122] Sonia, M.; and Mohamed, D. *In Vitro* Antioxidant Activities of *Aloe vera* Leaf Skin Extracts. Journal de la Societe Chimique de Tunisie 10(2008): 101-109.
- [123] Ranzo, B.; Giancalo, V.; Anna, L.; and Alessandro, C. Formation of Dehydrodieugenol from the Reaction of Isoeugenol and Eugenol with DPPH Radical and Their Role in the Radical Scavenging Activity. Food Chemistry 118(2): 256-265.
- [124] Patrik, C.E.; Otto, K.L.; Johan, P.W.; and Tapio, O. Chemical Studies on Antioxidant Mechanisms and Free Radical Scavenging Properties of Lignans. Org. Biomol. Chem 18(3): 3336-3347.
- [125] Ayse, K.; Beraat, O.; and Samim, S. Review of Method to Determine Antioxidant Capacities. Food Analytical Methods 2(1): 41-60.
- [126] Ruby, A. J.; Kuttan, G.; Dinesh, B. K.; Rajasekharan, K. N.; and Kutta, R. Antitumor and Antioxidant Activity of Natural Curcuminoids. Cancer Letters 94(1995): 79-83.
- [127] Slobodan, V. J.; Steenken, S.; Boone, C. W.; and Simic, M. G. H-Atom Transfer is a Preferred Antioxidant Mechanism of Curcumin. J. Am. Chem. Soc 121(1999): 9677-9681.
- [128] Toshiya, M.; Kayo, H.; Ayumi, S.; Tomomi, M.; Yoshio, T.; and Hidemasa, Y. Chemical Studies on Antioxidant Mechanism of Curcuminoid - Analysis of Radical Reaction Products from Curcumin. J. Agric. Food Chem 47(1999): 71–77.
- [129] Roberto, M.; Roberta, F.; Rekha, B.; and Colin, J. G. Curcumin, an Antioxidant and Anti-inflammatory Agent, Induces Heme Oxygenase-1 and Protects Endothelial Cells Against Oxidative Stress. Free Radical Biology & Medicine 28(8): 1303-1312.
- [130] L. Ross, C. B.; Melinda, R. V. On the Antioxidant Mechanism of Curcumin-Determine ASntioxidant Mechanism and Activity. Organic Letters 2(18): 2841-2843.
- [131] Venugopal, P. M.; and Adluri, R. S. Antioxidant and Anti-inflammatory Properties of Curcumin. Free Radical Biol Med 35(2003): 107-125.
- [133] Gopinath, D.; Ravi, D.; Rao, B. R.; Apte, S. S.; Renuka, D.; Rambhau, D. Ascorbyl palmitate Vesicles (Aspasomes) - Formation, Characterization and Applications.

- International Journal of Pharmaceutics 271(2004): 95–113.
- [134] Pokorski, M.; Gonet, B. Capacity of Ascorbyl Palmitate to Produce the Ascorbyl Radical *In Vitro* - an Electron Spin Resonance Investigation. Physiol. Res 53(2004): 311-316.
- [135] Julijana, K.; Breda, V.; Mirjana, G.; Marjeta, S.; and Polona, J. Effect of Colloidal Carriers on Ascorbyl Palmitate Stability. European Journal of Pharmaceutical Sciences 19(2003): 181–189.
- [136] Polona, J.; Marjeta, S.; Mirjana, G.; Julijana, K.; Slavko, P. Production of Ascorbyl Palmitate by Surfactant-Coated Lipase in Organic Media. European Journal of Pharmaceutics and Biopharmaceutics 56(2003): 59–66.
- [137] Tangsumranjit, A.; Pellequer, Y.; Lboutounne, H.; Guillaume, Y. C.; Lamprecht, A.; and Mille, J. Enhanced ascorbyl palmitate stability by polymeric nanoparticles. J. Drug Del. Ind. Pharm 16(2): 161-163.
- [138] Sangkil, L.; Jaehwi, L.; and Young, W. C. Characterization and Evaluation of Freeze-dried Liposomes Loaded with Ascorbyl Palmitate Enabling Anti-aging Therapy of the Skin. Bull. Korean Chem. Soc 28(1): 99-102.
- [139] Veerawat, T.; Rainer, H. M.; and Varaporn, B. J. Encapsulation of Ascorbyl Palmitate in nanostructured lipid carriers (NLC) - Effects of Formulation Parameters on Physicochemical Stability. International Journal of Pharmaceutics 340(2007): 198-206.
- [140] Veerawat, T.; Eliana, B. S.; Rainer, H. M.; and Varaporn, B. J. Physicochemical Characterization and In Vitro Release Studies of Ascorbyl Palmitate-loaded Semi-solid Nanostructured Lipid Carriers (NLC gels). Journal of Microencapsulation 25(2): 111-120.
- [141] Wittayasuporn, M.; Rengpipat, R.; Palaga, T.; Asawanonda, P.; Anumansirikul, N.; Wanichwecharungruang, S. P. Chitosan Derivative Nanocarrier: Safety Evaluation, Antibacterial Property and Ascorbyl Palmitate Encapsulation. Journal of Microencapsulation 27(3): 218-225.
- [142] Rangrong, Y.; Jatesuda, J.; and Kridsada, A. Encapsulation of Ascorbyl Palmitate in Chitosan Nanoparticles by Oil-in-water Emulsion and Ionic Gelation Processes Colloids Surf B Biointerfaces 76(1): 292-297.
- [143] Luadthong, C.; Tachaprutinun, A.; Wanichwecharungruang, S. P. Synthesis and Characterization of Micro/nanoparticles of Poly(vinylalcohol-co-vinylcinnamate) Deriva-

- tives. European Polymer Journal 44(2008) : 1285–1295.
- [144] Sheikh, F. A.; Barakat Nasser, A. M.; and Kanjwal, M. A. Novel Self-assembly Amphiphilic Poly(epsilon-caprolactone)-grafted-poly(vinyl alcohol) Nanoparticles and Hydrophilic Drugs Carrier Nanoparticles. Journal of Materials Science-Materials in Medicine 20(3): 821-831.
- [145] Yufeng, T.; Yiyang, Z.; Yan, L.; Yumin, D. A Thermosensitive Chitosan-poly(vinyl alcohol) Hydrogel Containing Nanoparticles for Drug Delivery. Polym. Bull 64 (2010): 791–804.
- [146] Seira, M.; Masaru, K.; Takashi, N.; Kimiya, G.; and Katsuhiko, H. Poly(vinyl alcohol) Nanocomposites with Nanodiamond. Macromolecules 44(2011): 4415-4421.
- [146] Semenzim V. L.; ; Basso, G. G.; and Silva, D. A. Synthesis and Characterization of Novel, Highly Crystalline Poly(vinyl alcohol) Microspheres for Chemoembolization Therapy. Journal of Applied Polymer 121(3): 1417-1423.
- [147] Semenzim, V. L.; Basso, D. A.; Grazielli, G.; Silva, D. A.; Vasconcellos, A.; Agreli, G.; Lima-Oliveira, G.; Marques, A. P.; Kawasaki-Oyama, R. S.; Braile, D.; and Nery, J. G. Synthesis and characterization of novel, highly crystalline poly(vinyl alcohol) microspheres for chemoembolization therapy. Journal of Applied Polymer Science 121(3): 1417-1423.

APPENDIX

APPENDIX

Encapsulation efficiency and loading of ascorbyl palmitate loaded into curcumin-grafted PV(OH) and cinnamate-grafted PV(OH) nanoparticles

Calibration curve of ascorbyl palmitate

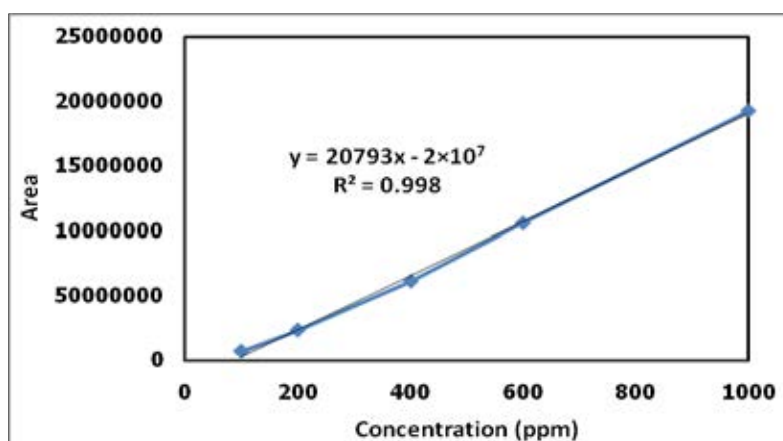


Figure A.1 Calibration curve of ascorbyl palmitate (AP) in methanol solution

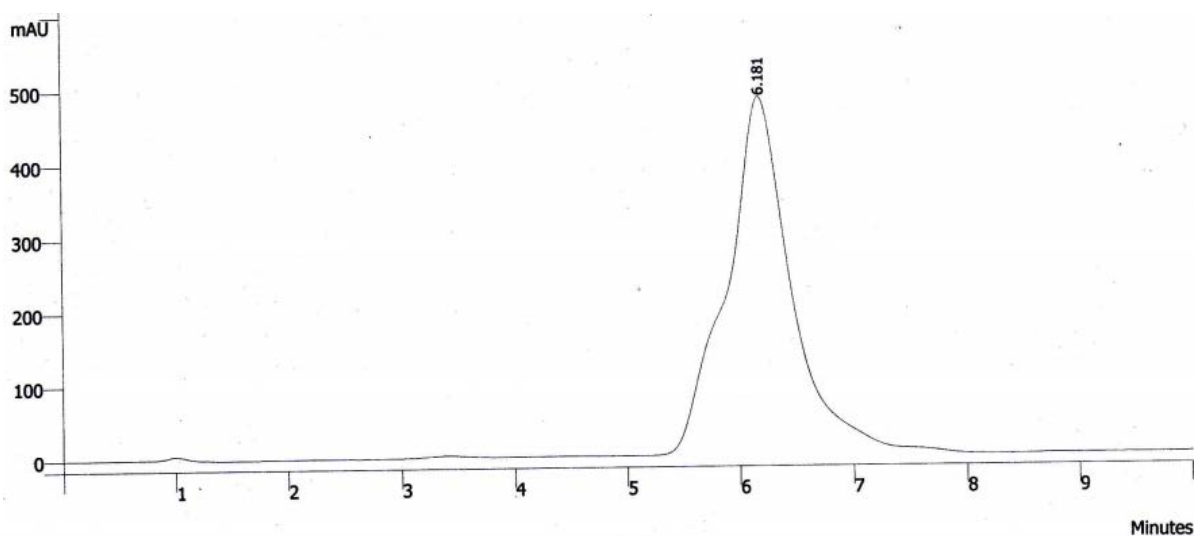


Figure A.2 Retention time and area of ascorbyl palmitate (AP) at 1,000 ppm

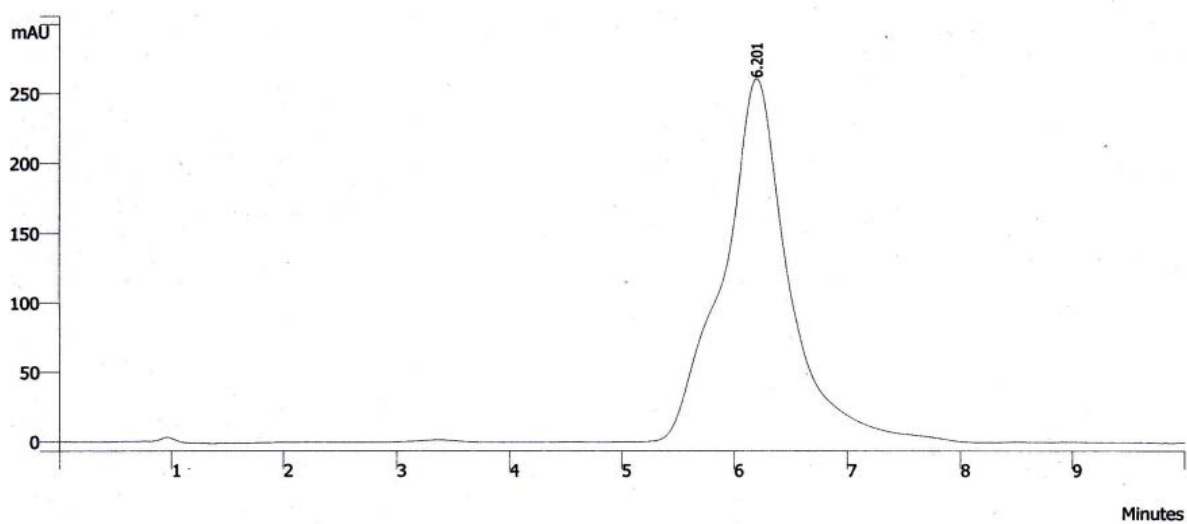


Figure A.3 Retention time and area of ascorbyl palmitate (AP) at 600 ppm

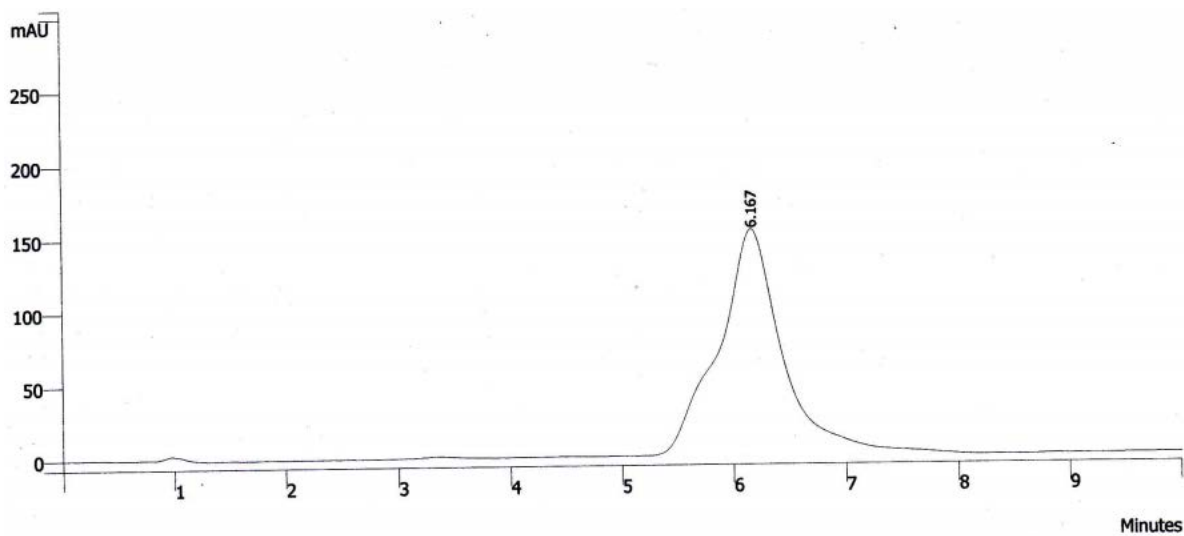


Figure A.4 Retention time and area of ascorbyl palmitate (AP) at 400 ppm

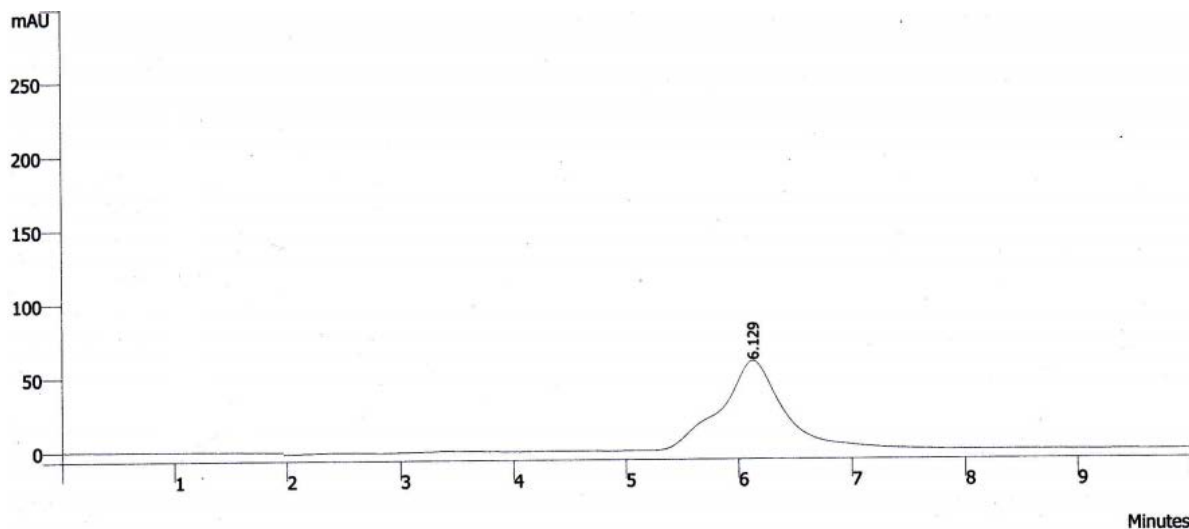


Figure A.5 Retention time and area of ascorbyl palmitate (AP) at 200 ppm

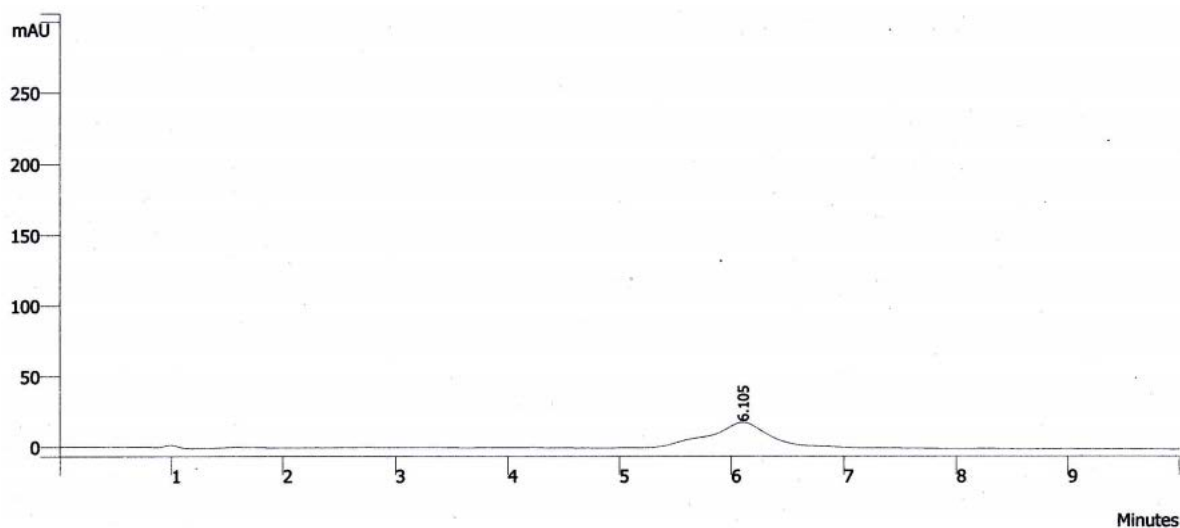


Figure A.6 Retention time and area of ascorbyl palmitate (AP) at 100 ppm

1) AP-encapsulated into curcumin-grafted PV(OH) nanoparticles

From the equation of calibration curve;

$$Y = 20793X - (2 \times 10^7), R^2 = 0.998 \quad (1)$$

1.1) Content of ascorbyl palmitate

The amount of ascorbyl palmitate loaded into curcumin-grafted PV(OH) nanoparticles was calculated by equation (1);

$$3846 = 20793X - (2 \times 10^7)$$

$$X = 86.249$$

Volume of the product 5 mL gave amount of ascorbyl palmitate (AP) in curcumin-grafted PV(OH) nanocarriers 86.249 ppm

$$\text{ppm} \longrightarrow \text{mg} / 1,000 \text{ mL} \quad \text{So, } 86.249 \text{ ppm} = 86.249 \text{ mg} / 1,000 \text{ mL}$$

Product volumetric 1,000 ml gave content of AP = 86.249 mg.

Product volumetric 34 ml gave content of AP = $\frac{86.249}{1,000} \times 34 = \underline{2.932}$ mg.

$$\begin{aligned} \text{\% encapsulation efficiency (\%EE)} &= \frac{(\text{weight of encapsulated AP})}{(\text{weight of AP used})} \times 100 \\ &= [(15.3 - 2.932) / 15.3] \times 100 \\ &= \underline{80.84 \%} \end{aligned}$$

$$\begin{aligned} \text{\% loading} &= \frac{(\text{weight of encapsulated AP})}{(\text{weight of polymer used})} \times 100 \\ &= [(15.3 - 2.932) / (12.37 + 30.3)] \times 100 \\ &= \underline{28.98 \%} \end{aligned}$$

1.2) Content of curcumin

The amount of curcumin that grafted on PV(OH) was calculated from peak area of ¹H-NMR spectrum between 1.22-1.74 ppm (-CH₂-CH-OH)_m-(CH₂-CH-O-C=O-CH₃)_n-(CH₂-CH-C=O-R)_o, br, 2H) of PV(OH) backbone and 6.02-6.14 ppm (-C=O-CH₂-C=O-, 2H) of curcumin.

g = (-C=O-CH₂-C=O-) of curcumin

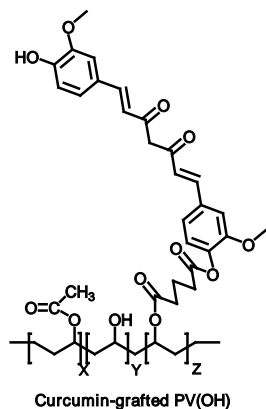
a = (-CH₂-CH-OH)_m-(CH₂-CH-O-C=O-CH₃)_n-(CH₂-CH-C=O-R)_o of
PV(OH)

backbone

$$\begin{array}{ccc} g & : & a \\ \underline{0.07} & : & \underline{1.18} \\ 2 & & 2 \\ 0.035 & : & 0.59 \\ \sim 0.059 & : & 1 \end{array}$$

So, degree of substitution of curcumin that grafted on PV(OH) is 0.059

But, we used PV(OH) 88% deacetylated



Mole ratio of

$$X = 0.88 - 0.059 = \underline{0.821}$$

$$Y = 1 - 0.821 - 0.059 = \underline{0.12}$$

$$Z = \underline{0.059}$$

Content of curcumin (g) was calculated from;

$$= \frac{(0.059 \times \text{MW. of curcumin})}{(0.12 \times 86) + (0.059 \times \text{MW. of monosubstituted glutarylcurcumin}) + (0.821 \times \text{MW. of PV(OH) 1 monomeric unit})}$$

$$= \frac{(0.059 \times 368.38)}{(0.12 \times 86) + (0.059 \times 508.38) + (0.821 \times 44)}$$

$$= \frac{21.73}{76.43}$$

$$= \underline{0.2843} \text{ g. curcumin}$$

So, Percentage of curcumin equal $0.2843 \times 100 = \underline{28.43} \%$ curcumin

2) AP-encapsulated cinnamate-grafted PV(OH) nanoparticles

From the equation of calibration curve;

$$Y = 20793X - (2 \times 10^7), R^2 = 0.998 \quad (1)$$

The amount of ascorbyl palmitate loaded into cinnamate-grafted PV(OH) nanocarriers was calculated by equation (1);

$$54130 = 20793X - (2 \times 10^7)$$

$$X = 86.501$$

Volume of the product 5 ml gave amount of ascorbyl palmitate (AP) in cinnamate-grafted PV(OH) nanocarriers 86.501 ppm

$$\text{ppm} \longrightarrow \text{mg} / 1,000 \text{ mL} \quad \text{So, } 86.501 \text{ ppm} = 86.501 \text{ mg} / 1,000 \text{ mL}$$

Product volumetric 1,000 mL gave content of AP = 86.501 mg.

Product volumetric 42 mL gave content of AP = $\frac{86.501}{1,000} \times 42 = \underline{3.633}$ mg.

$$\begin{aligned} \text{\% encapsulation efficiency (\%EE)} &= \frac{(\text{weight of encapsulated AP})}{(\text{weight of AP used})} \times 100 \\ &= [(15.1-3.633) / 15.1] \times 100 \\ &= \underline{75.94} \% \end{aligned}$$

$$\begin{aligned} \text{\% loading} &= \frac{(\text{weight of encapsulated AP})}{(\text{weight of polymer used})} \times 100 \\ &= [(15.1-3.633) / (11.47+30.5)] \times 100 \\ &= \underline{27.32} \% \end{aligned}$$

3) AP (together with curcumin)-encapsulated cinnamate-grafted PV(OH) nanoparticles

From the equation of calibration curve;

$$Y = 20793X - (2 \times 10^7), R^2 = 0.998 \quad (1)$$

3.1) Content of ascorbyl palmitate

The amount of ascorbyl palmitate (AP) loaded into cinnamate-grafted PV(OH) nanoparticles was calculated by equation (1);

$$\begin{aligned} 10127 &= 20793X - (2 \times 10^7) \\ X &= 86.281 \end{aligned}$$

Volume of the product 5 ml gave amount of ascorbyl palmitate (AP) in cinnamate-grafted PV(OH) nanocarriers 86.281 ppm

ppm \longrightarrow mg / 1,000 ml So, 86.281 ppm = 86.281 mg / 1,000 ml

Product volumetric 1,000 mL gave content of AP = 86.281 mg.

Product volumetric 42 mL gave content of AP = $\frac{86.281}{1,000} \times 66.5 = \underline{5.738}$ mg.

$$\begin{aligned} \text{\% encapsulation efficiency (\%EE)} &= \frac{(\text{weight of encapsulated AP})}{(\text{weight of AP used})} \times 100 \\ &= [(15.3-5.738) / 15.3] \times 100 \\ &= \underline{62.50} \% \end{aligned}$$

$$\begin{aligned} \text{\% loading} &= \frac{(\text{weight of encapsulated AP})}{(\text{weight of polymer used})} \times 100 \\ &= [(15.3-5.738) / (9.56+9.36+30.3)] \times 100 \end{aligned}$$

$$= \underline{19.43} \%$$

3.2) Content of curcumin

The amount of ascorbyl palmitate loaded into cinnamate-grafted PV(OH) nanocarriers was calculated by equation (1);

$$9833 = 20793X - (2 \times 10^7)$$

$$X = 86.279$$

Volume of the product 5 mL gave amount of curcumin in cinnamate-grafted PV(OH) nanocarriers 86.279 ppm

$$\text{ppm} \longrightarrow \text{mg} / 1,000 \text{ mL} \quad \text{So, } 86.279 \text{ ppm} = 86.279 \text{ mg} / 1,000 \text{ mL}$$

Product volumetric 1,000 mL gave content of AP = 86.279 mg.

Product volumetric 42 mL gave content of AP = $\frac{86.279}{1,000} \times 66.5 = 5.737 \text{ mg}$.

$$\begin{aligned} \text{\% encapsulation efficiency (\%EE)} &= \frac{(\text{weight of encapsulated curcumin})}{(\text{weight of curcumin used})} \times 100 \\ &= [(15.1 - 5.737) / 15.1] \times 100 \\ &= \underline{62.01\%} \end{aligned}$$

$$\begin{aligned} \text{\% loading} &= \frac{(\text{weight of encapsulated curcumin})}{(\text{weight of polymer used})} \times 100 \\ &= [(15.1 - 5.737) / (9.56 + 9.36 + 30.3)] \times 100 \\ &= \underline{19.02} \% \end{aligned}$$

VITAE

Ms. Sirinapa Janesirisakule was born on January 29th, 1985 in Bangkok, Thailand. She obtained a Bachelor's Degree of Science in Chemistry from Chulalongkorn University in 2004. After that, Miss Janesirisakule started her master study in the Program of Petrochemical and Polymer Science at Chulalongkorn University. During her study Miss Janesirisakule contributed academically to the 14th Asian Chemical Congress 2011 (14ACC) via a research presentation entitled "Co-encapsulation of ascorbyl palmitate and curcumin"

Her address is 35/171 Phyathai Road, Phyathai, Radchadavee, Bangkok, 10400, Tel. 02-2466832 and 081-8873456.